ELECTROSTATIC COALESCER AND CROSS FLOW ULTRAFILTRATION FOR CUTTING OIL WASTEWATER TREATMENT AND SEPARATION

Miss Thaksina Poyai

A Thesis Submitted in Partial Fulfillment of the Requirements
for the Degree of Master of Science Program in Environmental Management
(Interdisciplinary Program)
Graduate School
Chulalongkorn University
Academic Year 2014

การเพิ่มประสิทธิภาพการแยกและบำบัดน้ำเสียปนเปื้อนน้ำมันตัด โดยกระบวนการร่วมระหว่าง อิเล็กโทรสตาติกโคอะเลสเซอร์และอัลตราฟิลเตรชัน

นางสาวทักษิณา โพธิ์ใหญ่

วิทยานิพนธ์นี้เป็นส่วนหนึ่งของการศึกษาตามหลักสูตรปริญญาวิทยาศาสตรมหาบัณฑิต
สาขาวิชาการจัดการสิ่งแวดล้อม (สหสาขาวิชา)
บัณฑิตวิทยาลัย จุฬาลงกรณ์มหาวิทยาลัย
ปีการศึกษา 2557

Thesis Title	ELECTROSTATIC COALESCER AND CROSS FLOW ULTRAFILTRATION FOR CUTTING OIL WASTEWATER TREATMENT AND SEPARATION
By	Miss Thaksina Poyai
Field of Study	Environmental Management
Thesis Advisor	Associate Professor Pisut Painmanakul, Ph.D.
Thesis Co-Advisor	Dr. Aunnop Wongrueng, Ph.D.

Accepted by the Graduate School, Chulalongkorn University in Partial Fulfillment of the Requirements for the Master's Degree

.....Dean of the Graduate School
(Associate Professor Sunait Chutintaranond, Ph.D.)

THESIS COMMITTEE

.....Chairman
(Assistant Professor Chantra Tongcumpou, Ph.D.)
.....Thesis Advisor
(Associate Professor Pisut Painmanakul, Ph.D.)
.....Thesis Co-Advisor
(Dr. Aunnop Wongrueng, Ph.D.)
.....Examiner
(Dr. Seelawut Damrongsiri, Ph.D.)
.....External Examiner
(Dr. Srayut Rachu, Ph.D.)

ทักษิณา โพธิ์ใหญ่ : การเพิ่มประสิทธิภาพการแยกและบำบัดน้ำเสียปนเปื้อนน้ำมันตัดโดยกระบวนการร่วมระหว่าง อิเล็กโทรสตาติกโคอะเลสเซอร์และอัลตราฟิลเตรชัน (ELECTROSTATIC COALESCER AND CROSS FLOW ULTRAFILTRATION FOR CUTTING OIL WASTEWATER TREATMENT AND SEPARATION) อ.ที่ปรึกษาวิทยานิพนธ์หลัก: รศ. ดร. พิสุทธิ์ เพียรมนกุล, อ.ที่ปรึกษาวิทยานิพนธ์ร่วม: อ. ดร. อรรณพ วงศ์เรือง, 144 หน้า.

งานวิจัยนี้ มีจุดประสงค์เพื่อที่จะศึกษาประสิทธิภาพการแยกน้ำเสียปนเปื้อนน้ำมันตัด ซึ่งเป็นน้ำมันที่มีความคงตัวสูงและยากต่อการบำบัด โดยกระบวนการที่ทำการศึกษา ได้แก่ การทำลายเสถียรภาพด้วยสารเคมี กระบวนการโคอะเลสเซอร์ และการกรองแบบอัลตราฟิลเตรชัน ในกระบวนการทำลายเสถียรภาพ จะใช้สารแคลเซียมคลอไรด์เป็นสารทำลายเสถียรภาพแบบประจุบวก โดยสามารถหาปริมาณสารเคมีที่เหมาะสมได้จากวิธีจาร์เทส ในส่วนของอุปกรณ์โคอะเลสเซอร์ ได้ใช้ตัวกลางทรงกระบอกกลวงที่ผลิตจากพลาสติกโพลีโพรพิลีน และมีการดำเนินระบบด้วยความเร็วการไหล 1.2 มิลลิเมตร/วินาที สำหรับกระบวนการอัลตราฟิลเตรชัน ได้มีการศึกษาปัจจัยต่างๆ ที่มีผลกระทบต่อระบบ อาทิเช่น ความดัน อุณหภูมิ และพีเอช หลังจากนั้น ได้ทำการศึกษาความเป็นไปได้ ในการประยุกต์ใช้กระบวนการเหล่านี้ร่วมกัน โดยมีระบบหมุนเวียนน้ำกลับระหว่างอุปกรณ์โคอะเลสเซอร์และอัลตราฟิลเตรชันเกิดขึ้นด้วย

จากผลการทดลอง แสดงให้เห็นว่า กระบวนการการทำลายเสถียรภาพ มีสัดส่วนปริมาณสารแคลเซียมคลอไรด์ที่เหมาะสมต่อความเข้มข้นน้ำมัน อยู่ในช่วง 1:1 ถึง 5:1 โดยมีประสิทธิภาพการบำบัดสูงสุดที่ 70% ในขณะที่ กระบวนการโคอะเลสเซอร์ ให้ประสิทธิภาพการบำบัดสูงสุดที่ 40% เมื่อดำเนินระบบกับน้ำเสียที่มีความเข้มข้นน้ำมันต่ำกว่า 0.5% โดยมวลต่อปริมาตร แต่อย่างไรก็ตาม เมื่อนำน้ำเสียปนเปื้อนน้ำมันมาทำลายเสถียรภาพในเบื้องต้น ก่อนที่จะเข้าสู่กระบวนการโคอะเลสเซอร์ พบว่า ประสิทธิภาพการบำบัดของโคอะเลสเซอร์เพิ่มขึ้นถึง 50% สำหรับการกรองแบบอัลตราฟิลเตรชัน กระบวนการนี้มีประสิทธิภาพการบำบัดน้ำมันที่ค่อนข้างสูง (มากกว่า 95%) เมื่อดำเนินระบบภายใต้สภาวะที่เหมาะสม คือ ความดัน 3 บาร์ อุณหภูมิ 28 องศาเซลเซียส และพีเอชเป็นเบส อย่างไรก็ตาม กระบวนการนี้ยังมีข้อจำกัดในเรื่องการอุดตันของเมมเบรน ที่ส่งผลต่อค่าใช้จ่ายที่สูงขึ้นในการเดินระบบ จากการทดลอง ยังพบได้ว่า การประยุกต์ใช้กระบวนการร่วม สามารถลดเวลากักของอุปกรณ์โคอะเลสเซอร์ได้ถึง 50% มีประสิทธิภาพการกำจัดซีโอดีสูงถึง 97% และยังช่วยลดปัญหาการอุดตันของเมมเบรนได้อีกด้วย นอกจากนี้ ได้มีการทดลองนำกระแสไฟฟ้าในปริมาณต่ำๆ ใส่ไว้เหนือตัวกลางโคอะเลสเซอร์ ทั้งนี้ เพื่อให้เกิดการเคลื่อนที่ของประจุบนผิวเม็ดน้ำมัน ทำให้น้ำมันที่ผ่านชั้นตัวกลางแล้วสามารถรวมตัวกันได้อีก ซึ่งส่งผลให้ระบบมีประสิทธิภาพที่ดีขึ้น ในแง่การอุดตันของเมมเบรนที่ลดลง

สาขาวิชา การจัดการสิ่งแวดล้อม ลายมือชื่อนิสิต .....

ปีการศึกษา 2557 ลายมือชื่อ อ.ที่ปรึกษาหลัก .....

ลายมือชื่อ อ.ที่ปรึกษาร่วม .....

5687535820 : MAJOR ENVIRONMENTAL MANAGEMENT
KEYWORDS: CUTTING OIL WASTEWATER / COALESCER / CHEMICAL DESTABILIZATION / ULTRAFILTRATION

THAKSINA POYAI: ELECTROSTATIC COALESCER AND CROSS FLOW ULTRAFILTRATION FOR CUTTING OIL WASTEWATER TREATMENT AND SEPARATION. ADVISOR: ASSOC. PROF. PISUT PAINMANAKUL, Ph.D., CO-ADVISOR: DR. AUNNOP WONGRUENG, Ph.D., 144 pp.

This research aims to study the performance of various treatment processes on cutting oil wastewater, which is highly stabilized and difficult to deal with. The application of chemical destabilization, conventional coalescer, and ultrafiltration (UF) were considered. Calcium chloride ($CaCl_2$) was employed as a positively charged electrolyte for destabilizing oil droplets, in which its optimal dosage was determined by the jar-test method. For the coalescer, the polypropylene material in tubular shape was used as the two-stage coalescing media with the influent velocity of 1.2 mm/s. The UF process was conducted under a cross-flow operation mode and its optimum conditions in terms of TMP, temperature, and pH were investigated. Once these methods were independently studied, they were finally integrated into a system with liquid recirculation and their combining performance was then evaluated.

Considering each process individually, the optimal ratio of the $CaCl_2$ dose and oil concentration varied from 1:1 to 5:1 with the highest efficiency of 70%. Without oil droplet destabilization, the coalescer could reach its maximum effectiveness of 40% when dealing with oil concentrations below 0.5% w/v. However, the combination of these two processes could enhance oil separation performance of the coalescer up to 50%. For the UF process, the optimal conditions were acquired at the TMP of 3 bar and 28ºC under an alkaline state, in which more than 95% oil removal could be attained. Nevertheless, the problem of rapid membrane fouling still needs to be concerned. In case of the combined process, the coalescer with chemical adding was applied as a pretreatment for the cross-flow UF. The results indicated that this combined process could lessen half the residence time for the coalescer. Also, the membrane fouling could be retarded when the coalescer was provided upstream. Moreover, the COD removal of 97% was achieved for the effluent from this combined process. Finally, an external low electric field was applied over the media layer in order to promote the migration of oil droplet surface charges, leading to further oil droplet coalescence and enhanced overall process efficiency in terms of oil recovery and flux decline intensity.

Field of Study: Environmental Management	Student's Signature .....
Academic Year: 2014	Advisor's Signature .....
	Co-Advisor's Signature .....

ACKNOWLEDGEMENTS

First of all, I wish to express my profound gratitude to my advisor, Associate Professor Dr. Pisut Painmanakul, for his valuable advice and support throughout this research. I am also grateful to my co-advisor, Dr. Aunnop Wongrueng, for his worthwhile encouragement and guidance. Additionally, my appreciation is also provided to Assistant Professor Dr. Chantra Tongcumpou, Dr. Seelawut Damrongsiri and Dr. Srayut Rachu for serving as a chairman and members of my thesis committee, including their helpful comments and suggestions.

My gratefulness is also extended to the Center of Excellent on Hazardous Substance Management (HSM), Department of Environmental Engineering, Chulalongkorn University, and the entire staffs for research grants, assistance, as well as experimental facilities.

Further, my sincere thanks should also be given to Mr. Nattawin Chawaloesphonsiya, Mr. Nattapong Tuntiwiwattanapun, my parents, and all laboratory colleagues for their worthy favor and inspiration.

Finally, I would like to express my wholehearted regard to Miss Akiko Uyeda for her valuable instructions on the English-writing skill, which is highly crucial to complete this thesis work.

CONTENTS

Page

Page

Page

LIST OF TABLES

Page

LIST OF FIGURES

Page

CHAPTER 1

INTRODUCTION

1.1 BACKGROUND

Currently, water pollution seems to be a part of serious environmental concerns due to its extensively potential effects on human health and the environment. Wastewater can originate from several sources, particularly from the municipal and industrial sectors. Moreover, the components from each source of wastewater vary, resulting in different wastewater characteristics. Nowadays, oil has generated a great deal of interest since it is a substance that has been intensely used by households and industries. Furthermore, oil usually contains a large amount of hydrocarbons, which might be toxic to aquatic environments and cause a poor taste and odor in water.

Oily wastewater can be classified into various forms, depending on the features of hydrocarbon within the water. Nevertheless, generated oily wastewater is mostly found as oil-in-water emulsions or stabilized oil emulsions, in which oil droplets are quite small and highly stable; therefore, they are difficult to be separated from water. Oil-in-water emulsions are extensively employed as cutting fluids or cutting oils for cooling and lubrication in metalworking and machining processes in several branches of industry. It, moreover, tends to lose requisite properties and become toxic after extended use (Perez et al., 2007), which ultimately ends up as hazardous waste. Thus, it is vital to find an exceptionally effective method for managing this problem.

A critical challenge is that, most conventional treatment processes (e.g., decantation and sedimentation) require extremely long residence time compared to

others (Li & Gu, 2005), particularly for the emulsion with substantially low concentration and droplet size of less than 20 microns (Chakrabarty et al., 2010). On the other hand, a number of physical processes have been widely implemented as primary treatments of oily wastewater by reason of their cost effectiveness, like the coalescence process, membrane filtration and air flotation.

For the treatment of oily emulsions, the coalescing approach using a coalescer bed normally acts as an effective method for inducing large oil droplets, which are easy to rise and separate from water. However, further treatments are still desired due to unachievable environmental standards of this process. Membrane technology particularly ultrafiltration (UF), has widely been accepted as an attractive physical technique that provides a relatively high treatment efficiency of oily wastewater, including the ability to deal well with finely dispersed oil droplets. This system, however, is frequently subject to the problem of particle fouling, which contributes to the need for regular maintenance and its lower oil separation efficiency.

The purpose of this research, therefore, is to primarily study coalescer's mechanisms on cutting oil wastewater. Afterwards, the cross-flow UF in terms of its optimal conditions and fouling mechanisms is investigated in order to implement the coalescer process as well as improve the performance itself. Additionally, other technologies such as chemical additions and electrostatic fields are also applied in order to enhance the overall system efficiency, regarding oil droplet destabilization and coalescence approach. Finally, the synergistic effects along with optimization of the combined processes are then proposed.

1.2 OBJECTIVES

The main objective of this research is to study the performance of combined processes (i.e., chemical destabilization, coalescer, and cross-flow UF) on cutting oil wastewater treatment and separation.

The specific aims can be expressed below:

1.2.1 To individually investigate optimal operating conditions and enhance oil separation efficiency of each treatment process.

1.2.2 To develop an integrated process for effective cutting oil wastewater treatment

1.3 HYPOTHESES

1.3.1 The coalescence of stabilized oil droplets could be enhanced by the aid of chemical adding and electrostatic fields.

1.3.2 Oil recovery and membrane fouling could be improved when coupling the cross-flow UF with coalescer device.

1.4 SCOPE OF THE STUDY

1.4.1 The experiments in this study were carried out on a pilot scale with a batch system at HSM on the 10th floor of the Chulalongkorn University Research Building and the Department of Environmental Engineering under the Faculty of Engineering of Chulalongkorn University.

1.4.2 The oily wastewater was synthesized from a mixture of tap water and the commercial cutting oil.

1.4.3 Coalescence process:

- A cylindrical transparent acrylic column with a diameter of 10 cm and height of 150 cm was used as both the coalescer apparatus (a lower part) and a decantation tank (an upper part).
- The coalescing media were made of polypropylene plastic in a tubular shape, used as a two-step media bed (each layer was 5 cm high).

1.4.4 Optimal conditions for the membrane process were investigated from its flux declinations due to trans-membrane pressure, temperature and pH.

1.4.5 Supplements for enhancing oil droplet coalescence:

- An external electric field of 10 A/m^2 was offered to the coalescer process, in which two Al plates with an effective area and a gap of 100 cm^2 and 2 cm, were used as electrodes.
- Calcium chloride ($CaCl_2$) was used as an electrolyte for oil droplet destabilization.

1.5 EXPECTED ADVANTAGES

1.5.1 The applicable concepts of the hybrid process, involving chemical destabilization, coalescence, and cross-flow UF, for the effective treatment of oily wastewater.

1.5.2 A combined process that could be modified and adapted to deal effectively with produced oily wastewater from industries.

CHAPTER 2

BACKGROUND AND LITERATURE REVIEW

2.1 OILY WASTEWATER

2.1.1 Characteristics

Hydrocarbon or oil is considered to be a hazardous pollutant due to its harmful effects when released into the environment, particularly water bodies. Oily wastewater has an extremely high chemical oxygen demand (COD), which makes it difficult to degrade by natural self-purification systems. Moreover, it might consist of other components aside from oil and water such as surfactants, co-surfactants and some additives (e.g., anti-corrosion agents, bactericides and dyes). These substances are usually added to improve oil properties; however, they might cause treatment problems.

In this study, substances that can be identified as "oil" are based on the following physical characteristics:

Liquidity: Only oil in liquid form will be accounted in this study.

Solubility: Oil and water in this study are assumed to be two immiscible liquids; therefore, the oil should not dissolve well in water (i.e., oil with relatively low solubility in water is required)

Density or specific gravity: Oil in this study must have a density or specific gravity that is less than that of water.

2.1.2 Classification of Oily Wastewater

Oily wastewater exists in the environment in various forms, depending on the characteristics of the oils or hydrocarbons mixed in water. When treatment technologies, especially separation processes, are investigated, the oil-water mixture can be categorized by three major criteria according to its physical properties as described in the following section (Rachu, 2005).

2.1.2.1 Categorization by the type of continuous phase

A system with an immiscible liquid mixture will compose of two major phases: the dispersed phase and continuous phase, which is the majority of the system.

Direct emulsion: When the mixture has water as the continuous phase, it will be called a "direct emulsion" and can also be written as an "O/W emulsion," which is short for an "oil-in-water emulsion."

Inverse emulsion: When oil is the continuous phase of the mixture, it will be called an "inverse emulsion" or a "water-in-oil emulsion (W/O emulsion)"

In this research, however, I will concentrate on direct emulsions, in which water is in the continuous phase and oil is in the dispersed phase.

2.1.2.2 Categorization by the stability of oily wastewater

With regard to this criterion, oily wastewater can be categorized into two types as follows:

Emulsion with the absence of surfactants (non-stabilized emulsion)

In general, oil droplets in this type of emulsion can spontaneously combine with each other to form large molecules, depending on the degree of dispersion or oil droplet size. The longer the droplets disperse and stay in the water phase, the

higher the stability of the droplets are. A major factor affecting the degree of dispersion is the mixing characteristics, which provide energy and cause turbulence to the system.

Emulsion with the presence of surfactants (stabilized emulsion)

Oily wastewater of this type is composed of surface-active agents (i.e., surfactants and co-surfactants). These substances serve as the mechanical and electrical barriers that abate oil-water interfacial tension, leading to the inhibition of oil droplets from colliding and coalescing. Therefore, this type of emulsion will contribute to producing finely dispersed and very highly stable oil droplets.

Normally, surfactants or surface-active substances can be divided into four groups (i.e., non-ionic surfactants, anionic surfactants, cationic surfactants and amphoteric surfactants). Each molecule of a surfactant is composed of a hydrophilic part and hydrophobic part as shown in Figure 2.1.

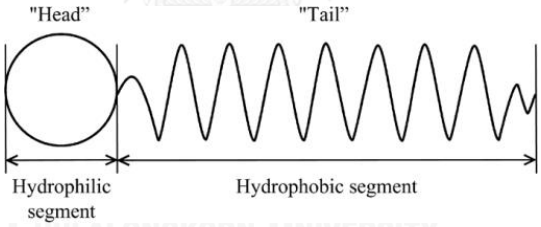

Figure 2.1 *The surfactant molecular structure*

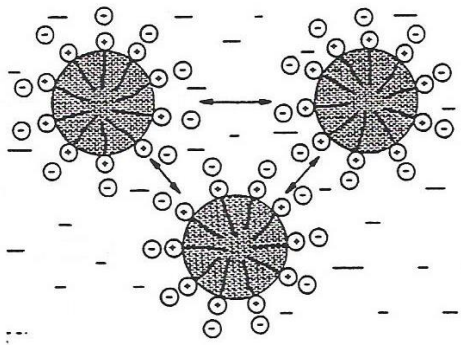

Figure 2.2 *The pushing between oil droplets resulting from a surfactant (Aurelle, 1985)*

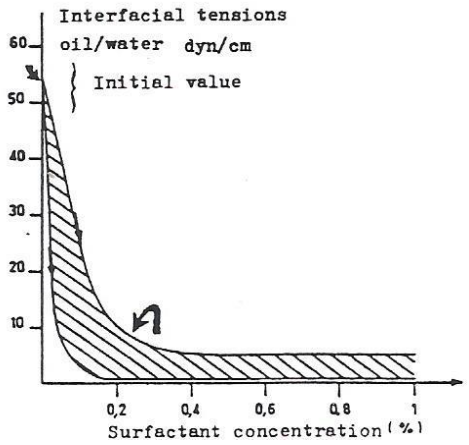

Figure 2.3 *The relationship between oil-water interfacial tension and surfactant concentration (Aurelle, 1985)*

According to Fig. 2.3, a surfactant is capable of lessening oil-water interfacial tension even at quite low concentrations. Additionally, the diagram also shows that the interfacial tension is inversely proportional to the surfactant concentration; in other words, interfacial tension tends to decrease as the concentration of a surfactant increases.

2.1.2.3 Categorization by the degree of dispersion

This criterion is governed by droplet size and the properties of the mixture, which influence the characteristics of the oil droplet rising velocity. When considering this criterion, oily wastewater can be classified into the following five classes:

- *Floating film or oil layer*

Wastewater in this group contains oil and water that are definitively separated from each other. Since oil floats as a layer over the water surface, it is quite easy to be treated. This type of wastewater, however, usually causes a problem on the transference of light and oxygen into the water body.

- *Primary emulsion*

  The oil droplet size in oily wastewater is mainly greater than 100 microns.

- *Secondary emulsion*

  The oil droplet size in oily wastewater is mainly less than 20 microns.

- *Macroemulsion*

This emulsion generally contains surfactants and the oil droplet size is mostly in the range of 0.06 to 1.0 microns and has a milky appearance.

- *Microemulsion*

This emulsion constitutes surfactants and co-surfactants in a large amount, which contributes to very tiny droplets within the size range of 10 to 60 nanometers.

The schematic diagram in Fig. 2.4 shows an overview of oily wastewater classifications based on the three criteria mentioned previously.

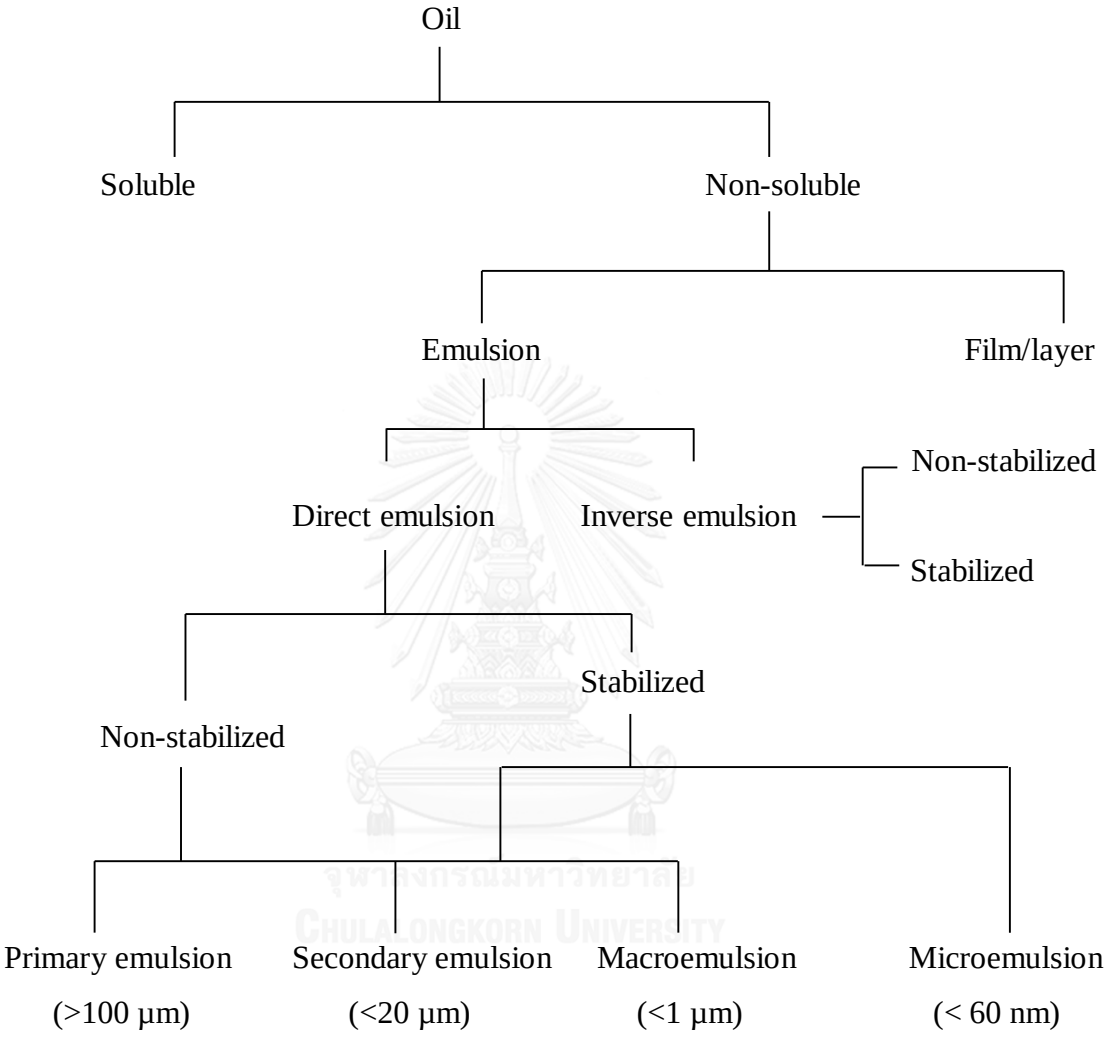

Figure 2.4 *A diagram of oily wastewater classification (Adapted from (Rachu, 2005))*

In conclusion, the categories of oily wastewater in this study were determined based on its physical properties (i.e., type of the continuous phase, oily wastewater stability and degree of dispersion). As a result, it is vital to use standard methods for analyzing and classifying oily wastewater in order to acquire correct data and suitable options for treatment processes.

2.2 CUTTING OIL

2.2.1 Characteristics and Functions

Metalworking fluids or cutting fluids are extensively used by industries for numerous mechanical and metalworking processes (e.g., boring, cutting, drilling and grinding). Since most machining operations generate enormous friction and a large amount of heat, metalworking fluids have been employed to reduce these effects and also improve cutting conditions in order to achieve the qualitative requirements of products.

It is widely agreed that cutting fluids can provide two major functions: cooling and lubrication. The most conventional substance used as a metalworking fluid is a type of oil-in-water emulsion (also known as cutting oil), in which water provides its cooling property and oil acts as its lubricating agent.

Coolants: The main advantages of the coolant are the reduction of thermal stress within the metallic work during operation, including the decrease of temperature on the cutting area of the tool edge and metal surface.

Lubricants: A major function of lubricant is to decrease the friction on the interface between a workpiece and tool, leading to the reduction of energy required.

2.2.2 Types of Metalworking Fluids

In general, cutting fluids can be sorted into the following four groups (Occupational Safety & Health Administration (OSHA), 1999):

2.2.2.1 Straight oil or neat cutting oil

Straight oil is mainly produced from mineral oils or vegetable oils and may be composed of some additives such as sulfur and chlorinated substances. Moreover, it is the only kind that is being used without being diluted with water. The appearance of the straight oil, therefore, tends to be oily and viscous. This material is preferable for lubricating action in machining work and regularly functions well at low cutting speeds.

2.2.2.2 Soluble oil

Soluble oil or emulsifiable oil consists of lubricating oil and emulsifiers as base materials. In addition, it usually contains some colorants and additives for improving its quality and performance. This product normally performs effectively as both a lubricant and coolant; on the other hand, corrosion prevention and mixture stability remain concerns.

2.2.2.3 Semisynthetic

This type of cutting fluid generally contains the same elements as the soluble oil; nevertheless, only a tiny amount of base oil (a concentration of 5-30%) is required. Additionally, semisynthetic fluids can provide desirable characteristics of lubricating action, rust control, heat reduction and extended sump life.

2.2.2.4 Synthetic

This material offers the advantages like those of semisynthetics; however, it provides better performance. Apart from detergent-like composition and some additives, no petroleum oil is contained in synthetics. Moreover, this product is transparent and not influenced by hard water.

As mentioned, besides oil and water as base materials, cutting fluid generally contains other additives in order to improve its performance and meet commercial specifications. Examples of some common additives as well as their functions are shown in Table 2.1

Table 2.1 *Lists of some additional additives in metalworking fluids*

Type of additive	Examples	Functional purpose
Emulsifiers	- Non-ionic surfactants - Petroleum sulfonate - Salts of fatty acids	To improve the dispersion of oil in water
Extreme pressure agents (EP)	- Phosphorus derivatives - Chlorinated paraffins - Sulfurized fatty materials	For lubrication under extraordinarily high pressure
Biocides	- Triazine - Oxazolidine	To resist microorganisms or bacterial growth
Oiliness agents	- Vegetable oil - Polyol ester	For enlargement of film strength
Corrosion inhibitors	- Calcium sulfonate - Fatty acid soaps	To prevent tools and workpieces from corrosion

2.2.3 Problems and Impacts

Environment:

The impact of metalworking fluids on the environment mostly takes place resulting from the difficulty of degrading and disposing of them. During the use of metalworking fluids in machining or cutting operations, a large quantity of cutting oil mist is released and subject to cause several adverse effects. Apart from smoke, fumes and odors that lead to air contamination, discharged wastewater from the process is also contaminated with cutting fluids and probably causes water and soil pollution.

Some types of metalworking fluid are flammable and might increase the risk of fires. Moreover, in western countries, a manipulation of lubricants having carcinogenic oil as a base material has become a serious problem that has to be addressed (El Baradie, 1996; Ii et al., 2000).

Health:

Exposure to metalworking fluids, particularly by virtue of dermal contact and inhalation, can cause various severe effects on health (Occupational Safety & Health Administration (OSHA), 1999):

Skin disorders: There are two types of diseases resulted from dermal exposure to cutting fluids: acne and dermatitis. Risk of dermatitis generally occurs from the exposure to synthetic and semisynthetic oils, while acne is mostly caused by straight oils.

Respiratory diseases: Exposure to metalworking fluids via inhalation can contribute to irritation on various parts of the body (i.e., the nose and throat, including the upper respiratory tract).

Cancer: After prolonged use of metalworking fluids, cancer might appear, for example, cancer of the skin, rectum, bladder and pancreas.

The potentially environmental and health problems from machining operations, however, generally result from the improper selection and application of cutting fluid in the process. Therefore, it is important to have a fundamental knowledge of metalworking fluid properties as well as its impacts on the environment and human health.

2.2.4 Lifecycle and Disposal

The lifecycle of metalworking fluids within a machining operation normally undergoes four steps (Grzesik, 2008): (1) storage and handling, (2) mixing with water, (3) use, and (4) disposal. After extended use, cutting fluids lose their properties and become contaminated. A coolant, for instance, is normally subject to a circulating system; therefore, its quality eventually deteriorates as a result of bacteria degradation, contamination with metal fines or dirt, and high mineral concentration due to water evaporation (Sutherland, 2008).

In many cases, wastewater contaminated with cutting oil should not be directly discharged to the public drainage system. Generally, prior to disposing of cutting oil wastewater, impure oil must be separated from the water. The most common method is a phase formation technique, which involves with the addition of some additives (e.g., salts, mineral acids and polyelectrolytes) for destabilizing or breaking down the emulsion. Rios et al. (1998), for example, found that inorganic salts (i.e., $CaCl_2$ and $AlCl_3$) could be effectively used as coagulants for the demulsification of a cutting oil emulsion. After that, the oil and water can be further managed by conventional processes (e.g., a centrifugal separator, coalescence, flotation and sedimentation). Electroflocculation, which is a combined technique using electroflotation and electroprecipitation, can also perform demulsification and purification in the oil separating process, including the ability to remove finely dispersed oil drops or heavy metals from the emulsions. Additionally, biological process such as an anaerobic thermophilic fluidized bed reactor (Perez et al., 2007) was also found to be an effective method for the treatment of cutting oil wastewater. Some

other treatment processes for this kind of wastewater, however, will be described later in Table 2.2.

2.3 STOKE'S LAW

The terminal settling or rising velocity by the gravitational separation process of a small spherical particle or droplet, which corresponds to the flow in the laminar zone (Re < 1), can be explained using Stoke's equation as shown below (Aurelle, 1985):

$$U = \frac{\Delta\rho.g.D_p^2}{18.\mu_c} \quad (2.1)$$

Where U is the terminal velocity of the dispersed phase particles;

$\Delta\rho$ is the difference of the densities of dispersed and continuous phases;

g is the gravitational acceleration;

D_p is the diameter of the dispersed phase particles;

μ_c is the viscosity of the continuous phase.

In this study, the dispersed phase comprises oil droplets and water contaminated with oils make up the continuous phase.

Regularly, the most common process for the separation of the dispersed phase from the continuous phase, particularly in an oil-in-water emulsion, is decantation. However, this technique still has limitations to dealing effectively with the small oil droplets due to the large separation area and long residence time that it requires.

According to the volumetric flow rate equation (Q = AU), with a constant flow rate, the increase of terminal velocity can lessen the size of a separating area. From Stoke's law, four main methods have been exhibited to enhance the terminal velocity:

1. The increase of the continuous phase temperature (a thermal process) to decrease its viscosity (μ_c).

2. The increase of the density difference between the dispersed phase and continuous phase ($\Delta\rho$), e.g., a floatation process.

3. The increase of gravitational acceleration (g), e.g., a hydrocyclone process.

4. The increase of the oil droplet size (D_p), e.g., a coalescing process.

2.4 OILY WASTEWATER TREATMENT

Recently, a large number of industrial processes have generated oily wastewater, which has to be properly managed to meet legislative and environmental requirements. Several effective treatment methods have been used for the treatment of oily wastewater. However, it is important to primarily consider the manners in which the oil-water are mixed and the oily wastewater characteristics—i.e., the oil proportion, oil conditions (free, dispersed or emulsified), and the amount of other contaminants—before determining an appropriate method.

The following are significant factors that have to be considered when selecting oil separation processes.

- Oil quantity in the wastewater
- Size of dispersed oil droplets in the wastewater
- Use of surfactants or emulsifiers
- Specific gravity of the oil
- Specific gravity of the wastewater
- Temperature of the oily wastewater
- Concentration of suspended compounds in the wastewater

Table 2.2 *Oily wastewater treatment processes*

Method	Advantages	Limitations
Gravity separation	- can remove suspended solids, free oil and dispersed oil in water - a simple and economical process	- a large volume decantation or sedimentation tank is required - flow velocity needs to be low - cannot treat dissolved and emulsion oil
Chemical process	- can be used as an effective primary treatment process - can deal with a high amount of suspended solids	- chemical sludge is produced
Flotation	- can remove suspended solids and dispersed oil - oil emulsion can be treated when some chemicals are added	- high energy consumption - chemical sludge is produced
Filtration	- can remove suspended solids - free oil, dispersed oil and emulsion oil can be treated	- needs a backwash process to clean the filter
Centrifugal separator	- high separation efficiency - flexible to use and a small area is required - can be used with a very high flow rate	- high initial investment and operating cost
Hydrocyclone	- inexpensive and very simple to operate	- a couple of hydrocyclones are required to attain effective separation

Coalescence	- all types of oil can be removed, except for soluble oil	- needs a primary treatment - media clogging problem
Biological process	- low excess sludge production - low energy consumption - high stability and efficiency	- an oil proportion in the wastewater should be low (less than 5%)
Thermal process	- can increase Brownian's motion in the system, leading to microdroplet conglomeration	- high energy consumption - a preliminary destabilization process is required
Membrane process	- can treat all types of oil, depending on the membrane pore size - no need for chemical additives	- needs a primary treatment - membrane fouling problem - needs frequent cleanings
Incineration	- low operation cost and easy to manipulate	- not suitable for heavy oily wastewater
Electrochemical or electrostatic process	- high efficiency and easy to control - requires a short operating time and small operating area	- consumes a lot of electrical energy - high maintenance cost

2.5 CHEMICAL DESTABILIZATION

Chemical processes (e.g., chemical coagulation and advanced oxidation processes) are widely used in wastewater treatment, particularly for wastewater disinfection, phosphorus precipitation and particle coalescence. Furthermore, they have been developed to be applied together with several physical operations for an effective secondary treatment of wastewater.

In general, the performance of colloidal particles in wastewater will be influenced by the following factors (Metcalf & Eddy, 2004): (1) Number and size of particles, (2) Shape and flexibility of particles, (3) Surface properties and electrical characteristics, (4) Interactions between particles, and (5) Interactions between particles and the solvent. Among them, an electrical manner on the particle's surface has been considered as a parameter that most affects the interaction between two approaching particles.

Under natural conditions, the surface of colloidal particles in wastewater is generally negatively charged, which is governed by two forces: (1) the zeta potential or a stabilizing repulsive force and (2) Van der Waals force or a destabilizing attractive force. A phenomenon that promotes the colloid's stability is known as the electrical double layer as displayed in Fig. 2.5. The value of an electrical potential on the slipping plane—i.e., zeta potential (ζ)—is a key indicator used for determining the degree of particle's stability. In other words, an increase in absolute zeta potential results in higher electrostatic repulsive force, which prevents the particles from an agglomeration.

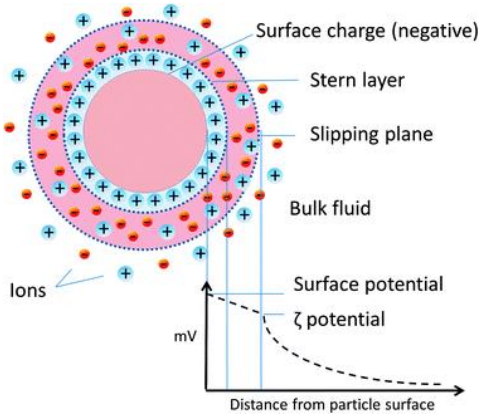

Figure 2.5 *A diagram of the electrical double layer on a charged particle*

The fundamental phenomena for the treatment of oily wastewater through chemical process, which involves directly with the emulsifying agents, can be expressed as follows (Bensadok, 2007):

- Emulsion destabilization (coagulation): the energy barrier of droplets will be declined in this mechanism, leading to the reduction of electrostatic or Van der Waals forces among the dispersed phase.
- Agglomeration of the destabilized droplets
- Oily phase separation: the coalesced oil drops will be separated from the wastewater by gravitational methods (e.g., decantation, centrifugation, flotation and filtration)

Therefore, the chemical demulsification process will be carried out in this study in order to improve the performance of oil droplet agglomeration.

2.6 MEMBRANE PROCESS

2.6.1 Theoretical Background

Recently, in the application of filtration and separation, the membrane process has become one of the most attractive techniques due to its high efficiency, compactness and low energy consumption. Moreover, it can be employed for a wide range of separations, extending from colloidal or particulate matter to dissolved components. A key role of the membrane is to serve as a selective or semipermeable barrier that allows and retains the transportation of certain constituents. Additionally, the manipulation of membrane technology has been accepted as a potential method for treating micro-sized particles, especially the separation of emulsion drops from oily wastewater (Chakrabarty et al., 2010).

Membrane processes have been classified into various types based on the pore size, amount and type of driving force, or molecular weight cut-off (MWCO). Microfiltration (MF), ultrafiltration (UF), nanofiltration (NF), reverse osmosis (RO), pervaporation, dialysis, and electrodialysis (ED) are the most well-known types of membrane processes. In addition, a membrane system can be operated either in dead-end (through-flow) or cross-flow (tangential flow) mode according to the flow direction of the feed or wastewater.

Nevertheless, among the numerous filtration methods for wastewater treatment, UF has been extensively studied for the treatment of oily wastewater (Chakrabarty et al., 2010; Hesampour et al., 2008b; Hilal et al., 2004; Salahi et al., 2010) because of the wide range of pore sizes, including its high potential to deal with

micro-droplet sized oily emulsions. This study thus focuses on UF operated in the cross-flow mode, which is described in the following part.

2.6.2 Ultrafiltration (UF)

2.6.2.1 Characteristics

UF membrane is generally considered as an anisotropic structure limited by the pore size range of 10 to 1000 Å (i.e., 0.001 - 0.1 μm). It normally is composed of two layers: (1) a finely porous surface layer, which undertakes the separation and permeation, and (2) a microporous supported layer, which provides a mechanical strength to the surface layer. The molecular weight of components or solutes is used to characterize the cut-off of the UF membrane, which is commonly known as the molecular weight cut-off (MWCO).

A large number of studies have shown that the operation of UF under appropriate conditions can deal effectively with oil, even as a microemulsion. Additionally, up to 100% oil removal efficiency can be achieved by UF. Nevertheless, several parameters should be of concern to select the appropriate membrane materials. These parameters can be sorted into the following three major criteria (Rachu, 2005):

- *Membrane pore size*: The pore size should be at least 1/4 to 1/3 of the average oil droplet size; in other words, the pore size of the membrane must be smaller than the oil droplets in order to prevent oil penetration through the membrane's pores.
- *Membrane characteristics*: In general, membrane material should not respond to components in the wastewater. To separate oil from water, a hydrophilic membrane is preferable in order to avoid oil clogging within the membrane's pores.

- *Operating conditions*: Membranes should be operated under a driving force that is less than the capillary pressure (i.e., the pressure required to push oil droplets into the membrane pores). The significant factors affecting the capillary pressure are the pore size and hydrophobicity of the membrane. With careful selection, on the other hand, the maximum pressure allowed to operate the membrane is usually lower than the capillary pressure.

2.6.2.2 Concentration polarization and membrane fouling

The deposition of retained components or colloids upon the membrane surface normally leads to membrane fouling. This phenomenon has been known as concentration polarization (CP), which is the main mechanism determining UF performance. During the initial period of membrane filtration, the permeate flux immediately falls due to the formation of a cake layer caused by the effect of CP. Subsequently, flux declination becomes constant as a result of internal membrane fouling or the penetration of macromolecules through the membrane's pores. The CP is normally a reversible mechanism and can be reduced by suitable cleaning agents, whereas membrane fouling is considered to be irreversible due to the permanent adsorption of solutes within the membrane's pores. Additionally, the degree of fouling is largely dependent on three significant factors: feed characteristics, membrane characteristics, and operating parameters (Salahi et al., 2010). Therefore, UF membranes with relatively low MWCOs are commonly used to avoid the occurrence of internal fouling and acquire more sustained fluxes.

2.6.3 Cross-flow Filtration

The components of the wastewater or feed stream that can penetrate through the membrane's pores is commonly called the *filtrate* or *permeate*, while the remainder, which is obstructed by the membrane, is known as the *retentate* or *concentrate*. In cross-flow membrane filtration, the feed is fed in a tangential direction and transported parallelly to the membrane surface (see Fig. 2.6).

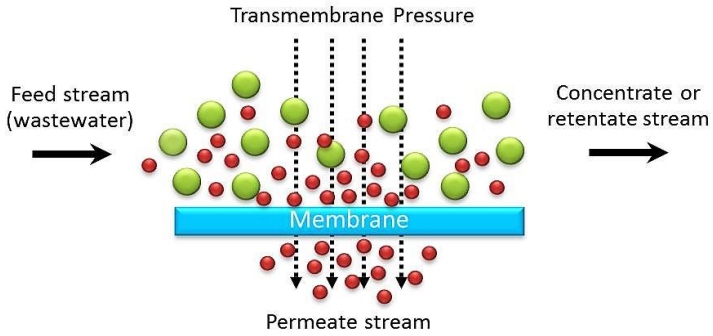

Figure 2.6 *The mechanisms of cross-flow filtration*

The cross-flow mechanism is governed by a pressure-driven force or trans-membrane pressure (TMP), which is the pressure difference between the concentrate and permeate. After a certain time of filtration, the retained components will increase, leading to a CP layer. Particle accumulation occurs until its maximum concentration is achieved, and cake layers form continuously between the CP layer and membrane surface until the steady state is acquired. However, it is widely agreed that the separation of colloidal particles by the cross-flow operation is more favorable than that of the dead-end mode, resulting from the high-shear conditions, which can diminish the effects of CP and rapid flux decline.

2.7 COALESCER

2.7.1 Principles and Performance

Coalescers have been rapidly developed and modified to improve the separation efficiency of conventional physical processes (e.g., decantation and sedimentation). Moreover, a coalescer can be effectively used as a primary method for separating two immiscible liquids (i.e., an oil-in-water emulsion). The mechanisms of a coalescer are based on Stokes' law in which the rising velocity of droplets (U) is directly proportional to the squared function of the droplet diameter (D_p^2); in other words, the oil rising velocity is most influenced by the variance of the droplet diameter. Therefore, the main function of a coalescer is to promote an enlargement of the dispersed microdroplets into relatively larger drops that can be rapidly separated from the continuous phase by ordinarily gravitational methods.

A coalescing bed, which is a layer of media or collector particles, is generally partially installed within the coalescer in order to provide a surface at which microdroplet agglomeration can occur. There are two major properties of the coalescing material (i.e., hydrophilic and oleophilic properties). The separation efficiency, however, depends on the compatibility of the dispersed phase with the coalescing media.

Coalescers can be divided into two groups according to the physical features of the media layer:

1. Granular bed coalescers (e.g., glass beads, resin or sand)
2. Fibrous bed coalescers (e.g., plastic brush, metal wool or stainless)

The approach of the coalescer equipped with a coalescing bed is that, while oily wastewater is flowing up through the media bed, oil droplets will be subject to several mechanisms and then agglomerate themselves with others into larger drops. Finally, these large droplets can be easily removed downstream of coalescing bed.

2.7.2 The Mechanisms within the Coalescer

The three major stages of a single collector inside the coalescer are described as follows (Rachu, 2005):

2.7.2.1 Transportation of microdroplets through the coalescing bed (Interception)

This stage is similar to the mechanisms of filtration, which can be categorized into three phenomena (i.e., direct interception, sedimentation and diffusion). A schematic diagram of the three transport models is shown in Fig. 2.7 and the explanation of each phenomenon will be expressed later.

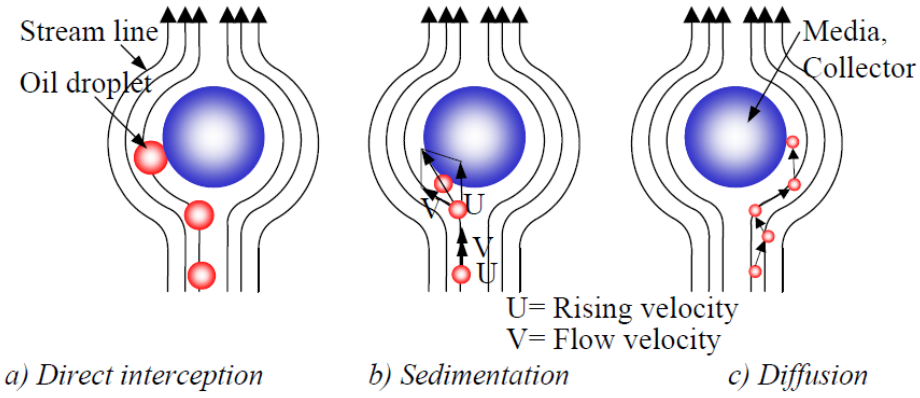

Figure 2.7 *The diagram of three transport phenomena within the coalescing bed (Rachu, 2005)*

- *Direct interception*

This phenomenon occurs when oil droplets with a diameter (D_p) flow along the stream line within the distance less than $D_p/2$ from the medium surface. These oil droplets, thus, will be caught by the medium. The efficiency of this mechanism can be calculated by Eq. 2.2, where D is the media diameter.

$$\eta_{Int} = \frac{3}{2}\left(\frac{D_p}{D}\right)^2 \tag{2.2}$$

- *Sedimentation*

According to Fig. 2.7b, the direction of the rising velocity (U) and flow velocity (V) is the same at the beginning. When droplets come closer to the medium, they undergo the resultant direction effect from the rising velocity and flow velocity, while the streamline swerves. Therefore, some droplets will occasionally collide and settle onto the medium. The efficiency of this phenomenon is shown in Eq. 2.3.

$$\eta_{sed} = \frac{U}{V} = \frac{\Delta\rho g D_p^2}{18\mu_c V} \tag{2.3}$$

- *Diffusion*

This phenomenon involves Brownian's motion of oil droplets with a diameter of less than 5 microns. This random motion can promote collisions between droplets and a medium. The efficiency of this phenomenon is shown in Eq. 2.4.

$$\eta_D = 0.9\left(\frac{KT}{\mu_c D_p D V}\right)^{\frac{2}{3}} \tag{2.4}$$

From the three phenomena described earlier, the theoretical efficiency factor of this stage (interception) can be figured out from the summation of all phenomena efficiencies as presented in Eq. 2.5. Moreover, this equation also shows that the theoretical efficiency factor definitely fluctuates with the diameter of the oil droplets.

$$\eta_{theo} = \eta_{Int} + \eta_{sed} + \eta_{D}$$

Therefore,

$$\eta_{theo} = \frac{3}{2}\left(\frac{D_p}{D}\right)^2 + \frac{\Delta\rho g D_p^2}{18\mu_c V} + 0.9\left(\frac{KT}{\mu_c D_p D V}\right)^{\frac{2}{3}} \qquad (2.5)$$

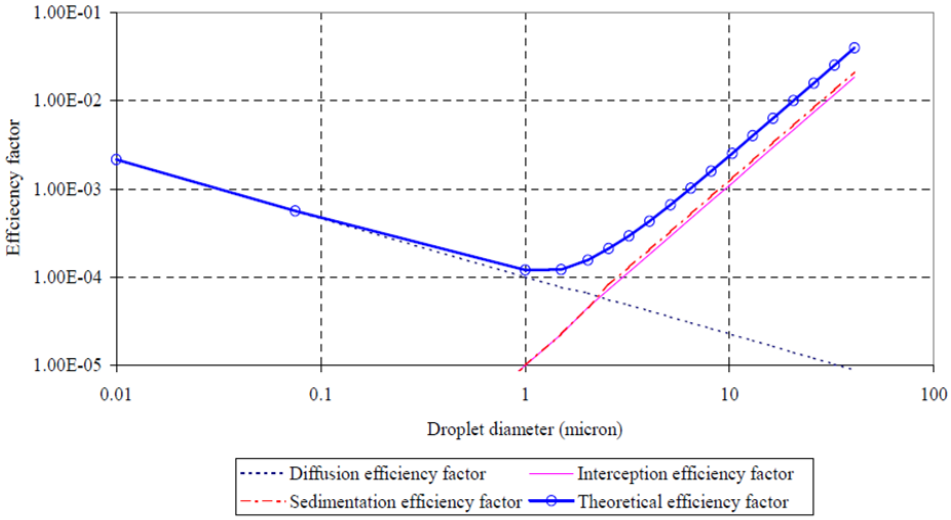

Figure 2.8 *A Relationship between the efficiency factor of each transport phenomenon and oil droplet diameter (Rachu, 2005)*

From Fig. 2.8, it can be seen that oil droplets in the range of 0.25 to 5.0 microns contribute to the minimum theoretical efficiency factor. Therefore, these droplets would theoretically be difficult to separate.

What mentioned previously is the single collector's efficiency. To adapt it with the whole media particles, a spherical single medium in a laminar flow system, as shown in Fig. 2.9a, will be considered.

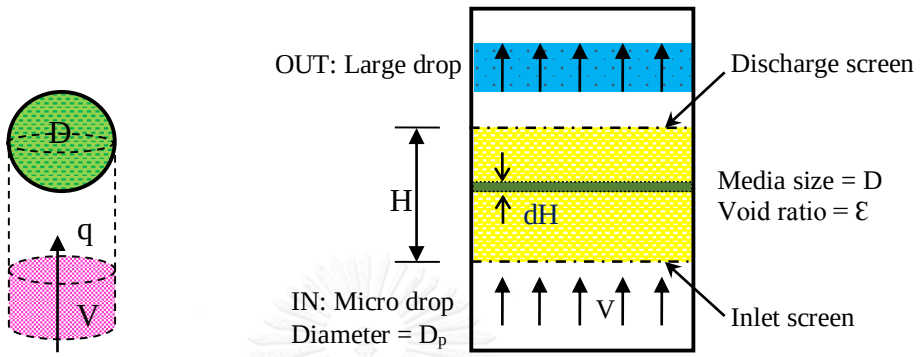

Figure 2.9 *Configuration of (a) a single collector and (b) the entire coalescing bed (Adapted from Rachu (2005))*

The portion of oily wastewater that flows past the single medium will be equivalent to the flow moving toward the projected area of the medium, for which the flow rate (q) is shown in Eq. 2.6. Consequently, there would have to be some oil droplets in this portion caught by the medium, and the amount of these droplets (c') can be calculated by Eq. 2.7, where C is the concentration of the emulsion at the inlet.

$$q = \frac{\pi}{4} D^2 V \tag{2.6}$$

$$c' = \eta_{theo} \frac{\pi}{4} D^2 V C \tag{2.7}$$

When focusing on the entire coalescing bed, a small layer of the bed (regarded as dH in height) will be of consideration (see Fig. 2.9b). The quantity of media in this thin layer can be calculated by Eq. 2.8 from the void ratio of the bed (ε), collector diameter (D), and cross sectional area of the bed (A).

$$\text{The quantity of media in the dH layer} = \frac{dH(1-\varepsilon)A}{\frac{\pi}{6}D^3} \tag{2.8}$$

In theory, the total concentration of attached oil drops in this thin layer can be determined from the number of c' and the total amount of media; nevertheless, all the droplets that are caught do not completely adhered onto the media. Thus, the number of attached drops (c") will be calculated by applying the number of intercepted drops with the probability coefficient (α) as shown in Eq. 2.9.

$$c'' = \alpha \cdot \eta_{theo} \frac{\pi}{4} D^2 VC \cdot \frac{dH(1-\varepsilon)A}{\frac{\pi}{6}D^3}, \ \alpha < 1 \tag{2.9}$$

If dC is the difference of the oil concentration before and after going through the media layer dH, Eqs. 2.10 and 2.11 can be expressed as follows:

$$-V \cdot A \cdot dC = c'' \tag{2.10}$$

$$-V \cdot A \cdot dC = \alpha \cdot \eta_{theo} \frac{\pi}{4} D^2 VC \cdot \frac{dH(1-\varepsilon)A}{\frac{\pi}{6}D^3} \tag{2.11}$$

Therefore,

$$\frac{dC}{C} = -\frac{3}{2D}(1-\varepsilon)\alpha\eta_{theo} dH \tag{2.12}$$

For the total number of adhered oil drops in the whole coalescing bed, the integration of Eq. 2.12 is needed to acquire Eq. 2.13.

$$\log\left(\frac{C}{C_o}\right) = -\frac{3}{2}(1-\varepsilon)\alpha\eta_{theo}\frac{H}{D} \tag{2.13}$$

Finally, the theoretical removal efficiency, based on the first stage of the coalescer (interception), can be represented as Eq. 2.14.

$$\eta_{d,\,theo} = \left(1-\frac{C}{C_o}\right)\cdot 100\% = \left(1-e^{-\frac{3}{2}(1-\varepsilon)\frac{H}{D}(\alpha\cdot\eta_{theo})}\right)\cdot 100\% \tag{2.14}$$

2.7.2.2 Droplet entrapment and coalescence

After the first step has been completed, some of oil droplets that are attached to the collector surface will aggregate with each other and form themselves into larger drops until they have an individual flow separate from the water stream.

As mentioned, collector particles have hydrophobic and hydrophilic properties. For a direct emulsion (O/W emulsion), however, it is preferable to use a hydrophobic (or oleophilic) material as the coalescing bed due to its ability to deal with the high loading rate of the emulsion.

2.7.2.3 Enlargement or salting out of coalesced droplets

The coalesced droplets that flow along the media will ultimately rise to the top of the bed. In the case of a good coalescing performance, the oil droplets will form and leave the bed with a diameter of 2-3 mm or more, depending on the phenomenon happening at the bed surface. Additionally, to avoid the occurrence of oil re-fragmentation, it is preferable for the salting out surface to be made of hydrophilic material. Furthermore, the oil proportion and inlet flow velocity should not be too high.

2.8 ELECTROSTATIC COALESCENCE

An electrostatic coalescer contains an electric field to enhance the agglomeration of microdroplets, which is generally called “electrocoalescence.” In an electrocoalescer system, electrodes are equipped inside the coalescing vessel; at least one acts as a grounded electrode and the other is a charged electrode. Normally, coalescence can take place spontaneously as a result of two mechanisms (i.e., differential settling and Brownian motion). The effect from these two actions, on the

other hand, is inconsiderable when compared to coalescence from the electrostatic mechanism (Eow & Ghadiri, 2003).

Two oil droplets are prevented from agglomerating by their stability or the height of potential energy, which results from the electrostatic interactions between their surface charges (Ichikawa et al., 2006). A low external electric field, nevertheless, can be applied to reduce the repulsive double layer force on oil droplet surfaces due to the rearrangement of surface charges upon the oil droplets, as illustrated in Fig. 2.11.

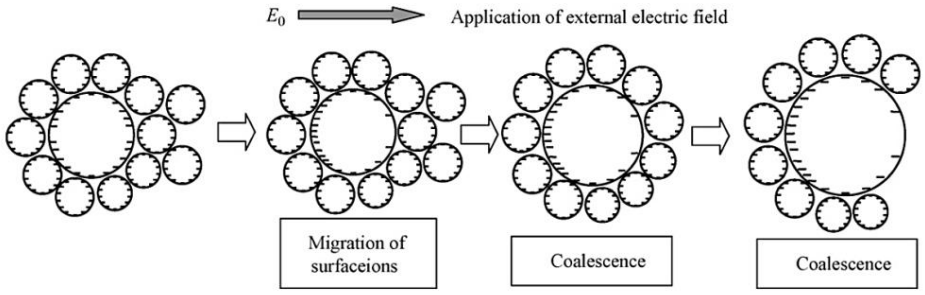

Figure 2.10 *Mechanisms of electrical demulsification on oil droplets (Ichikawa, 2007)*

The potential energy barrier on the surface of two oil droplets can be expressed as follows (Ichikawa, 2007):

$$U = \frac{\varepsilon_l \kappa \zeta^2 e^{-\kappa\omega}}{8(h+1)} \left[\frac{\left[[4(h+1)+3h(a_1-a_2)E_0\cos\eta/\zeta]\right]^2}{h+1+(h-1)e^{-\kappa\omega}} - \frac{[3h(a_1+a_2)E_0\cos\eta/\zeta]^2}{h+1-(h-1)e^{-\kappa\omega}} \right] - \frac{A_H}{12\pi\omega^2} \quad (2.15)$$

where $h = z_s e\zeta\left(s_{+,0}+s_{-,0}\right)/\left[kT\left(s_{+,0}-s_{-,0}\right)\right]$

(z_s: the surface ion valence; e: the unit charge; $s_{+,0}$ *and* $s_{-,0}$: the number densities of positive and negative surface ions; kT: the thermal energy at temperature T);

ε_l is the dielectric constant of water;

κ is the Debye reciprocal length;

ζ is the zeta potential;

ω is the separation between the front surfaces of approaching two droplets with the radii a_1 and a_2;

E_0 is the intensity of the external electric field;

η is the angle between the axis of approach and the external field;

A_H is the Hamaker constant of the droplets.

However, the external electric field applied to assist oil droplet coalescence should be adequate to fulfill the condition below:

$$|E_0| \geq \left| \frac{2\left[z_s e\zeta\left(s_{+,0}+s_{-,0}\right) + kT\left(s_{+,0}-s_{-,0}\right)\right]}{3z_s e\left(s_{+,0}+s_{-,0}\right)a} \right| \quad (2.16)$$

where a is the radius of the larger droplet.

2.9 LITERATURE REVIEW

2.9.1 Oily Wastewater

Maiti et al. (2011) investigated the removal of oil-in-water emulsions and found that the stability of oil emulsions is largely dependent on factors such as the surfactant concentration, agitation, and the mixing time. The effects of each of these parameters are described as follows:

- ***Surfactants***: The emulsion stability increases as the concentration of the surfactant increases; however, this condition is limited by the optimal surfactant concentration.

- ***Agitation***: This action provides a mechanical energy to the emulsions, causing higher shearing force and turbulence in the system. The intensity and type of agitation, moreover, can determine oil droplet size, which inversely corresponds with the emulsion's stability.

- ***Mixing time***: An increase in the mixing time leads to smaller sized oil droplets, which results in higher emulsion stability. On the other hand, this effect takes place only from the initial stage to approximately 20 minutes of stirring time and then remains nearly constant**.**

Oily waste is mostly produced from several branches of industrial processes; moreover, the oil concentration from each source is different, as illustrated in Table 2.3.

Table 2.3 *Oil and grease concentration of effluent from different industrial processes (Cheryan & Rajagopalan, 1998)*

Source of effluent	**Oil and grease concentration (mg/l)**
Metal finishing	4,000-6,000
Petroleum refinery	10-3,200
Wool scouring	1,605-12,260
Tanning waste, hide curing	40,200
Aluminum rolling	5,000-50,000
Can production (forming)	200,000
Steel-rolling mills	
- Hot rolling	20
- Cold rolling	700
- Cold rolling coolant	2,088-48,742

2.9.2 Membrane Process

Cross-flow UF membrane has been extensively applied for treating several types of industrial effluent particularly oily wastewater. A large number of researchers have investigated the effect of influential parameters on membrane performance and oil separation efficiency. Various factors, for instance, trans-membrane pressure (TMP), feed concentration, and particle size have been widely examined.

Chakrabarty et al. (2010) and Khiewpuckdee (2011) have studied the performance of UF on an oil-in-water emulsion treatment. The effects of TMP have been discussed. During the initial stage of filtration, an increase in TMP leads to a higher driving force and then increases the permeate flux; on the other hand, a sharp flux declines until an almost steady state is observed in this stage due to the effect of rapid pore blocking resulting from the size distribution of the oil droplets and membrane pores. In addition, a greater number of TMP at certain levels can cause adverse effects on the system because of the accelerated hydraulic resistance and higher particle deposition rate on the cake layer. In other words, at a very high TMP, oil droplets may be broken into smaller particles that penetrate through the membrane pores, resulting in a decrease in the permeate flux and oil rejection (%R). The results in Sarkar and De (2011) verified this. An increase of pressure from 0.22 to 0.36 MPa and 0.36 to 0.64 MPa enhanced the flux by approximately 19.4% and 12.4%, respectively. A declination of flux, however, was also influenced by membrane properties (i.e., hydrophobicity, pore size distribution, porosity and morphology). At a constant pressure, for example, the permeate flux probably increases with the higher porosity of membranes. Additionally, permeate flux as well as oil rejection also corresponds directly to the oil

concentration. In other words, an increase in the oil concentration results in a reduction in flux which differs from that of oil rejection. It can be explained that the rate of cake formation increases with the oil concentration and leads to more total resistance on the membrane surface. The effect of the oil concentration, nonetheless, contrasts with that of the oil droplet size (Chakrabarty et al., 2008; Hong et al., 1997).

Besides the mentioned operating parameters, the influence of pH, temperature and salt concentration on flux and emulsion properties have been also investigated. The result from Chakrabarty et al. (2008) showed that the effect of pH was fluctuated by different compositions of membrane, which indicated the interactions between oil droplets and membrane materials (e.g., hydrophobic or hydrophilic interactions, hydrogen bonding and electrostatic effects). In addition, the emulsion viscosity and density were found to be decreased with higher temperature, leading to an increase in droplet collision and coalescence as well as permeate flux. Lastly, the simultaneous effect of pH and salt ($CaCl_2$) was also observed as influential factors on emulsion stability regarding the change in zeta potential (Hesampour et al., 2008a).

2.9.3 Coalescer Process

The separation of oily wastewater has been studied using various treatments, particularly using physical methods. The conventional technique that has been commonly applied is a coalescer equipped with a media layer. Numerous significant operating factors of this process have been investigated, including the flow rate, feed and media characteristics, oil concentration, and pressure drop across the media.

Maiti et al. (2011) examined the effects of the oil concentration, flow rate and media height on a coalescer's performance. The treatment efficiency is observed to be improved with increased inlet oil concentrations due to the considerable number of oil droplets, which enhances the chance of coalescence. In contrast, the removal efficiency corresponds inversely with the emulsion flow rate. In other words, an increase in the feed flow rate causes the reduction of contact time within the media bed, which adversely affects the coalescence of oil droplets and leads to lower oil removal efficiency.

In addition, the media characteristics also have an impact on coalescing equipment. Coalescing performance can be enhanced by the height of the media bed, especially when it is in the range of 3 cm to 10 cm. Moreover, the stage coalescing media or step bed was found to be advantageous over the conventional one. Also, when compared with stainless steel media, media made of plastic is considered to be more suitable for separating oil-in-water emulsions due to its higher hydrophobicity (Kongkangwarn, 2009).

2.9.4 Electrostatic Coalescence

Electrostatic coalescers have been widely applied to separate oil-in-water emulsions in cooperation with an electrochemical process. This equipment is the most common apparatus used for providing electrocoalescence, which is an irreversible mechanism related to particle interactions. This application is governed by an applied external electric field that encourages the agglomeration of particles. The phenomena that seem to be the driving force of electrocoalescence include electrophoresis,

dielectrophoresis, intermolecular bonds formation, dipole coalescence and drop polarization (Shin et al., 2004).

According to Ichikawa (2007), the stability of oil-in-water emulsions has been found to be substantially affected by the external electric field during the migration of ions upon the particle surface. Elektorowicz et al. (2006) found that the intensity of applied electrical potential had a strong effect on demulsification and the aggregation rate of particles. In other words, the oil droplets were rapidly demulsified and the phase separation was improved under a relatively low electrical potential (0.5 V/cm). The rearrangement of oil droplet surface charges led to the lowering of energy barriers for oil droplet coalescence. This phenomenon occurred within the whole area between two electrodes, resulting in three separate layers in the system: a water layer, an emulsion layer, and an oil layer. Furthermore, demulsified emulsions under the electric field have to be subject to three major conditions: (1) the emulsion type must be oil-in-water; (2) the emulsified oil droplets must stay closely with each other; and (3) the emulsified oil droplets are separated due to the electrostatic force from their surface charges (Ichikawa et al., 2004). The performance of this mechanism, however, has been considered to be effective under a low applied external electric field, which corresponds to the findings of Elektorowicz et al. (2006).

However, the electrocoalescence process is also influenced by the characteristics of the electrode. The amount of electric field that must be provided to serve an adequate energy depends on the distance between two electrodes, which is limited by the effects of the fringing field or electrode edge (Eow & Ghadiri, 2002). Similarly, the performance of an electrocoalescer on palm oil wastewater treatment was investigated by Titasupawat (2009), and it was found that the distance between

electrodes (cathode and anode) largely affected the intensity of the electric field. Moreover, among three types of electrodes (i.e., aluminum, iron and graphite), aluminum plates were found to be the most favorable material. Additionally, the application of electrocoalescence with coalescing media could enhance the treatment efficiency up to 10% over that without media. The position of electrodes also had a significant effect on oil removal; in other words, the electrodes equipped over the media bed resulted in better oil separation with a 25% greater efficiency than those under the media layer.

According to several previous studies, oil-in-water emulsions can be considered to be highly stable and complicated to deal with. A number of techniques, therefore, have been developed to address this concern. Membrane processes, particularly UF, have been applied to treat and separate oily wastewater effectively; however, the problem of pore blogging or fouling usually takes place rapidly with high concentrations of oily influent and results in the need for frequent cleaning as well as increased operating cost. Moreover, the application of the coalescer apparatus has also been largely investigated in terms of its oil separation performance. Various related parameters, such as media characteristics and flow velocity, have been considered to determine the preferable conditions for operating the process. Nevertheless, its efficiency is still low when being applied as the sole treatment.

As a result, this research aims to enhance the efficiency of oily wastewater treatment and separation by combining the coalescer with cross-flow UF. Each process will be independently investigated before conducting the combined processes. Functional manners of the coalescer, for instance, separation kinetics as well as removal efficiency, will be taken into concern for determining the optimal conditions.

Subsequently, the factors affecting membrane performance (i.e., TMP, temperature and pH), including fouling mechanisms will be considered. Also, the application of chemical and electrical approach will be provided in order to improve oil coalescence and phase separation. Lastly, performance of the hybrid processes will be evaluated.

CHAPTER 3

METHODOLOGY

3.1 AN EXPERIMENTAL FRAMEWORK

The overall experimental framework in this study is displayed as follows:

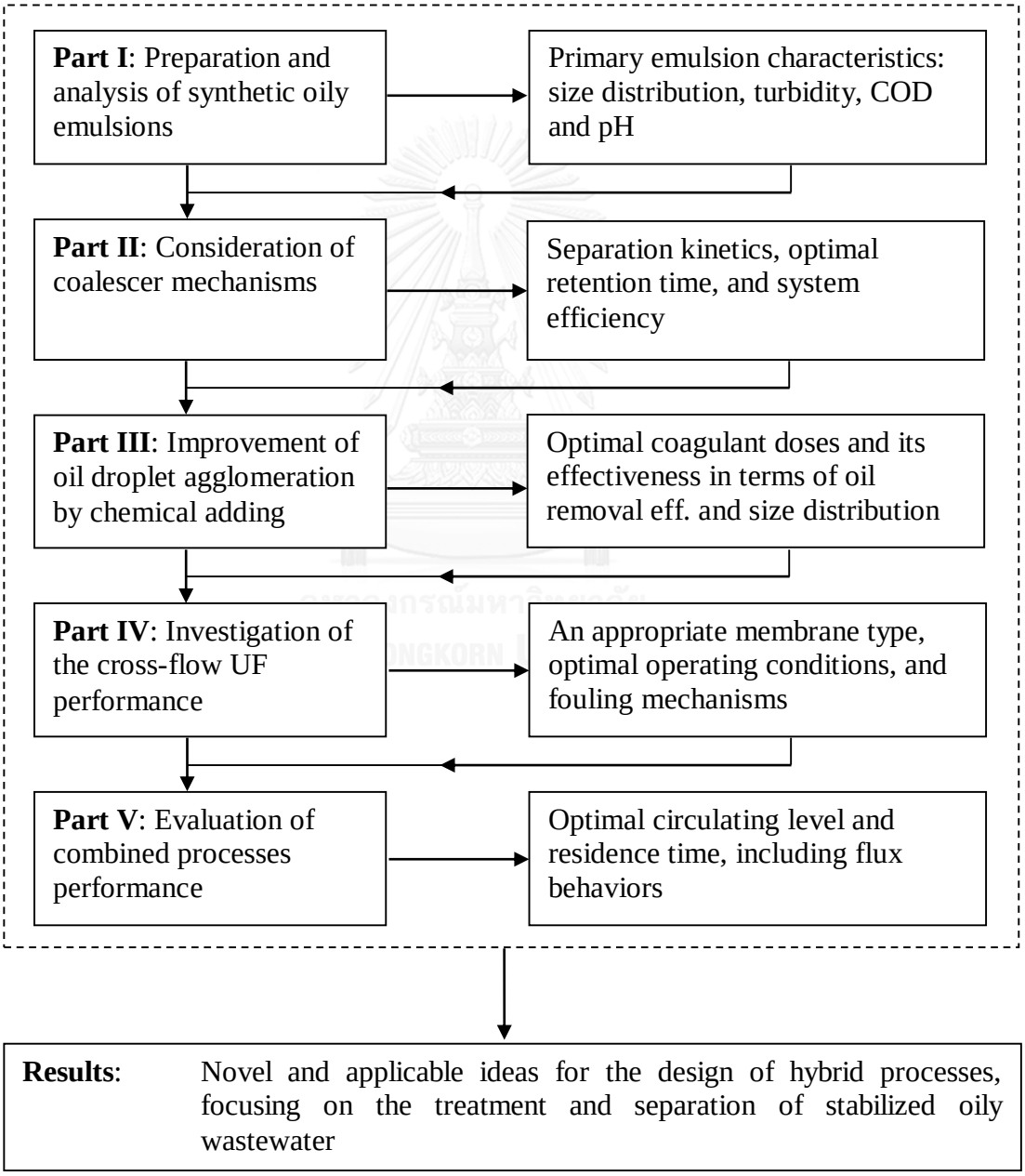

Figure 3.1 *Experimental framework*

3.2 EXPERIMENTAL SCHEMATIC

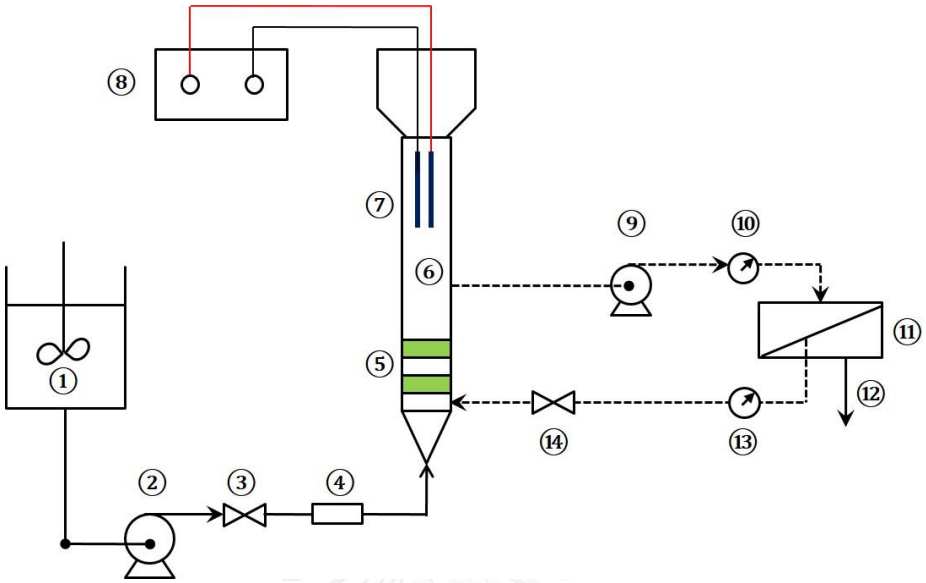

Figure 3.2 *An experimental set-up diagram*

The experimental setup in this study is illustrated in Fig. 3.2. The arrangement of materials was divided into four sections: emulsion preparation, media coalescer, electrostatic coalescence, and membrane filtration. A destabilized cutting oily emulsion was prepared in the feed tank (1) and then fed to the coalescer (6) by the centrifugal pump (2), at which the flow rate was controlled by the globe valve (3) and flow meter (4). After the influent passed through step-bed media (5), the coalesced oil droplets would raise and being demulsified by the aid of an electric field (i.e., electrodes (7) and DC power supply (8)), leading to further agglomeration. Later, the coalesced oil droplets would accumulate and float on the upper side of the coalescer (i.e., a decantation tank). The sample was kept in the reactor for a certain time and then pushed into the cross-flow membrane module (11) by the magnetic gear pump (9), in which the pressure gauges (10&13) and globe valve (14) were also provided to control

pressure drop across the membrane. Finally, the concentrate would be circulated into the coalescer, while the permeate (12) would be collected in order to analyze oil removal efficiency of the process.

3.3 MATERIALS

- **Apparatus**

1. The coalescer equipment made of transparent acrylic glass in cylindrical shape with diameter and height of 10 cm and 120 cm, respectively. The upper side of this column was served as a decantation tank with 25 cm in diameter and 30 cm in height as shown in Fig. 3.3

Figure 3.3 *The configuration of coalescer column*

2. Tubular coalescing media made of polypropylene (PP) with the diameter and height of 5 and 10 mm, respectively

Figure 3.4 *The tubular coalescing media*

3. A two-step media container made of stainless steel with 9 cm in diameter and 15 cm in height. The lid of this container is also used as the salting out device, which is illustrated in Fig. 3.5a and 3.5b

(a) (b)

Figure 3.5 *(a) A two-step media container and (b) salting out device*

4. Emulsion storage tank
5. Membrane module (Nitto Denko C-10T test cell) with filtration area of 60 cm^2

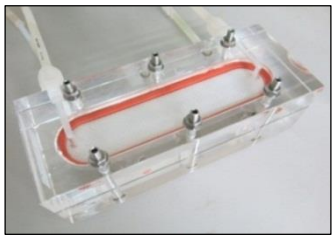

Figure 3.6 *Membrane module with cross-flow operation*

6. UF flat sheet membranes, preserving in DI-water at temperature of 4 °C

Table 3.1 *Characteristics of the membranes used in this study*

Membrane type	Parameter			
	Pore size (μm)	**pH**	**Pressure (bar)**	**Hydrophobicity**
Polysulfone (PSU)	0.020	2-12	1-10	hydrophilic
Polyethersulfone (PES)	0.005	2-12	1-10	hydrophilic

7. Magnetic gear pump purchased from Iwaki Co., Ltd., Japan with the maximum pressure and capacity of 0.55 MPa and 2.4 l/min, respectively

Figure 3.7 *The magnetic gear pump used in cross-flow UF*

8. Pressure gauge with the capacity of 0 - 0.5 MPa
9. Centrifugal pump
10. Globe valve
11. Magnetic stirrer bar
12. Turbidimeter (TURB 350 IR, WTW, Germany), providing the measurement in the range of 0.2 to 1000 NTU

Figure 3.8 *A turbidimeter*

13. Hot air oven

Figure 3.9 *An oven used for water evaporation*

14. Digital hotplate stirrer purchased from Thermo Scientific

Figure 3.10 *A digital hotplate stirrer*

15. DC Power Supply (Model S303E: 0-30 V; 0-3 A)

Figure 3.11 *A DC power supply machine*

16. Aluminium plates with effective area of 100 cm^2 (4 cm in width and 25 cm in height)

Figure 3.12 *Electrode plates made of Al*

17. COD Test equipment set
    - Hot air oven 600, Memmert (temperature range of 150 ± 2 °C)
    - Test tube (16 × 150 mm in size) with Tetrafluoroethylene (TFE) cap
    - Volumetric flask
    - Cylinder
    - Pipet
18. pH meter (PH-200, HM Digital, Inc., USA)

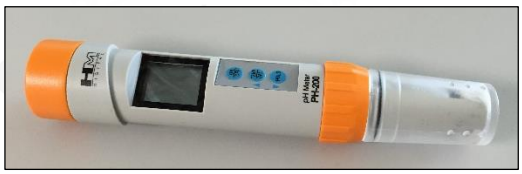

Figure 3.13 *A pH meter*

- **Reagents**

1. Cutting oil, Castrol Cooledge BI, purchased from BP-Castrol (Thailand) Co., Ltd.

Table 3.2 *Physical characteristics of the cutting oil used in this study*

Concentrate	
Appearance	Clear blown liquid
Mineral content (%wt)	More than 60
Density @ 30 ºC	0.882
Viscosity @ 25 ºC (cps)	9.13
Surface tension (mN/m)	47.02
Emulsion	
Appearance	Milky emulsion
pH (5% concentration)	9.5

2. Deionized Water (DI-Water)
3. Calcium chloride ($CaCl_2$)
4. COD test chemical agents:
   - Standard Potassium Dichromate digestion solution ($K_2Cr_2O_7$)
   - Conc. Sulfuric acid (H_2SO_4)
   - Silver Sulfate (Ag_2SO_4)
   - Ferrous Ammonium Sulfate (FAS)
   - Ferroin indicator
5. Hydrochloric acid (HCI)
6. Sodium Hydroxide (NaOH)
7. Isopropyl alcohol (IPA)

3.4 EXPERIMENTAL PROCEDURES

3.4.1 Preparation and Analysis of the Synthetic Oily Emulsions

The oily emulsions used in this study were synthesized in various concentrations. The mixtures were made of tap water and the commercial cutting oil (Castrol Cooledge BI) by 15 minutes of 300 rpm agitating. Their characteristics, including size distribution, turbidity, COD, and pH, were then investigated in order to understand the oily emulsion's behaviors.

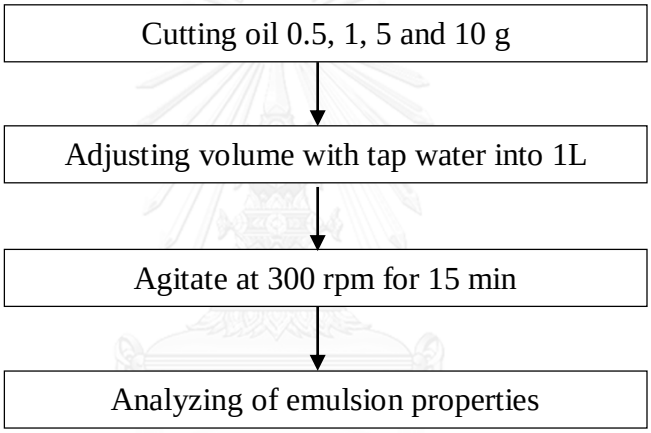

Figure 3.14 *Preparation process of the synthetic cutting oil emulsions*

Table 3.3 *Measured variables for the synthetic cutting oil emulsions*

Fixed factors	**Parameters**
Water type	Tap water
Oil type	Cutting oil
Independent factors	**Controlled parameters**
Emulsion concentration	0.05, 0.1, 0.5 and 1.0% w/v
Dependent factors	**Measured parameters**
Average oil droplet size	Sauter mean diameter (d_{32})
Emulsion properties	COD, Turbidity, and pH

3.4.2 Consideration of the Coalescer Mechanisms

An objective of this part was to study kinetics of the coalescer during the separation of cutting oil wastewater. As mentioned previously, the coalescer column used in this work is divided into two parts: the media section at the bottom and the settling section on the top. All experiments were carried out by pumping the oily influent into the lowest part of the coalescer under the flow velocity of 1.2 mm/s.

The system was primarily operated for 3 hours by the sole decantation process in order to identify the saturated time for the media coalescence, in which the turbidity was an indicator concerned in this step.

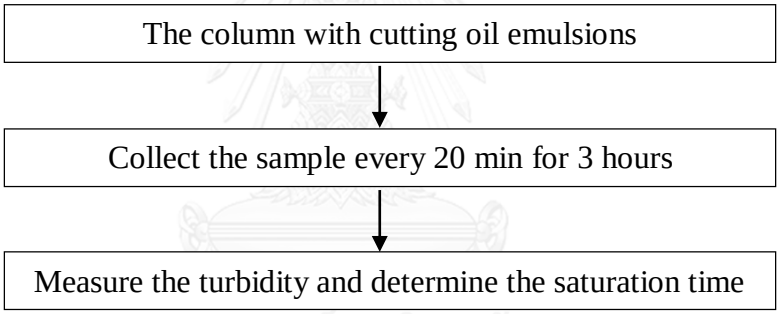

Figure 3.15 *Determination of the saturation time for the coalescer process*

Once the operating time was obtained, the coalescer was conducted using the tubular PP as the coalescing media, at which the separation kinetics and treatment efficiency were considered.

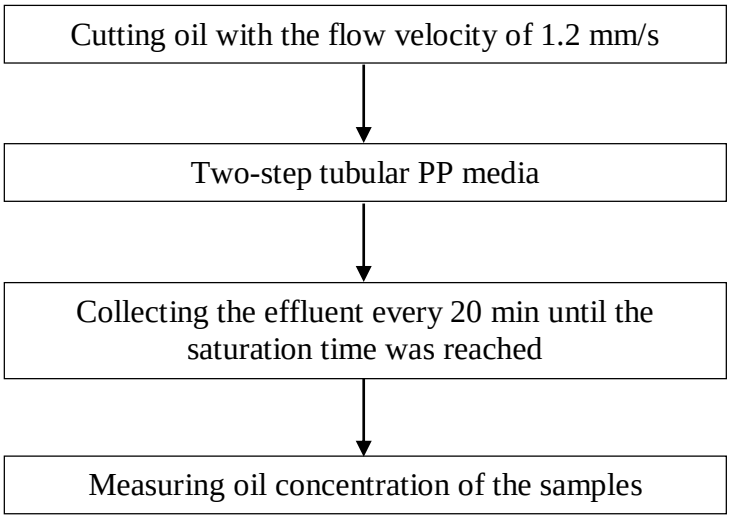

Figure 3.16 *Operating process of the coalescer equipment*

Table 3.4 *Measured variables for the coalescer performance*

Fixed factors	**Parameters**
Flow velocity	1.2 mm/s
Coalescing media	10-cm tubular PP
Independent factors	**Controlled range**
Emulsion concentration	0.05, 0.1, 0.5, and 1.0% w/v
Sampling time	Every 20 min
Dependent factors	**Measured parameters**
Effluent quality	Oil concentration

3.4.3 Enhancement of Oil Droplet Agglomeration by Chemical Destabilization Process

The purpose of this step was to promote oil droplet destabilization using a positively charged coagulant or an electrolyte, which is calcium chloride ($CaCl_2$). Each oil concentration was operated with $CaCl_2$ concentrations varied from 0.5 to 2.0 g/l, in which jar-tests method was used for determining the most optimal coagulant dosage regarding two parameters: residual oil concentration and turbidity.

Figure 3.17 *Experimental setup of the jar-test technique*

The process of jar-tests is illustrated in Fig. 3.17. All experiments were carried out in four parallel stirrers. The emulsion was poured into a beaker and stirred for 1 minute at 100 rpm. After that, the paddle velocity was decreased to 30 rpm for 30 minutes in order to control the system stability. Lastly, the system was then stopped and two hours was allowed for particle settling.

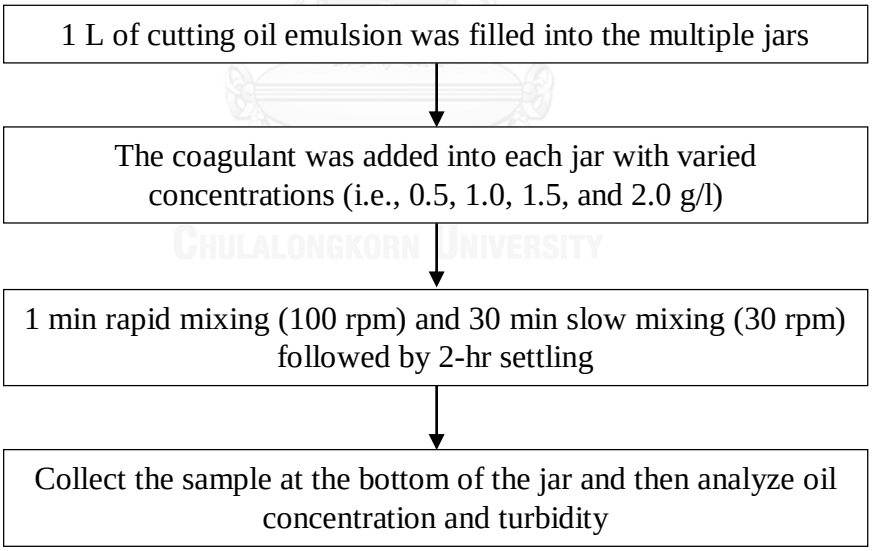

Figure 3.18 *Jar-tests procedures for the optimal coagulant dosage*

After the results from jar-tests were acquired, each emulsion concentration was provided with the optimal dose of $CaCl_2$ and then operated through the coalescer device in order to investigate oil separation efficiency.

3.4.4 Investigation of Membrane Performance

3.4.4.1 Membrane type selection

An objective of this step was to determine a type of membrane that is compatible with the cutting oil separation. Two types of hydrophilic membrane that were examined in this study were described in Table 3.1.

The examination included the following two steps:

1. Investigate and compare flux declines of each membrane type during an oil separation process.
2. Select an appropriate type of membrane that offered the highest permeate flux at the steady state of filtration.

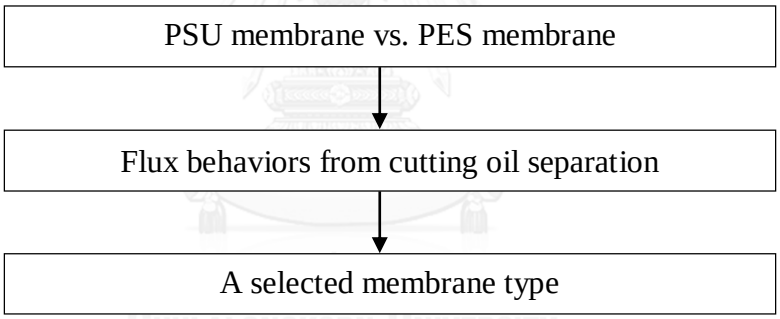

Figure 3.19 *The process of selecting a membrane type*

Table 3.5 *Measured variables for the selection of a membrane type*

Fixed factors	**Parameters**
Pure water	Deionized water
Emulsion concentration	0.1% w/v
Independent factors	**Controlled parameters**
Membrane type	PSU and PES
Trans-membrane pressure (TMP)	2, 3, and 4 bar
Dependent factors	**Measured parameters**
Flux behavior	Permeate flux

3.4.4.2 Determination of optimal operating conditions

This step aimed to find the optimal conditions of the cross-flow UF process for the treatment of oily wastewater. The operational parameters, for instance, TMP, temperature and pH, were varied in order to determine the most optimum value.

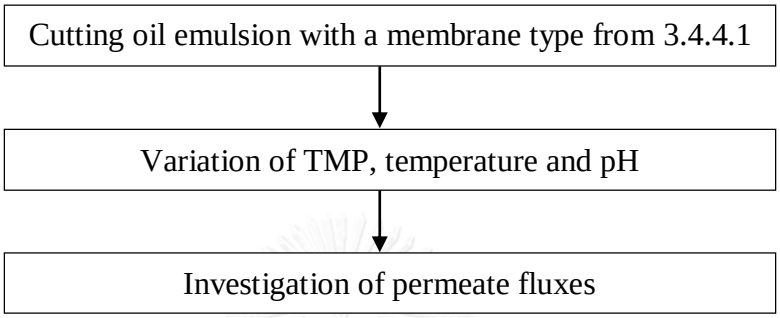

Figure 3.20 *Investigation process for optimal conditions of the UF*

Table 3.6 *Measured variables for determining optimal conditions of the UF*

Fixed factors	**Parameters**
Membrane type	From the experiment 3.4.4.1
Emulsion concentration	0.1% w/v
Independent factors	**Controlled parameters**
TMP	2, 3, and 4 bar
Temperature	16, 28, and 40 °C
pH	5, 7, and 9
Dependent factors	**Measured parameters**
Flux behavior	Flux decline rate

3.4.5 Combined Processes: chemical destabilization, coalescence, and cross-flow UF

In this part, the destabilized emulsions were governed by the collaboration between the coalescer and cross-flow UF process provided with a liquid recirculation system (see Fig 3.21). The 0.1% w/v cutting oil emulsion was used

throughout the experiments under the optimal conditions obtained from the previous steps.

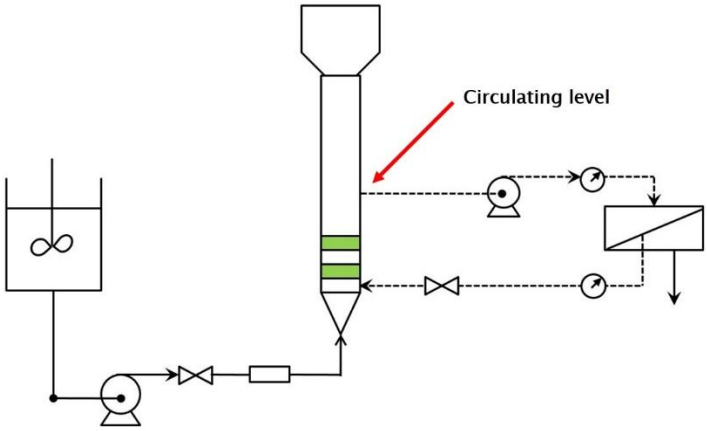

Figure 3.21 *Experimental schematic of the combined process*

3.4.5.1 Effect of different circulating levels on system performance

Once the influent reached the setting height of the reactor, the emulsion was then pumped to the membrane process. The retentate was recirculated into the coalescer under the media bed, in which the circulating lines were varied in four levels as illustrated in Fig. 3.22.

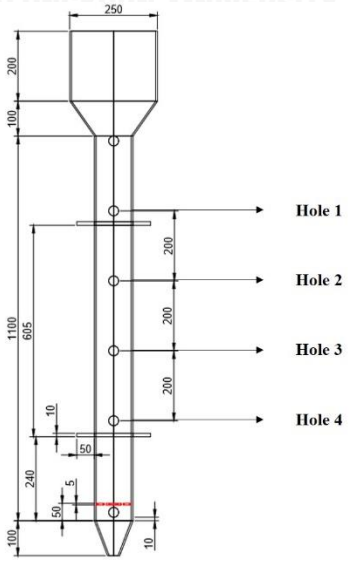

Figure 3.22 *The levels of a circulating line in the combined process*

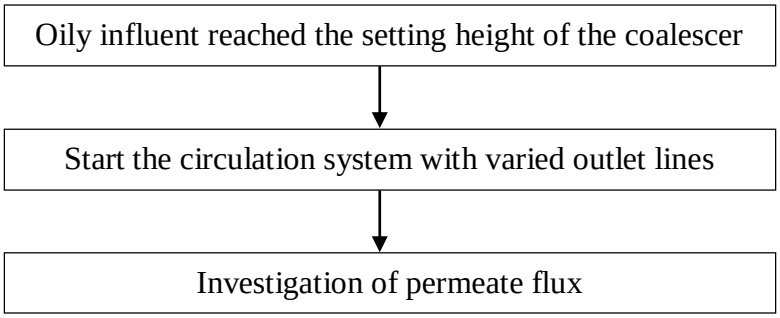

Figure 3.23 *A process of determining an optimal circulating line*

3.4.5.2 Determination of an optimal decantation time

After the optimal circulating level was attained, the combined process was investigated regarding the effect of different decantation times on flux behaviors, which focused on the coalescer apparatus.

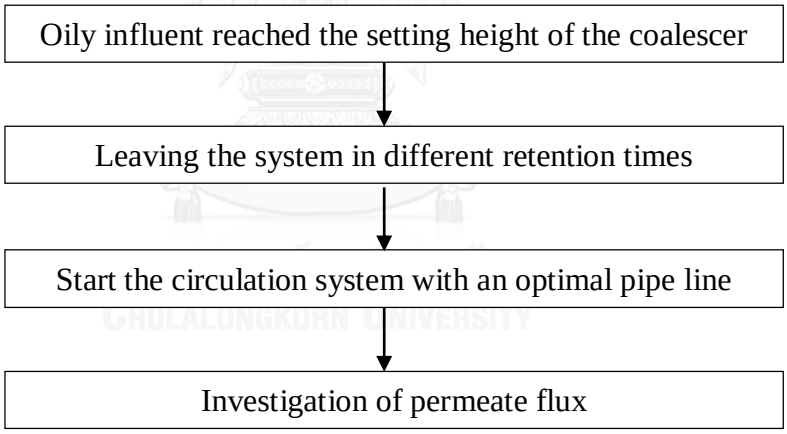

Figure 3.24 *Steps for choosing a residence time of the combine process*

Table 3.7 *Measured variables for the combined processes*

Fixed factors	**Parameters**
Circulating level	From the experiment 3.4.5.1
Independent factors	**Controlled parameters**
Retention time	0.5, 0.75, 1 and 2 hours
Dependent factors	**Measured parameters**
Flux behavior	Permeate flux

3.4.5.3 Improvement of the combined process via an electric field

An objective of this final phase was to increase the performance of the combined processes, focusing on the application of electrostatic coalescence. An external electric field was provided to the coalescer column over the media bed during the feed of oily influent, where the coalesced oil droplets could be further demulsified and agglomerate.

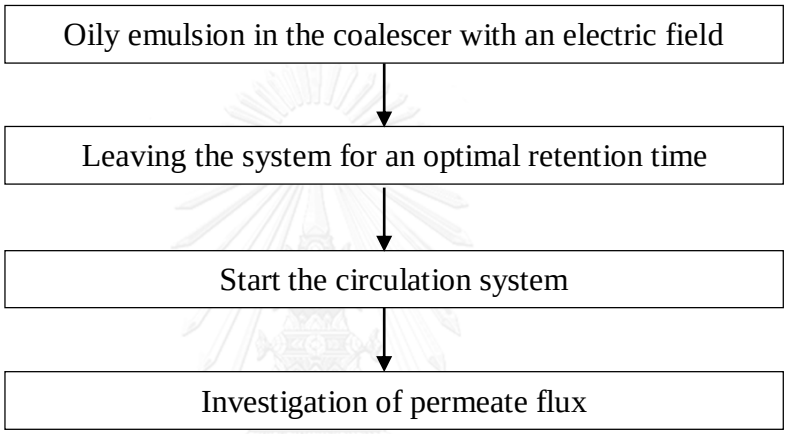

Figure 3.25 *Investigating procedures of the combined process with an E-field*

Table 3.8 *Measured variables for the combined processes with an electric field*

Fixed factors	**Parameters**
Circulating level	From the experiment 3.4.5.1
Residence time	From the experiment 3.4.5.2
Current density	10 A/m^2
Electrode gap	2 cm
Dependent factors	**Measured parameters**
Flux behavior	Permeate flux

3.4.6 Analytical Methods

3.4.6.1 Chemical oxygen demand (COD)

The COD values were triplicately analyzed by closed reflux titration method (American Public Health Association, 2005).

3.4.6.2 Turbidity

The turbidity measurement was done immediately after collecting the samples and instrument calibration was performed regularly. Moreover, a dilution of 100 times was required for the samples with the turbidity above 1000 NTU due to the detection limit of the apparatus.

3.4.6.3 Temperature

The temperature was controlled by ice addition for cooling, while heating was conducted using the digital stirring hotplate. In addition, a thermometer was immersed in the samples during experiments in order to constantly ensure the accuracy.

3.4.6.4 pH

The pH meter was frequently calibrated before the measurements and the pH of samples were adjusted by HCl and NaOH.

3.4.6.5 Oil concentration

In this work, the cutting oil existing in the system was analyzed by the high performance liquid chromatography (HPLC) under the conditions as follows:

Detector type: Evaporative Light Scattering

Flow velocity: 0.5 ml/min

Mobile phase: Isopropyl alcohol

Injection volume: 20 µL

The effluent was collected at a sampling point and then incubated at 105.5 °C for 2 hours approximately. Once the water completely evaporated, the residual oil would be dissolved in IPA and subject to the HPLC for measuring oil concentration.

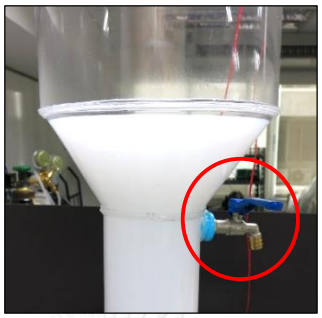

Figure 3.26 *A sampling point of the coalescer apparatus*

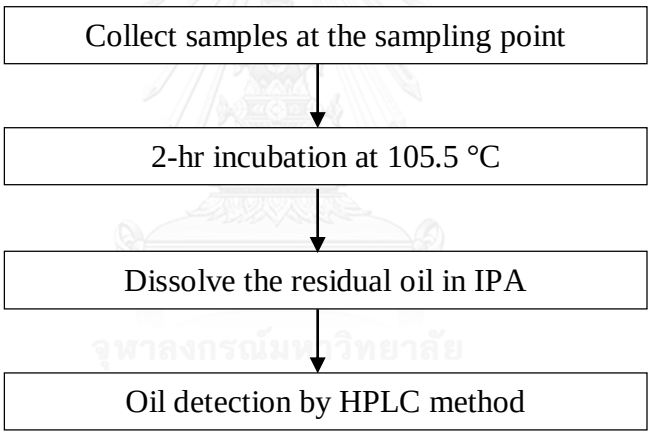

Figure 3.27 *Measurement steps of oil concentration*

(a) (b)

Figure 3.28 *The collected sample (a) before and (b) after evaporation process*

3.4.6.6 Oil removal efficiency

$$\text{Eff}\,(\%) = \left[1 - \frac{C_{in}}{C_{out}}\right] \times 100 \quad (3.1)$$

where C_{in} is the oil concentration in the influent;

C_{out} is the oil concentration in the effluent.

3.4.6.7 Permeate fluxes (J_p) as a function of time

$$J_p = \frac{V_p}{A\Delta t} \quad (3.2)$$

where V_p is the permeate volume;

A is the effective area of the membrane;

Δt is the sampling time;

3.4.6.8 Flux declination (FD)

$$FD_t(\%) = \left[1 - \frac{J_{pt}}{J_{pi}}\right] \times 100 \quad (3.3)$$

where J_{pi} is the initial permeate flux;

J_{pt} is the permeate flux at a certain time.

3.4.6.9 Membrane fouling mechanisms

In order to comprehend the interactions between oil droplets and the membrane surface, the fouling mechanism of each operating condition was predicted via mathematical models proposed by Hermia (1982) as follows:

1. Complete pore blocking model

$$\text{Ln}(J) = \text{Ln}(J_0) - K_b t \quad (3.4)$$

2. Standard pore blocking model

$$1/J^{1/2} = 1/J_0^{1/2} + K_s t \quad (3.5)$$

3. Intermediate pore blocking model

$$1/J = 1/J_0 + K_i t \quad (3.6)$$

4. Cake formation model

$$1/J^2 = 1/J_0^2 + K_c t \quad (3.7)$$

where J is permeate flux at specific time ($l/m^2 \cdot h$)

J_0 is initial permeate flux ($l/m^2 \cdot h$)

K_b is complete pore blocking model constant ($1/s$)

K_s is standard pore blocking model constant ($1/s^3$)

K_i is intermediate pore blocking model constant ($1/m^3$)

K_c is cake formation model constant (s/m^6)

CHAPTER 4

RESULTS AND DISCUSSION

The results existing in this chapter are based on the experimental sequences carried out during this course with the purpose to effectively treat and separate the stabilized oily wastewater. Characteristics of the synthetic oily emulsions are described in the first section. The following three parts are subject to the study of coalescer mechanisms, oil droplet destabilization, and cross-flow UF performance in order to individually determine their optimal operating conditions, including oil removal efficiency. Then an integration of these processes was further implemented as a combined process, in which a liquid recirculation system was also provided. Finally, the aid of an external electric field was considered in order to improve the combined process efficiency for the treatment of highly stabilized oily wastewater.

4.1 CHARACTERISTICS OF THE SYNTHETIC CUTTIING OIL EMULSIONS

In this study, the oily wastewaters were synthesized from the mixture of commercial cutting oil and tap water in the concentrations of 0.05, 0.1, 0.5, and 1% w/v. The synthetic sample exists in the form of an emulsion with the milky appearance as shown in Fig. 4.1.

Figure 4.1 *The synthetic oily emulsion*

As can be seen in Table 4.1, several parameters including COD, turbidity, droplet diameter, and zeta potential were analyzed in order to determine the characteristics of the synthetic oily emulsions.

Table 4.1 *Characteristics of the synthetic cutting oil emulsions*

Parameter	**Unit**	**Feed concentration (% w/v)**			
		0.05	**0.1**	**0.5**	**1.0**
Chemical oxygen demand (COD)	mg/l	1,456	3,081	16,154	35,765
Turbidity	NTU	911	1,822	10,165	19,655
pH	-	8.1	8.5	8.7	8.9
Sauter mean diameter (d_{32})	µm	0.354	0.327	0.985	3.048
Zeta potential	mV	- 48			

The average oil droplet size was determined using the Sauter mean diameter or surface weighted mean diameter (d_{32}) as presented in Eq. 4.1.

$$d_{32} = \frac{\sum_{i=1}^{n} d_i^3}{\sum_{i=1}^{n} d_i^2} \tag{4.1}$$

The sauter diameter is extensively applied in the system of liquid/liquid or gas/liquid dispersions and generally subjected to the shape of droplet size distribution. This parameter offers the linkage between the area and volume of the dispersed phase, which

could be further referred to mass transfer and chemical reaction rates (Pacek et al., 1998). According to Shinnar (1961), d_{32} could imply the average droplet size in two ways: (1) $d_{32} \approx d_{max}$ for break-up systems and (2) $d_{32} \approx d_{min}$ for coalescence systems; however, only the latter one was taken into account in this study.

Table 4.1 expresses that the COD, turbidity, and oil droplet size varied directly with the amount of oils existing in water, whereas the pH and oil droplet size remained almost constant for all oil concentrations. Most commercial cutting oils contain ionic surfactants which make them relatively stable. As shown in Fig. 4.2, the majority of oil droplets was in the size of less than 20 μm, which could be defined as the secondary emulsion or macro-emulsion.

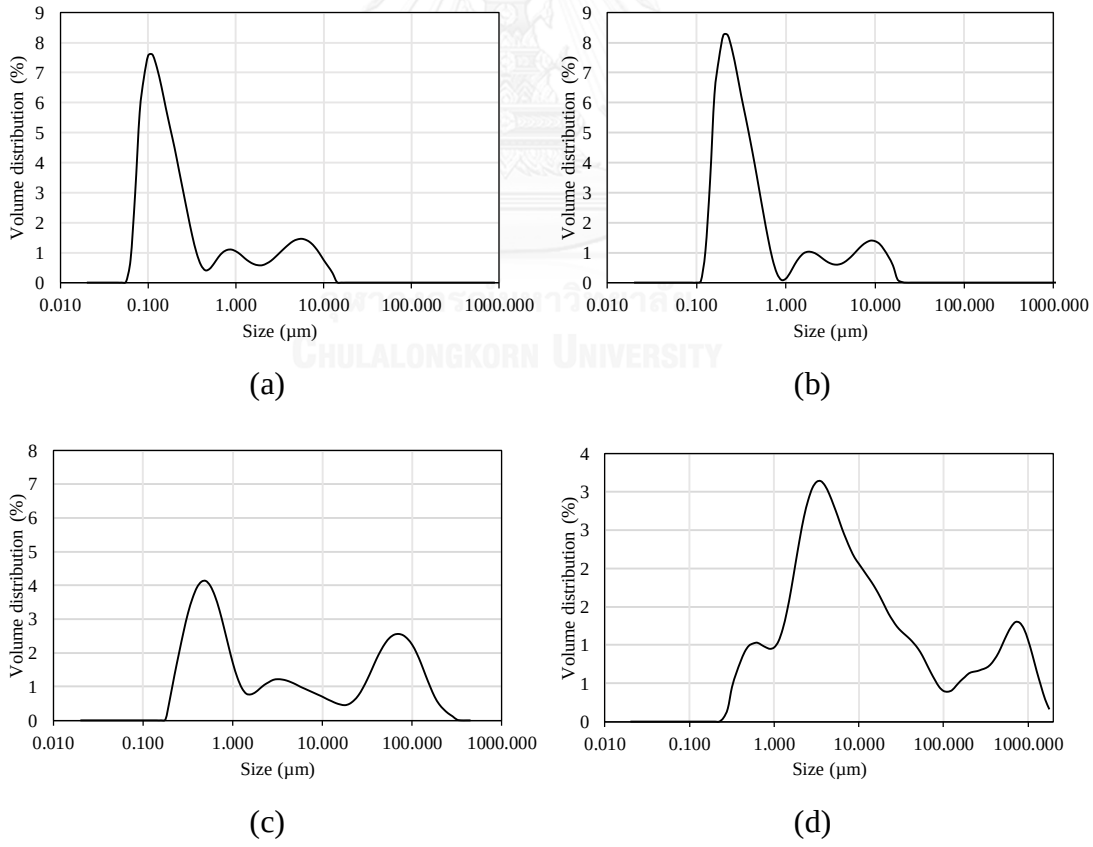

Figure 4.2 *Droplet size distribution of the synthetic cutting oil emulsions:* (a) 0.05%; (b) 0.1%; (c) 0.5%; (d) 1%

The zeta potential is also an important factor used for indicating the degree of particle stability. Regardless of an electrolyte adding, cutting oil emulsions generally have the large negative value of the zeta potential (Ríos et al., 1998b). This suggests that the emulsion is greatly electrically stabilized and well dispersed in the water; in other words, the main mechanism influencing the emulsion stability is an electrostatic repulsive force, which prevents oil droplets from agglomeration.

Besides, the calculated oil droplet velocity can be obtained from Stoke's law (Eq. 2.1) as illustrated in Table 4.2. It is clearly noticed that the oil droplet, particularly for the 0.05 and 0.1% w/v, had extremely low rising velocity and required long residence time for 1 cm rising.

Table 4.2 *Rising velocity of the synthetic oily emulsions*

Parameter	**Oil concentration (% w/v)**			
	0.05	**0.1**	**0.5**	**1**
d_{32} (μm)	0.354	0.327	0.985	11.317
Terminal velocity (cm/s)	6.8×10^{-7}	5.8×10^{-7}	5.3×10^{-6}	7.0×10^{-4}
Time for 1 cm rising	≈ 17 days	≈ 20 days	≈ 2 days	≈ 24 min

As discussed, cutting oil wastewater is relatively stable and difficult to deal with via conventional treatment processes. Therefore, an effective technique is needed in order to accomplish the satisfactory separation efficiency and environmental requirements.

4.2 CUTTING OIL SEPARATION BY THE COALESCENCE PROCESS

An objective of this section is to investigate oil separation efficiency by the coalescing technique using a coalescer device. The experiments were divided into two steps: (1) decantation and (2) media coalescer. The first investigation was done to find out the saturated operating time of the process. Then the coalescer's performance was evaluated in the second part.

4.2.1 Investigation of Oil Separation by Decantation Process

With the purpose of evaluating the coalescer's separation efficiency, it is vital to primarily observe the saturated operating time for this apparatus. This parameter was indicated by the decantation performance through the coalescer column. The turbidity of the synthetic cutting oils was measured every 20 minutes in order to investigate the equipment stability and determine the saturated time for further experiments. Afterwards, the efficiency of this process was finally observed.

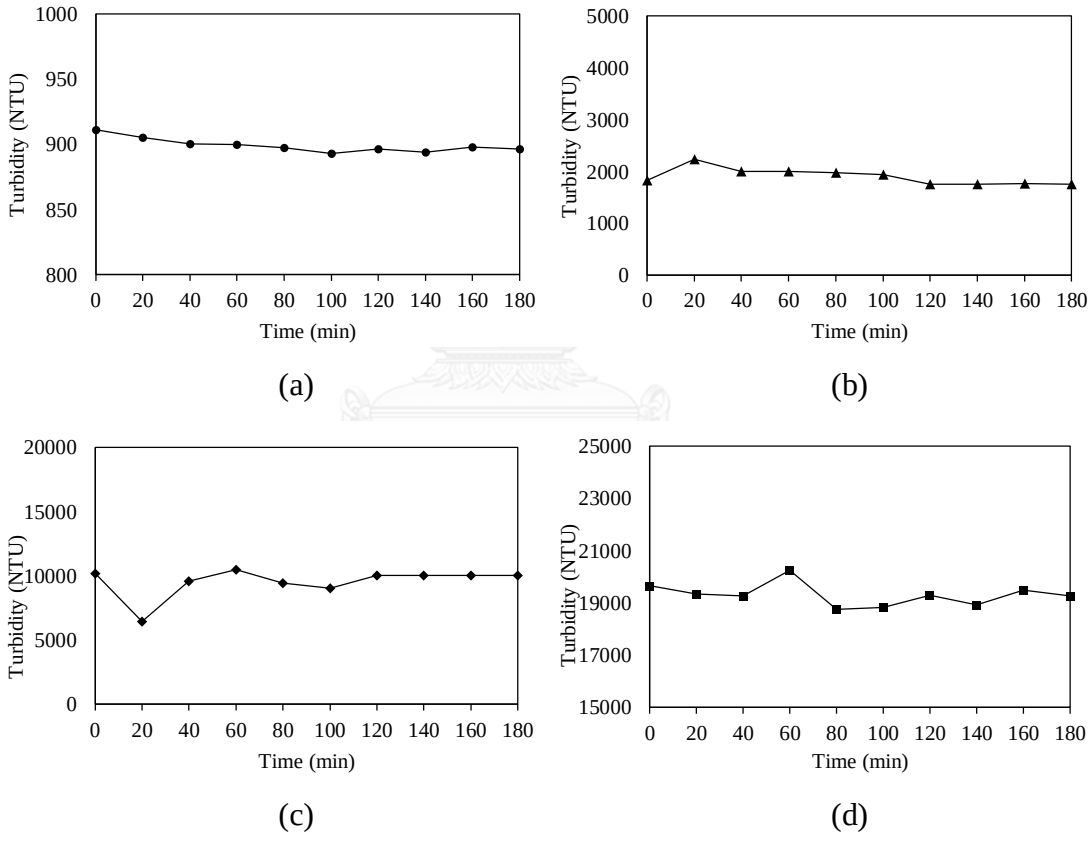

Figure 4.3 *Variations of the emulsion turbidity during the decantation process:* (a) 0.05%; (b) 0.1%; (c) 0.5%; (d) 1%

The results in Fig. 4.3 describes that the turbidity of 0.05 and 0.1% w/v emulsions were relatively constant during 3-hour operation. Resulting from less number and high stability of oil droplets, the decantation process could not provide considerable changes

within the system. On the other hand, for 0.5 and 1%, two stages of turbidity variation were clearly observed and could be explained as the following:

Fluctuated stage: this phase contained both rise and fall in turbidity. Due to the highly concentrated emulsions, the collisions in the oily stream might spontaneously occurred and thus promote coalesced oil drops, resulting in less oil droplet density and thus decreased turbidity. In contrast, an increase in turbidity might be probably affected by the dispersion of coalesced oil droplets throughout the system.

Stationary stage: the system reached a steady state, in which the turbidity did not change significantly.

As can be noticed in Fig 4.3, the turbidity became constant at approximately 120 minutes for all oil concentrations, which was considered as the saturation time of this device. Additionally, oil removal efficiencies at this point were 13.49, 14.25, 19.68 and 15.99% for 0.05, 0.1, 0.5 and 1%, respectively. It can be concluded that the decantation, which is one of the traditional treatment processes, is unable to provide acceptable efficiency for this type of wastewater. In order to fulfill this gap, the coalescing process will be discussed in the following part.

4.2.2 Separation Performance of the Coalescer Process

This part aims to investigate oil separation performance by means of a conventional coalescer, containing two separated sections: (1) a media layer and (2) a decantation tank. The experiments were carried out under the flow velocity of 1.2 mm/s with the 10-cm media height.

As stated previously, for the treatment of oily wastewater, the coalescer media should be highly hydrophobic in order to promote the agglomeration of oil droplets. An important factor frequently used for determining an appropriate medium type is the contact angle between an oil droplet and the medium surface (θ), which can be calculated from Young's equation as displayed in Eq. 4.2

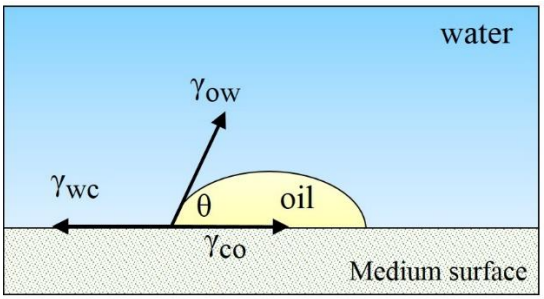

Figure 4.4 *The contact angle (θ) of an oil droplet on the medium surface in water*

$$\gamma_{wc} = \gamma_{co} + \gamma_{ow}\cos\theta \qquad (4.2)$$

where γ_{wc} is the interfacial tension between the medium and water

γ_{co} is the interfacial tension between the medium and oil

γ_{ow} is the interfacial tension between the water and oil

θ is the contact angle of an oil drop on the medium in water

The contact angle between the oil droplet and medium surface has been studied on various medium types (Chawaloesphonsiya, 2009; Kongkangwarn, 2009), for instance, polypropylene (68.37°), polyester base (87.88°), and stainless steel (90.97°). Since the polypropylene (PP) has the θ value of much less than 90°, it proposed that this material holds highly hydrophobic property (Aurelle, 1985) and offers the favorable surface for oil droplet attachment. In this study, therefore, the tubular PP was selected to apply as the coalescing media. Furthermore, a two-step

container was employed to contain the media due to its higher efficiency compared to the same height of a conventional one (Kongkangwarn, 2009).

(a) (b)

Figure 4.5 *Experimental setup of the (a) decantation and (b) coalescer*

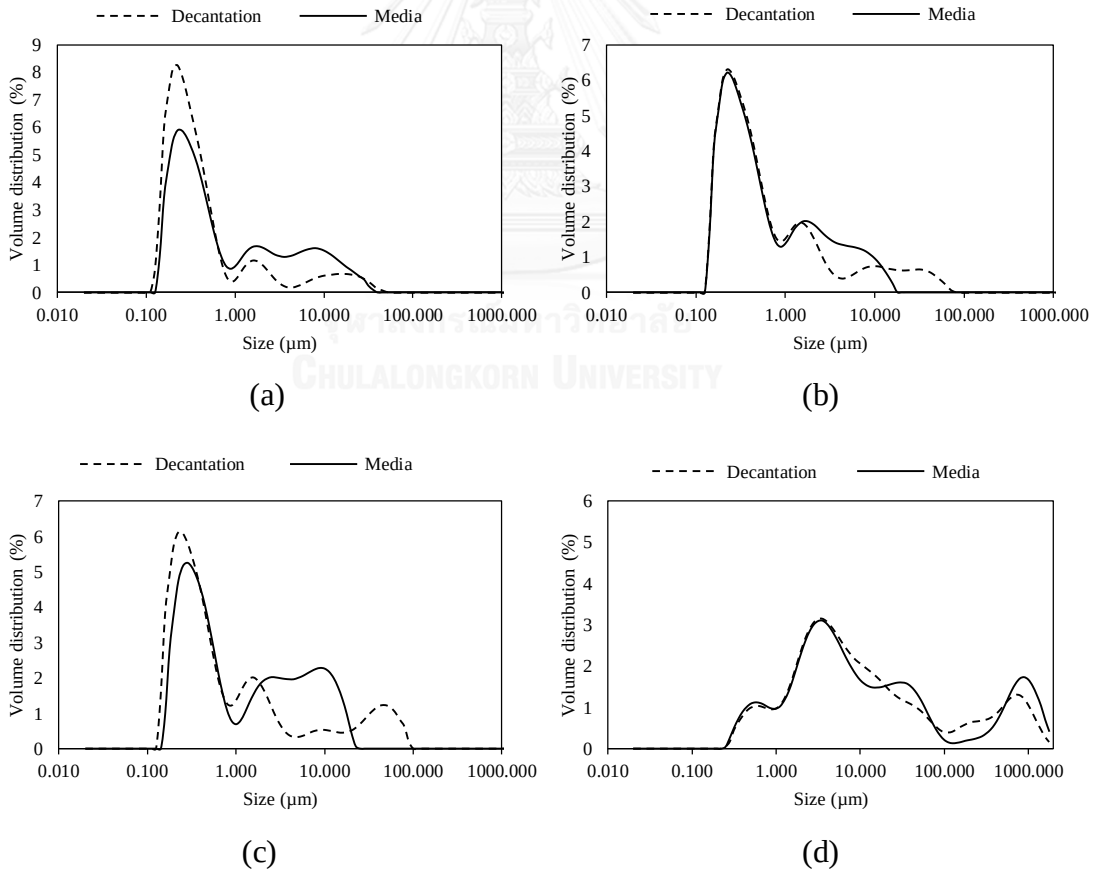

(a) (b)

(c) (d)

Figure 4.6 *Droplet size distribution of the emulsions after coalescer process:* (a) 0.05%; (b) 0.1%; (c) 0.5%; (d) 1%

Fig. 4.6 illustrates the volume distribution of oil droplet sizes, comparing between the decantation and coalescer process. It is noticed that the oil droplet sizes tended to be slightly larger after passing the media and thus possible to explain that the attachment between oil drops and coalescing media could promote oil droplet coalescence.

In addition to size characteristics, the coalescer performance was also studied in terms of separation kinetics as presented in Fig. 4.7. It is worth nothing that before conducting the experiments, the coalescing media were being soaked with oil in order to achieve its maximum effectiveness (Motta et al., 2014)

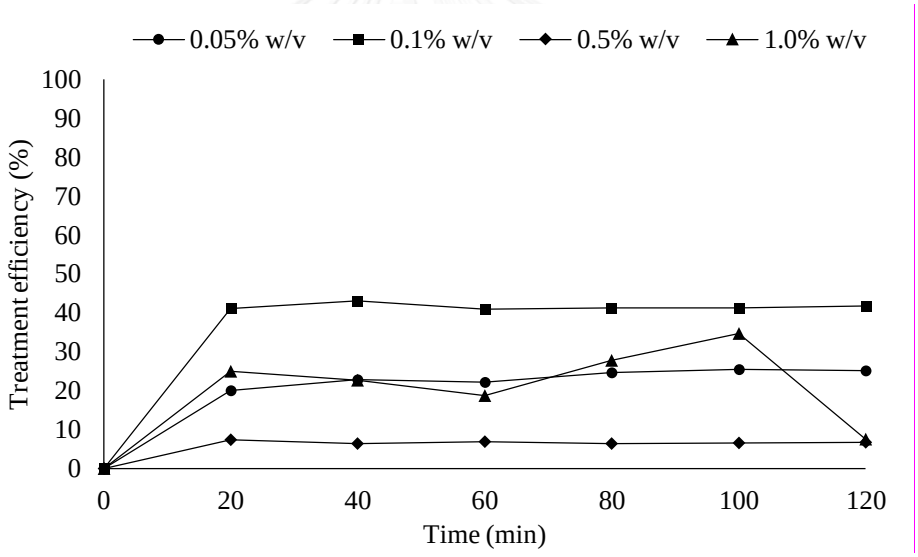

Figure 4.7 *Separation kinetics of the coalescer apparatus*

Once the system was proceeded over an extended time, the stability of the coalescer would generally be subject to the differential pressure across the coalescing bed, which influences the media permeability including system's performance. As seen in Fig. 4.7, regardless of 1% emulsion, the separation efficiency slightly fluctuated at certain time of the operation. This behaviors might probably result

from the explanation as follows: At the initial stage, there were a less number of oil droplets captured by the oil films, which primarily attached to the media surface. Therefore, the efficiency was still low in the beginning and then abruptly increased until a peak was reached. However, a mild decrease in efficiency was then found. It can be described by the effect of increased superficial velocity due to the reduction of media permeability. This occurrence probably caused an inadequate contact time within the media, resulting in an adverse effect on oil droplet agglomeration. Finally, the coalescer efficiency remained constant over time until the saturated state was achieved.

The results presented in Fig. 4.7 point out that the coalescer efficiencies were significantly different in each oil concentration. Once the system approached the saturation time (120 minutes), 25.24, 41.83, 6.76, and 7.54% of oil removal could be achieved for 0.05, 0.1, 0.5, and 1% w/v, respectively. The collisions within the coalescing bed take place regarding two mechanisms. First, the collision among oil droplets in the bulk emulsion. It corresponded directly with the results of 0.05 and 0.1%. Once the oil concentration increases, the coalescing efficiency might be improved due to higher oil droplet density and thus enhance the chance of oil droplet colliding and coalescing. Another one is the collision occurring between oil droplets in the stream and those on the media surface. This phenomenon retards oil droplet coalescence and plays an important role on the system with high oil concentrations, especially greater than 0.2% w/v (Li & Gu, 2005). Therefore, the treatment efficiency acquired for the 0.5% was found relatively low compared to others. In addition, the sharp decrease in coalescer efficiency was observed from the 1% w/v. Besides the stated reasons, it was anticipated to be the result of oil droplet detachment. Due to the highly concentrated emulsion, most coalesced oil droplets might be grasped inside the media layer. As time

passed, therefore, they might have been released and discharged with the effluent, resulting in lower efficiency.

In conclusion, the coalescer process could effectively serve as a primary treatment process for stabilized cutting oil separation. However, its efficiency was quite low when dealing with extremely concentrated emulsions (i.e., 0.5 and 1% w/v). Also, oil contents remaining in the discharge still much exceeded the industrial effluent standards of Thailand, which is below 15 mg/l (Ministry of Science, 1996). As a result, the approach of chemical addition will be studied in the next phase in order to increase the coalescer's effectiveness regarding oil droplet destabilization.

4.3 ENHANCEMENT OF THE COALESCING PERFORMANCE BY CHEMICAL DESTABILIZATION PROCESS

This section aims to investigate the effectiveness of coagulation process on oil separation performance. The experiments were conducted in jar-test apparatus under room temperature in order to determine an appropriate coagulant dose, which is calcium chloride ($CaCl_2$). This inorganic salt was preferable to use as the electrolyte throughout this study due to its outstanding manners compared to some other substances such as $Al_2(SO_4)_3$ and NaCl (Bensadok et al., 2007; Muniz et al., 2012). Afterwards, the optimal conditions attained from jar-tests would be performed to monitor their effects on the coalescer, relating to the treatment efficiency and droplet size variations.

4.3.1 Study of Optimal Coagulant Dosages for Emulsion Demulsification

Coagulation is the process involving with physical and chemical reactions. As mentioned before, the stability of suspended substances in water is normally subject to their negative surface charges. Therefore, the adding of $CaCl_2$,

which is positively charged coagulant, could promote neutralization and destabilization of the colloidal matters and then lead to particle's attraction and coalescence. Generally, the coagulation mechanisms can be controlled by numerous parameters, including water properties (i.e., density, viscosity, and temperature), the concentration of oil droplets as well as electrolytes, and the operational conditions (i.e., mixing velocity, detention time, and flow patterns). However, the significant factor concerned in this study was a relationship between the emulsion concentration and electrolyte dosage.

It is worth noting that the samples were drained from the bottom of the jar after 2-hr settling. Also, the optimal $CaCl_2$ dose was determined based on the lowest residual oil in the sample.

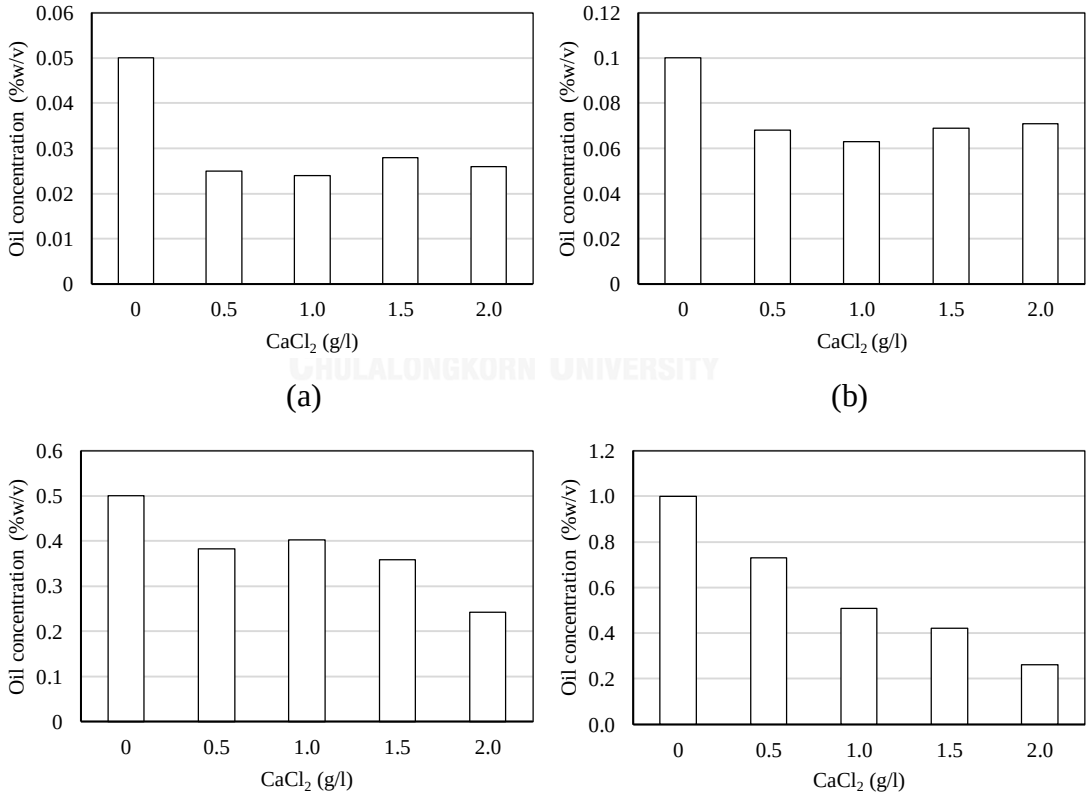

Figure 4.8 *Effects of different coagulant dosages on oil removal:*
(a) 0.05%; (b) 0.1%; (c) 0.5%; (d) 1%

The results demonstrated in Fig. 4.8 clearly reports that the chemical dosage varied directly with the oil concentration. The attained optimal coagulant doses are presented in Table 4.3. It should be noted that the effect of pH changes in each condition could be negligible due to a slightly variation compared to the beginning. The main mechanisms occurring in this process were mainly oil droplet demulsification and aggregation, which will be further discussed in the following part. In general, the turbidity of an emulsion is linearly proportional to the oil concentration or the quantity of oil droplets in the system; however, this can be altered by the effect of droplet size. Once the coalescence occurs, even in high emulsion concentrations, the droplet size become larger and the turbidity may decline resulting from a lower number of oil drops within the system (Ríos et al., 1998a). Nevertheless, the coagulation performance could be varied according to other factors such as pH, mixing conditions, and temperature.

Table 4.3 *Optimum coagulant doses for each oil concentration*

	Oil concentration (%w/v)			
	0.05	**0.1**	**0.5**	**1.0**
Coagulant dose (g/l)	0.5	1	2	2

4.3.2 Oil Droplet Size and Separation Efficiency by Coupling Coalescer with Chemical Destabilization Process

As mentioned previously, the zeta potential is a significant indicator for determining the stability of oil droplets. The addition of $CaCl_2$ would lessen the energy barriers among the dispersed phase and thus lead to droplets' coalescence.

It also should be noted that the droplet size distribution was analyzed in the oily phase withdrawn from the emulsion surface after 2-hr decantation time.

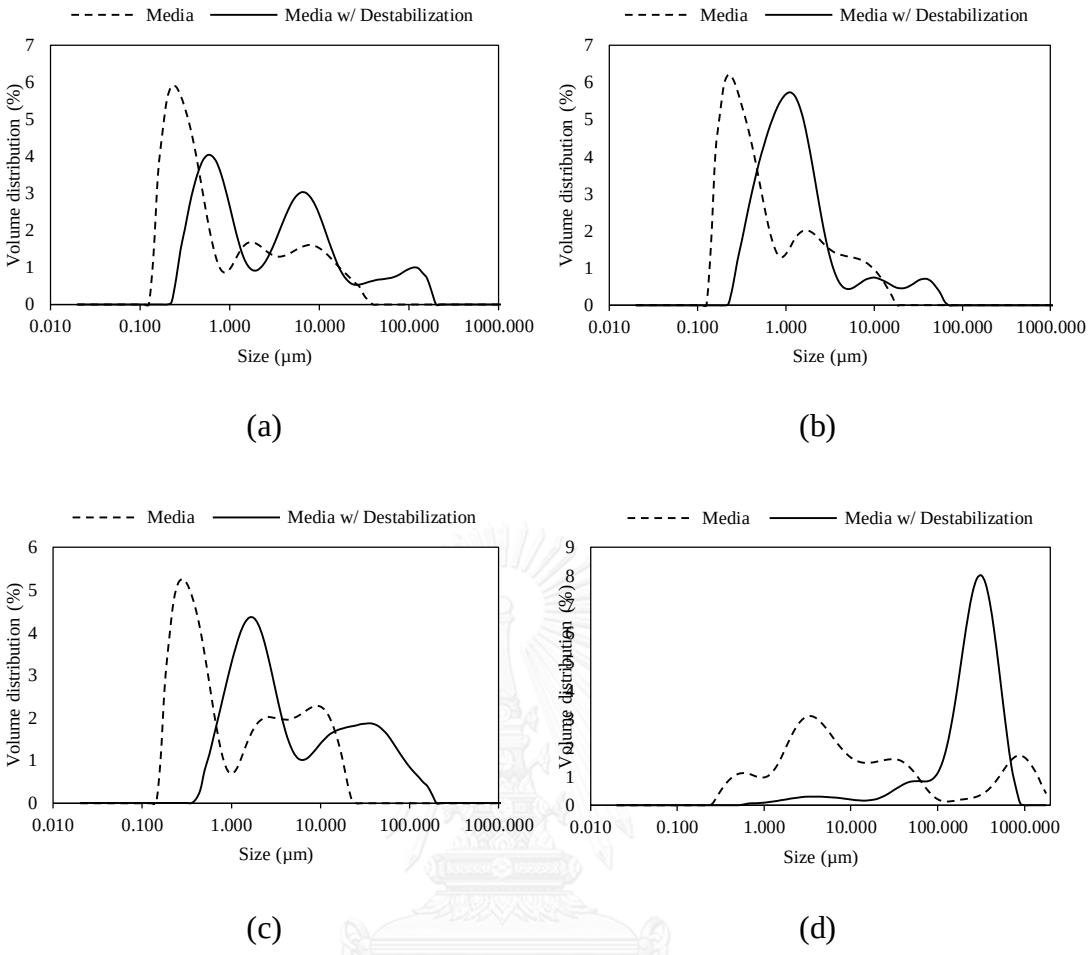

Figure 4.9 *Droplet size distribution by coupling coalescer with chemical destabilization: (a) 0.05%; (b) 0.1%; (c) 0.5%; (d) 1%*

With regard to Fig. 4.9 and Table 4.4, an increase in oil droplet size indicates that the electrolyte addition led to instantaneous aggregation of oil droplets and thus promoted the coalescer performance. The treatment efficiency achieved for 0.05, 0.1, 0.5 and 1% was respectively 42.02, 85.80, 91.65, and 67.30%, which were much higher than those of the sole coalescer process.

Table 4.4 *Oil droplet size via the coalescer after the $CaCl_2$ addition*

Oil concentration (% w/v)	**Surface weighted mean diameter: d_{32} (μm)**	
	Coalescer	**Coalescer w/ $CaCl_2$**
0.05	0.455	1.065
0.1	0.419	0.880
0.5	0.511	2.108
1	2.929	40.272

Another noticeable point from Table 4.4 is the shifted droplet size of the 1% emulsion. Resulting from an extremely high amount of stabilized oil droplets in the system, the collisions and aggregation could intensely occur, leading to a better phase separation (see Fig. 4.10). Additionally, this phenomenon can also be verified by a sharp decrease in turbidity as displayed in Fig. 4.8d.

(a) (b)

Figure 4.10 *Emulsion appearance after $CaCl_2$ addition (1% w/v): (a) during process; (b) left: over night settling; right: a sample suddenly collected from the process*

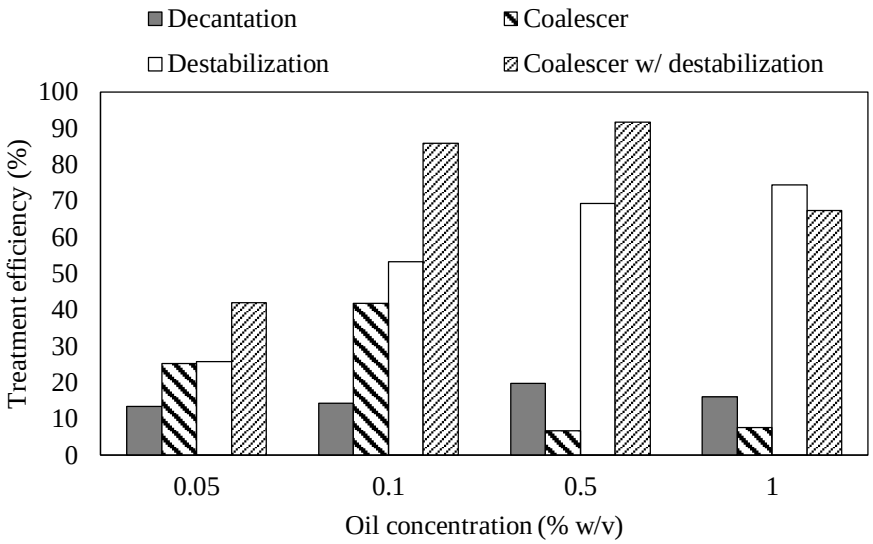

Figure 4.11 *Relationships between the oil concentration and treatment efficiency through various treatment processes*

On the other hand, as shown in Fig. 4.11, the treatment efficiency of the 1% emulsion was declined when coupling destabilization process with the coalescer. As a result of an inverse correlation between the emulsion stability and oil concentration (Muniz et al., 2012), it is possible to describe that the oil droplets formed such a diameter once they were being destabilized (see Fig 4.12b). Therefore, these coalesced droplets might have been fragmented while passing the media bed, which caused a decrease in separation efficiency.

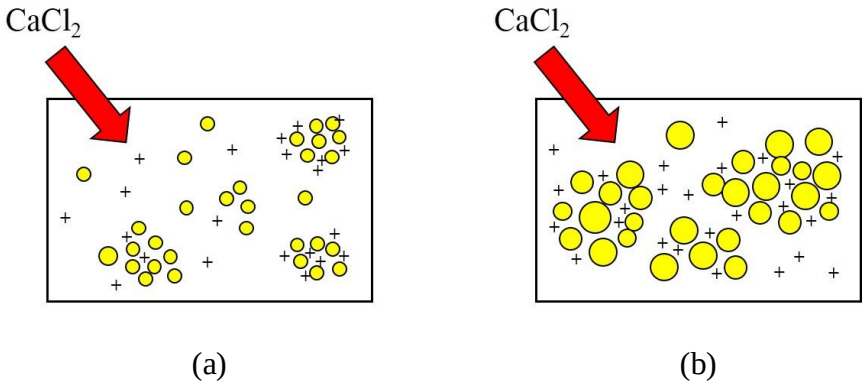

Figure 4.12 *Oil droplet coalescence after $CaCl_2$ addition: (a) 0.1% w/v; (b) 1% w/v*

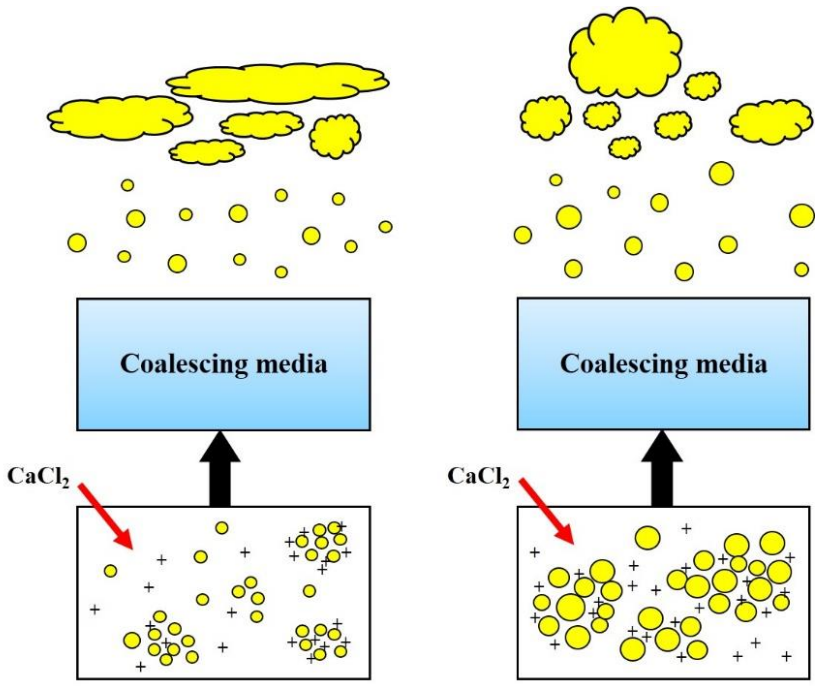

(a) (b)

Figure 4.13 *Oil droplet coalescence through the coupled process of coalescer and destabilization (a) 0.1% w/v; (b) 1% w/v*

The results in this part confirm that chemical destabilization could greatly improve the coalescer's performance in terms of droplet size and oil separation. However, a certain amount of relatively small oil droplets still remained in the system as presented in Fig 4.13. In order to accomplish a practical and effective treatment process for the stabilized oily wastewater, the application of UF technique will be considered in the following steps.

4.4 INVESTIGATION OF THE CROSS-FLOW UF MECHANISMS

This part demonstrates the characterization of factors correlating to a membrane filtration process. All experiments were conducted under the cross-flow operation mode, which is intensely employed by industries. The variation in UF performance due

to a membrane type, TMP, temperature and pH was discussed in details. Lastly, the fouling mechanisms as well as oil removal efficiency were then determined.

4.4.1 Membrane Type Selection

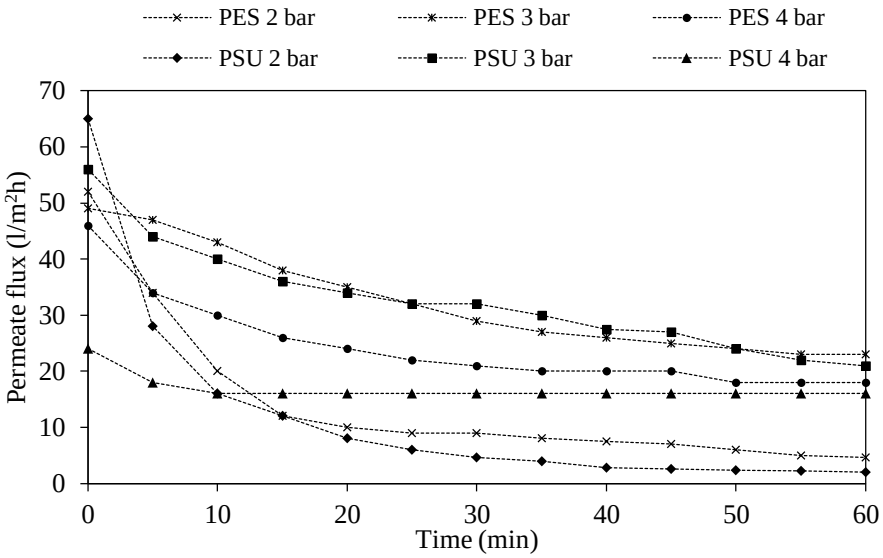

Figure 4.14 *Effect of membrane types on the permeate flux*

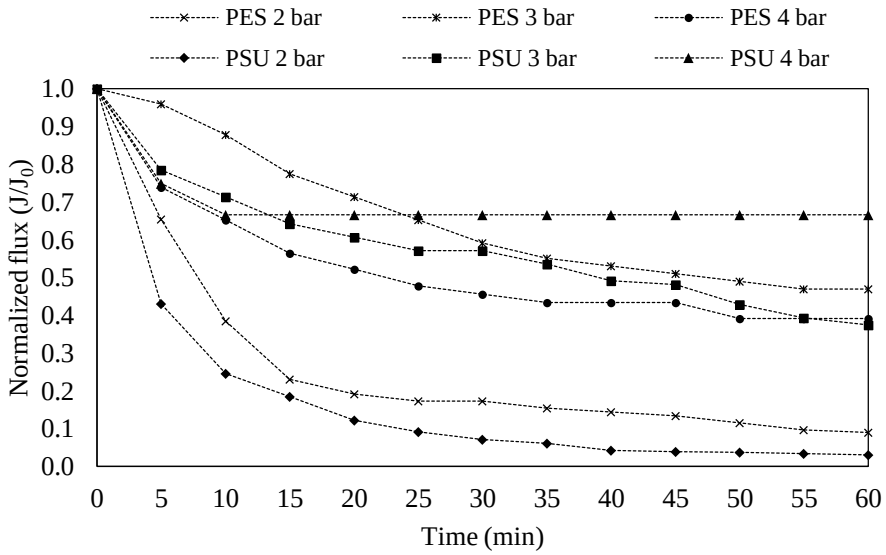

Figure 4.15 *Performance of different membrane types in terms of normalized flux*

The permeate flux as a function of time for PES and PSU membrane is presented in Fig. 4.14. The experiments were conducted under varied TMP (i.e., 2, 3, and 4 bar), whereas the oil concentration was kept constant at 0.1% w/v. In the application of UF, choosing a suitable membrane material that is compatible with the influent is a significant concern. Moreover, the filtration of oily wastewater is generally carried out with relatively hydrophilic or water-like materials in order to prevent filter's fouling.

Both PSU and PES polymer are fairly similar in structures. They contain the sulfur atom in an oxidation state, which provides them high polarity and thus the ability to deal well with hydrophobic oily emulsions. Fig. 4.14 describes that the permeate flux from all conditions tended to decrease over the initial period. Once the system approached the steady state, fluxes attained from the PES membrane were higher than those of the PSU under all TMP values. Generally, membrane characteristics can vary depending on several parameters, for instance, wettability and feed-membrane interactions (Chakrabarty et al., 2008). For this study, however, the membrane's pore appeared to be the most influential factor due to the substantially different pore size of two membranes (PES:0.005 μm; PSU:0.020 μm).

Another concern is the normalized flux decline exhibited in Fig 4.15. Whereas the lowest flux decline rate (≈ 33%) was obtained from the PSU membrane under 4 bar, only 16 l/m^{2}h of critical flux could be achieved. This might be the effect of large membrane's pore as can be supported by Hagen-Poiseuille equation as follows:

$$Q = \frac{\pi d^4 \Delta P_T}{128 \mu L} \quad (4.3)$$

where ΔP_T is the trans-membrane pressure; L is the pore length;

Q is the flow rate; d is the pore diameter; μ is the dynamic viscosity

Independent of other parameters, the feed flow rate is proportional to the fourth power of the pore diameter. Therefore, a larger pore size could lead to the accelerated membrane's fouling and thus fluxes immediately approach a stationary phase. However, the PES membrane was selected to be applied for further experiments due to its better performance in terms of an acceptable permeate flux.

4.4.2 Determination of the Optimal Operating Conditions

4.4.2.1 Trans-membrane pressure (TMP)

In this work, the filtration process was operated under a controlled pressure mode. The mechanisms generally taking place upon the membrane surface can be explained by the following schematic:

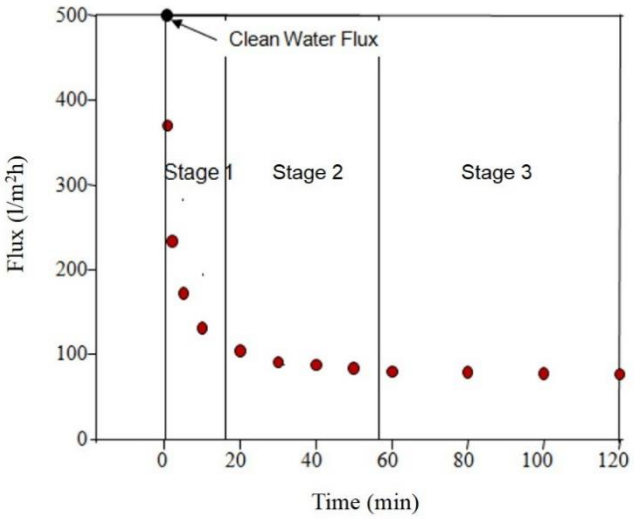

Figure 4.16 *Typical flux decline under a constant pressure mode (Yoon, 2015)*

As seen in Fig. 4.16, when the TMP is kept constant during the filtration process, three phases of flux behaviors can be observed (Yoon, 2015):

Stage 1: Rapid cake layer formation and compaction

Once the filtration starts, a relatively high initial flux is obtained in this stage due to the controlled TMP. This situation instantly enhances particle deposition rate and leads to rapid cake layer formation. Simultaneously, the cake layer gradually packs on the membrane surface, resulting in sharply flux decline.

Stage 2: Slow cake layer growth and compaction

As the cake layer grows, an increase in membrane resistance occurs and thus brings about the lowered flux. Resulting from flux decline, particle deposition rate as well as cake layer compaction are also retarded and thus the critical flux is approached.

Stage 3: Pseudo steady flux

In this stage, the membrane permeability is maintained at a fairly constant level and the particle deposition becomes insignificant. Even though the cake layer still packs gradually, it is considered as a long-term effect which could be negligible.

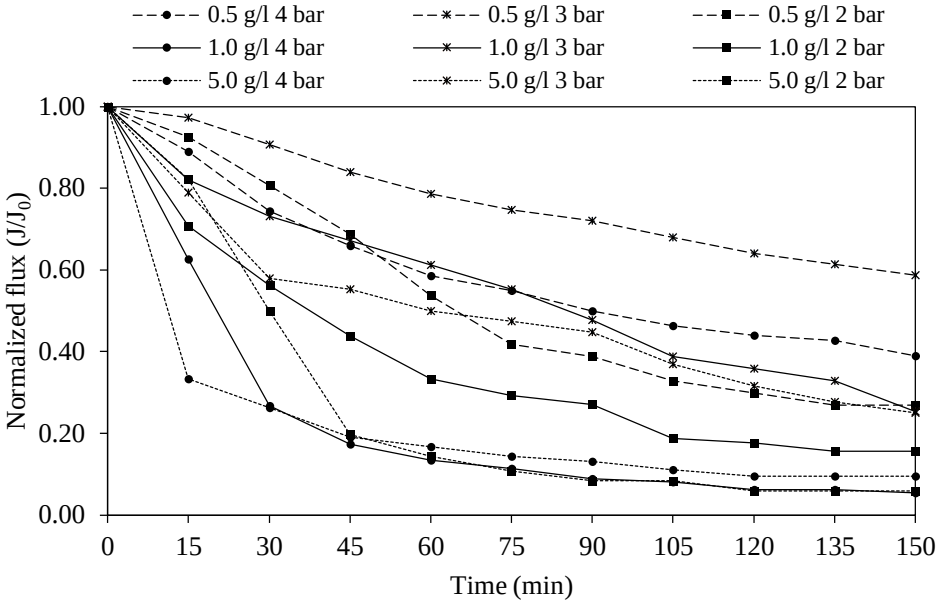

Figure 4.17 *Effects of TMP on flux decline rate*

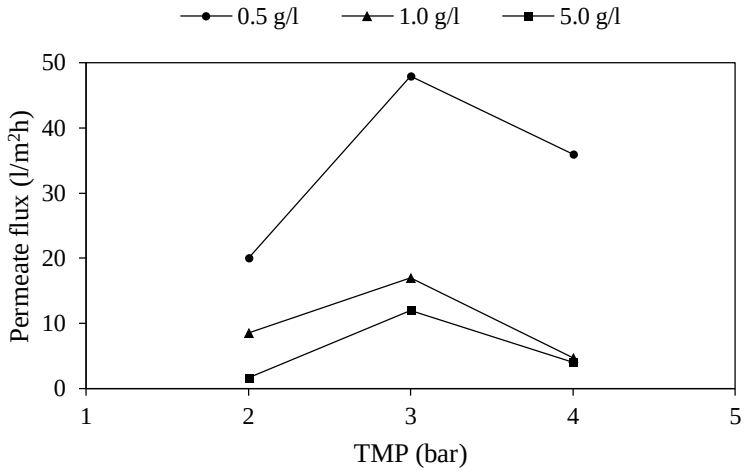

Figure 4.18 *The permeate flux of different TMP after 2-hr filtration (0.1% w/v)*

The effects of TMP on permeate flux is displayed in Fig. 4.17 and 4.18. During the filtration process, sharp flux decrease in the first hour was observed due to the rapid pore blocking or oil droplet deposition (Hong et al., 1997). Then the flux gradually declined until a steady state was reached. In general, an increase in TMP causes higher permeate fluxes as a result of a greater amount of driving force. On the

other hand, as obviously seen from the figures, the highest flux for all conditions was acquired at the TMP of 3 bar, which was considered as a critical pressure in this study. Once the TMP was raised to 4 bar, therefore, the fluxes were not enhanced any longer. An explanation is that the permeate flux could rapidly fall at a certain pressure caused by the high rate of particle accumulation and cake layer compactness on the membrane surface, which cause large hydraulic resistance and changes in flux behavior (Hong et al., 1997; Salahi et al., 2010).

4.4.2.2 Temperature

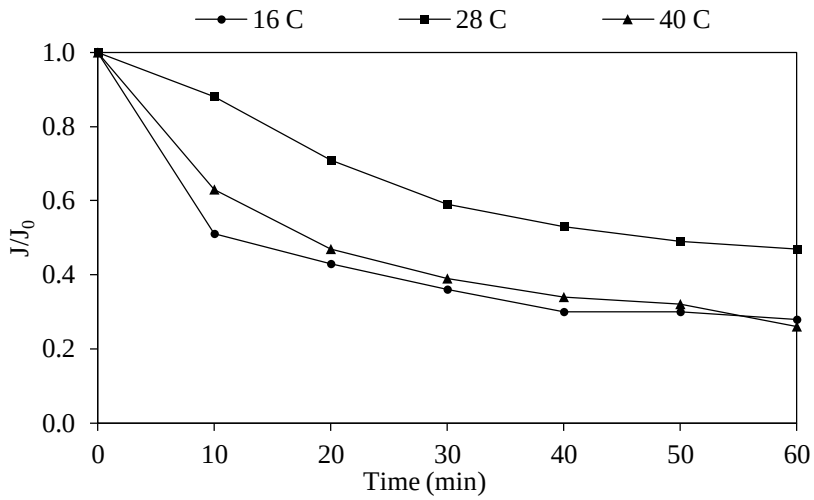

Figure 4.19 *Effects of temperature on permeate fluxes conducted with 0.1% w/v under 3 bar*

An increase in temperature generally improves the flux due to the reduction of liquid viscosity and concentration polarization. This mechanism promotes higher permeability and diffusion coefficient of liquids in the system. Nevertheless, an optimal temperature need to be specified for each treatment process (Salahi et al., 2013). The outcome illustrated in Fig. 4.19 points out that the highest flux was obtained at the temperature of 28 °C. This suggests that the emulsion properties, particularly

droplet size distribution and viscosity, might be largely affected at high temperature (40 °C). Therefore, some small oil droplets could penetrate and attach to the membrane's pores. Similarly, an oily emulsion was difficult to disperse and be separated under low temperature (16 °C) as a result of extremely high viscosity.

4.4.2.3 pH

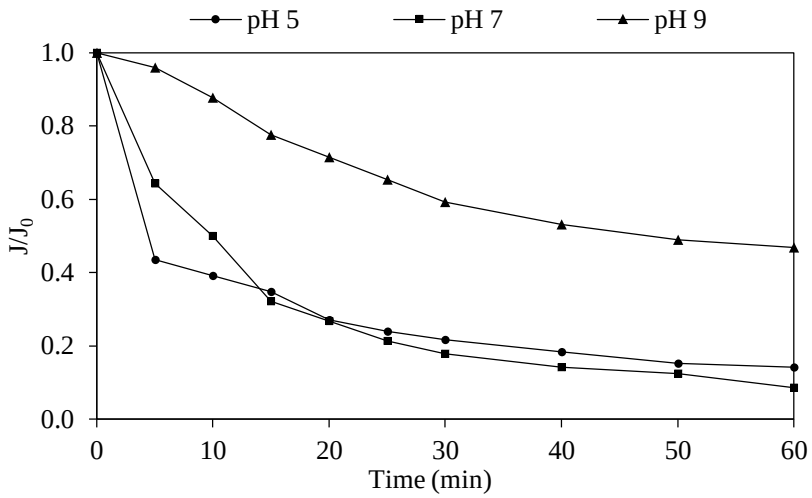

Figure 4.20 *Effects of pH on the permeate fluxes operated with 0.1% w/v under 3 bar and 28 °C*

The result in Fig. 4.20 reveals that pH has a significant effect on flux behaviors. This can be clarified by a mechanism of droplet surface charges. In an acidic condition (pH of 5), the negative surface charges of oil droplets could be destabilized by a high number of H^+ presented in the mixture. Thus the oil drops tended to coalesce, resulting in higher rate of cake layer formation as well as rapid flux declines (Hesampour et al., 2008a).

The most optimal pH was clearly observed at an alkaline condition (pH of 9), in which the NaOH was added for pH adjustment. Once a major area of the membrane surface was covered by OH^-, a considerable amount of a repulsive force

could take place when facing with the negative charges on the droplet surface. This results in lower membrane resistance and higher permeate fluxes. Nevertheless, the effects of pH may also vary according to either membrane compositions or surfactants in the system (Chakrabarty et al., 2008).

4.4.3 Prediction of the UF Fouling Mechanisms

Regardless of the membrane type, the filtration manners usually fluctuate due to different operating conditions, which might probably affect influent properties. The determination coefficient (R^2) of each blocking model was calculated from Hermia's equations (see Ch. 3.4.6). Various R^2 values of the same condition were compared in order to determine a characteristic of membrane's fouling, of which the most fitting model was identified by the highest R^2 value (see Appendix C).

The membrane fouling might result from various phenomena: (1) adsorption or blocking inside the membrane's pores; (2) concentration polarization; (3) particle deposition on the membrane surface as a cake layer; and (4) compression of a cake layer (Salahi et al., 2010). However, the most optimal conditions (3 bar, 28 °C, and pH of 9) corresponded well with the cake formation model, which can be schematically explained as follows:

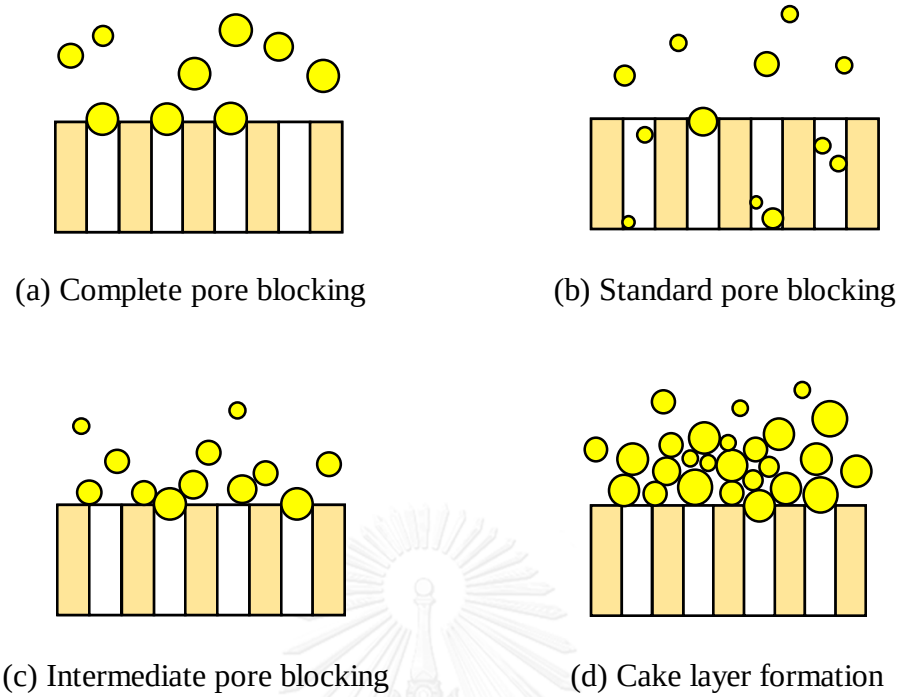

(a) Complete pore blocking (b) Standard pore blocking

(c) Intermediate pore blocking (d) Cake layer formation

Figure 4.21 *Schematics of the fouling mechanisms during a filtration process*

Table 4.5 *Description of each pore blocking model (Sarfaraz et al., 2012)*

Model	Explanation
Complete pore blocking	Oil droplets block the membrane's pores without any superposition
Standard pore blocking	Pore volume is reduced due to some penetrated oil droplets
Intermediate pore blocking	Some oil drops stay on others that already settled on the membrane surface
Cake formation	Oil droplets deposit upon the previous settled drops and form a cake layer at the membrane surface

According to Salahi et al. (2010), several factors affecting the degree of fouling could be feed characteristics, operating parameters, and membrane properties. The mechanisms depicted in Fig. 4.21a, 4.21b, and 4.21c are largely dependent on the size of feed particles as well as the membrane's pore. Various phenomena, for example, concentration polarization and adsorption/blocking inside the membrane's pores, could

take place through these mechanisms. In contrast, the cake formation generally takes place due to the operating conditions, for instance, an applied pressure, cross-flow velocity, and particle deposition rate. Besides, as aforementioned, the average size of oil droplets in this work was much larger than that of the membrane's pores. Also, the pressure applied to the system was quite large. These effects could result in a high rate of oil droplet deposition and intense cake layer on the membrane surface.

4.4.4 UF Treatment Efficiency

The experiments in this part were conducted with three emulsion concentrations: 0.05, 0.1, and 0.5% w/v. The effluent was subject to five-time concentrate before analytical process. The residual oil in all samples could not be measured due to a detection limit of the equipment, which is 0.025% or 250 mg/l. It is possible to describe that oil contents remaining in the effluent were lower than 50 mg/l. In other words, the separation efficiency at least 90% could be achieved for the treatment of cutting oil wastewater.

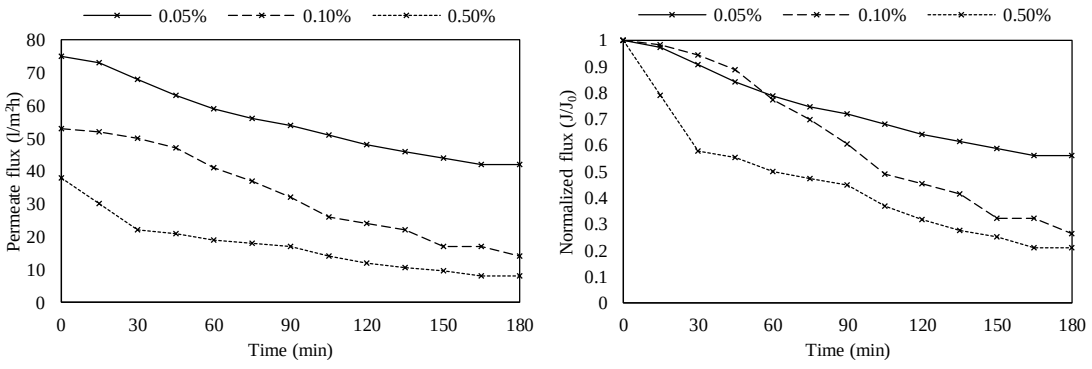

(a) (b)

Figure 4.22 *Flux behaviors as a function of time operated under 3 bar and 28 ºC in an alkaline condition: (a) actual flux; (b) normalized flux*

The results in Fig. 4.22 indicates the effect of oil concentration on the UF performance. Under a constant pressure, the degree of particle deposition as well as cake layer density are supposed to be in accordance with oil concentrations. Also, an oil layer formed upon the membrane surface is compressible, which make it even more compact during the filtration process. As a consequence, the highest flux was obtained from the 0.05% emulsion. Moreover, this fact also proposes that higher effectiveness of the cross-flow UF could be reached under low feed concentration, regarding less fouling and flux decline rate.

As aforementioned, it is clearly seen that the destabilization, coalescer, and ultrafiltration are able to deal with the stabilized oily wastewater. However, when these processes are conducted individually, a specific operational condition is required for the achievement of their maximum efficiency. As a result, these processes will be integrated into a system with liquid recirculation as schematically shown in Fig 4.23. This process was designed under the expectations to enhance oil recovery and improve the performance of each treatment method. The evaluation of the combined process will be discussed in the following section.

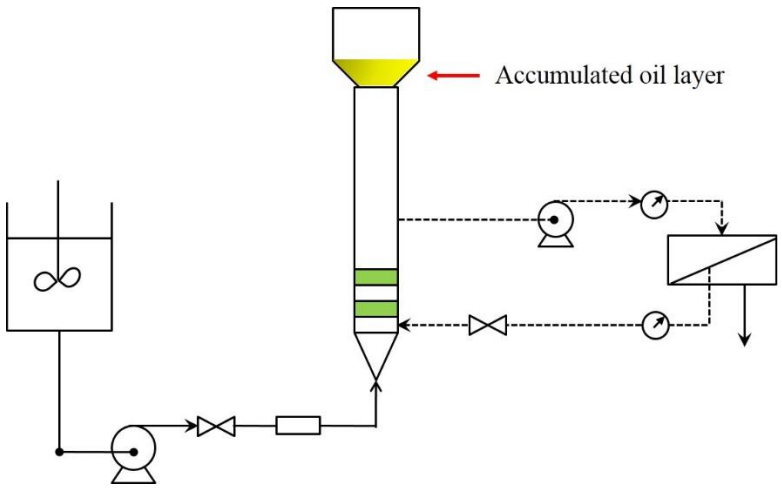

Figure 4.23 *Expected combined process performance*

4.5 OPTIMIZATION OF THE COMBINED TREATMENT PROCESSES: CHEMICAL DESTABILIZATION, COALESCER, AND CROSS-FLOW UF

The purpose of this section is to study synergistic effects of the combined process on oil separation performance. The 0.1% w/v emulsion was used throughout this section, in which three major methods were respectively applied (i.e., destabilization, coalescence, and cross-flow UF). Significant operating factors, for instance, a circulating level and retention time, were considered. Finally, an external electric field was applied to the system in order to enhance the treatment effectiveness.

4.5.1 Determination of an Optimal Circulating Level

In order to acquire the most favorable system's performance, the comparison of various circulating levels were examined, focusing on flux decline behaviors. It is worth noting that a recirculation was proceeded immediately after the feed reached the setting point.

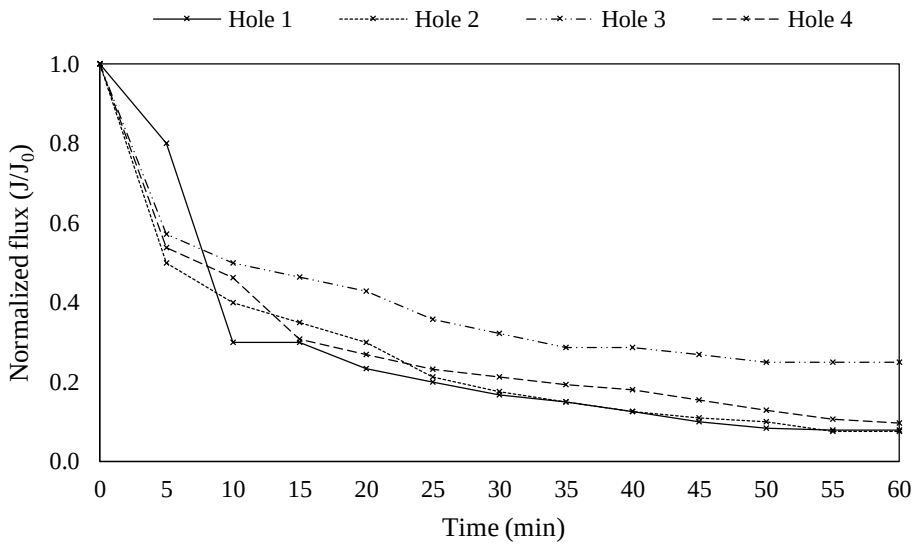

Figure 4.24 *Flux decline rate of various circulating levels*

Table 4.6 *Flux declination of different circulation levels at 1-hr operating time*

Hole No.	FD (%)
1	92.15
2	92.5
3	75.0
4	90.38

Focusing on the steady state, the similar trends of flux decline were found in Hole 1, 2, and 4. Fig. 4.24 and Table 4.6 obviously describe that the lowest flux decline was achieved from Hole 3 during 1-hr operation. This implied that the circulating level had an effect on the process and Hole 3 was then considered as an optimal outlet for a circulation system (see Fig. 4.25).

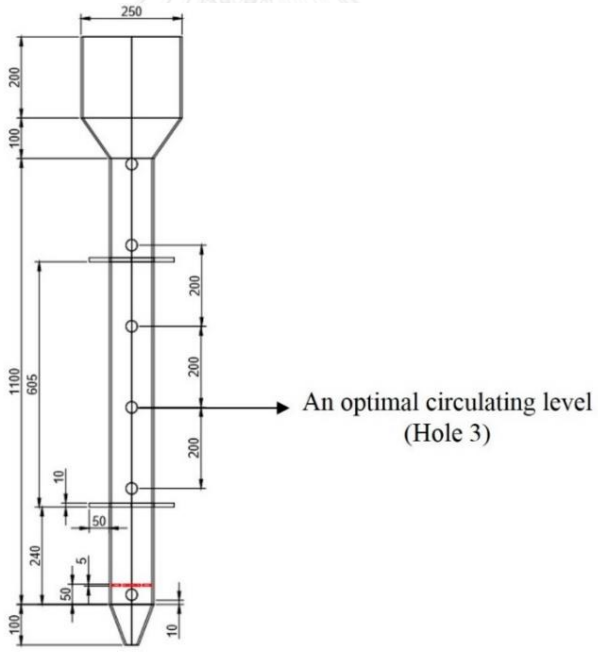

Figure 4.25 *The optimal level of a circulating line*

4.5.2 Optimum Decantation Time for the Combined Process

As discussed earlier, the UF process individual can provide relatively high treatment efficiency. However, the experiments in this phase aims to couple the coalescer with UF process for the improvement of oil removal efficiency and membrane fouling. The flux behavior through various residence times was investigated and compared with that of the sole UF in order to determine the most effective condition.

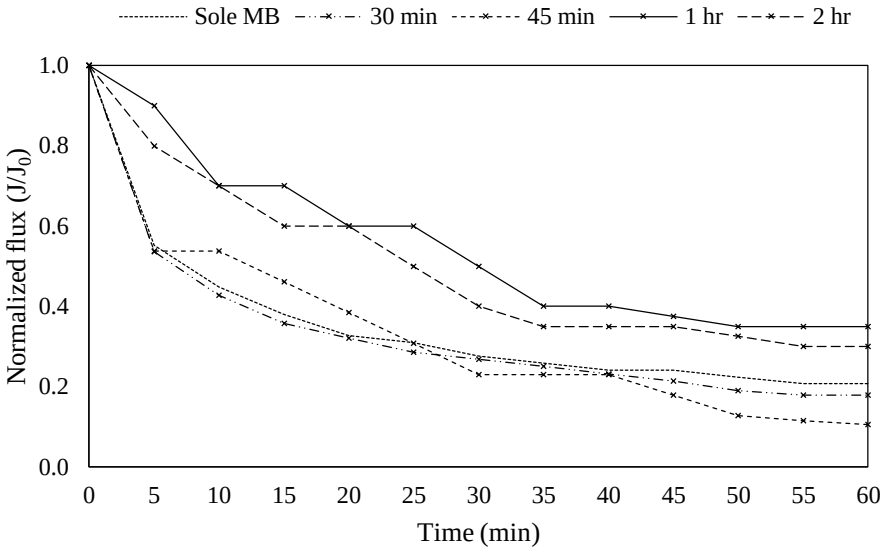

Figure 4.26 *Flux decline rate of the combined process at different decantation times*

The decantation time of 30 and 45 minutes offered similar trends of flux decline for the combined process, which was comparable to that of the sole UF method. As seen in Fig.4.26, the system performance was found to be improved at the retention time of more than one hour. This could be explained that only 30 and 45 minutes might not be adequate for the coalesced oil droplets to rise or decant efficiently. Once the recirculation starts, some large oil drops could be drawn to the UF and then lead to rapid particle deposition and pore blocking on the membrane surface.

Another fascinating point is the fluxes obtained from 1-hr and 2-hr decantation times, which were fairly similar. From this point, it is possible to propose that this combined process could enhance the coalescer and UF performance in terms of the reduction in residence time and membrane fouling, respectively.

However, the accumulated oil layer from this combined process could not be clearly noticed. This might be result from the relatively low oil concentration used in this experiment. Additionally, the permeate flux attained from the UF was quite low due to the extremely small membrane area. Therefore, the recirculated oily stream could not be enough concentrated.

4.5.3 Improvement of the Combined Process by Electrostatic coalescence

In this section, an external low electric field was applied over the media layer in order to improve the combined process performance (see Fig. 4.27). Once the coalesced oil droplets salted out from the media, the electric field could induce the migration of their surface charges, resulting in further coalescing performance.

During the influent feeding, the current denstiy was kept constant at 10 A/m^2 or approximately 1 V/cm. This is comparable to the study of Ichikawa et al. (2004), which suggests that the demulsification of O/W emulsions can be rapidly enhanced under an electric field of less than 10 V/cm.

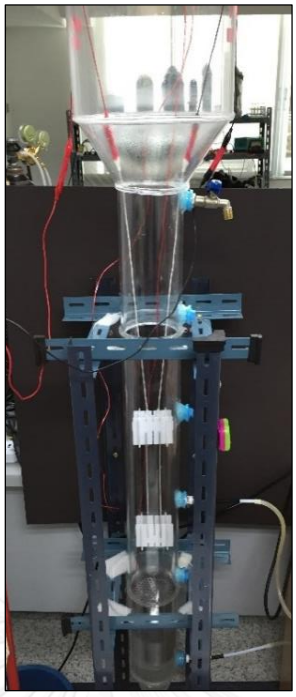

Figure 4.27 *Reactor setup under the electrocoalescence process*

In general, chemical reactions that may take place during this process includes the metal dissolution at the anode and hydrogen evolution at the cathode as expressed below:

Anode: $Al_{(s)} \longrightarrow Al_{(aq)}^{3+} + 3e^-$

Cathode: $2H_2O_{(l)} + 2e^- \longrightarrow H_{2(g)} + 2OH_{(aq)}^-$

Redox: $2Al_{(s)} + 6H_2O \longrightarrow 2Al_{(aq)}^{3+} + 3H_{2(g)} + 6OH_{(aq)}^-$

In contrast to the electrocoagulation process (Bayramoglu et al., 2004), Al^{3+} and OH^- ions generated at the electrode surfaces are inconsiderable in this study due to the extremely low electric field. The main mechanism here is the reduction of an energy barier caused by the migration of oil droplet surface charges, which results in accelerated oil droplet coalescence.

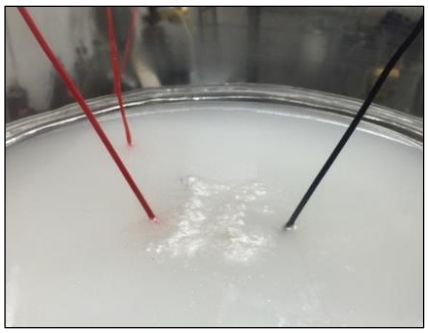

Figure 4.28 *The hydrogen gas (H_2) taking place during the electrocoalescence*

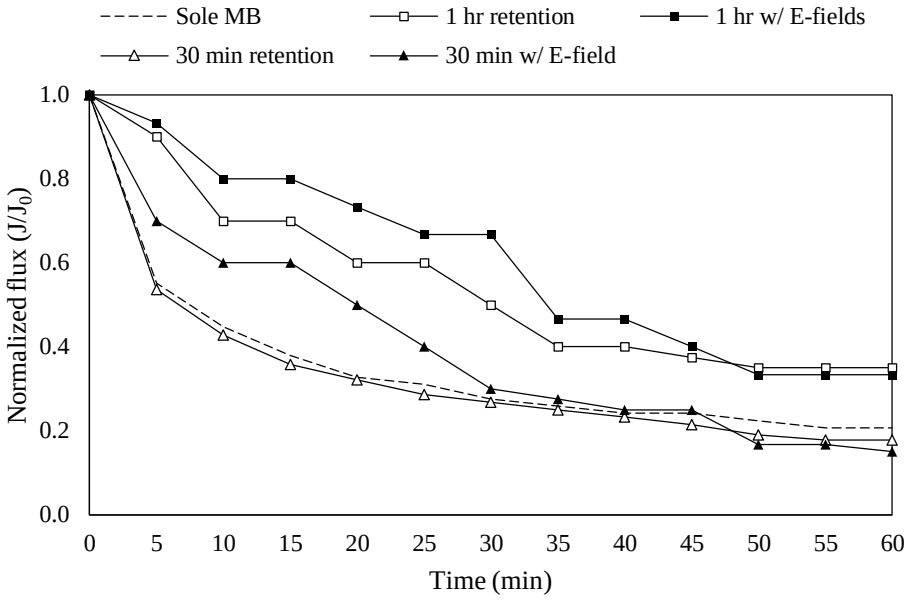

Figure 4.29 *Effect of an external electric field on flux behaviors*

The result in Fig. 4.29 points out the advantage of an external electric field on the combined process. Considering at the 1-hr decantation time, the membrane fouling could be retarded when equipped the system with an external electric field. Furthermore, as recently reported, the performance of the combined process was comparable to the sole UF under 30-min decantation time. Once the electrostatic coalescence was provided, the process was improved and could be longer operated until the flux reached half decline of the beginning. However, the $Al(OH)_3$ might be

gradually generated in the system, leading to rapid flux decline at a certain operating time.

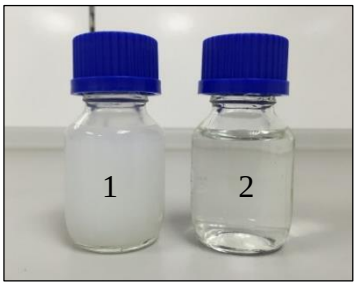

Figure 4.30 *Appearance of the 0.1% w/v emulsion: (1) before treatment; (2) after the combined process*

Additionally, in terms of treatment efficiency, the combined process could offer up to 97% oil removal. In other words, the effluent with the residual COD of below 80 mg/l was attained from the combined process.

4.5.4 System Design Proposal

This section aims to propose the applicability of the combined process in terms of design criteria, of which necessary information was based on the results in this work.

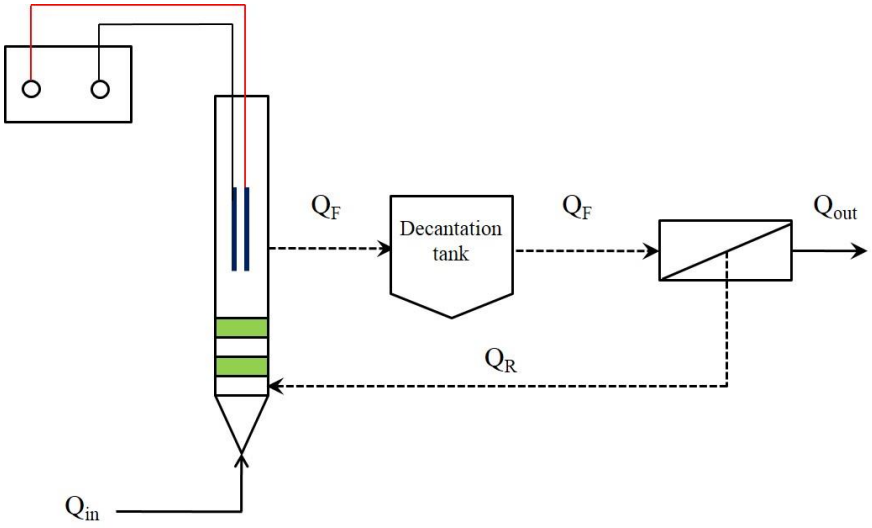

Figure 4.31 *A schematic for combined system design*

Given:

- The treated water (Q_{out}) of 1 m^3/d is required from the system
- The influent concentration (C_{in}) = 1000 mg/l
- The UF provides 97% oil removal with the steady permeate flux of 20 l/m^2hr
- The oily feed achieves 85% efficiency before entrance the UF
- Flow velocity of the coalescer = 1.2 mm/s
- The system is provided with 50% liquid recirculation
- Sludge retention time = 1 hr

Calculation:

Assume that no accumulation and loss in the system

Therefore, $Q_{in} = Q_{out} = 1\ m^3/d$

$Q_R = 0.5\ m^3/d$

$Q_F = Q_{in} + Q_R = 1.5\ m^3/d$

Considering the coalescer process:

$Q_{in} + Q_R = VA_{coalescer}$

$1.5\ m^3/d = (0.0012\ m/s)(86400\ s/1\ d)(A_{coalescer})$

$A_{coalescer} = 0.0145\ m^2 = 145\ cm^2$

$r_{coalescer} = 6.79\ cm \approx 7\ cm$

Considering the decantation tank:

Retention time = (Tank volume)/(Q_F)

(1 hr)(1 d/24 hr) = (Tank volume)/(1.5 m^3/d)

Tank volume = 0.0625 m^3 = 62.5 l

Considering at the UF process:

$$J = Q_{out}/A_{membrane}$$

$$(20\ l/m^2hr)(1\ m^3/1000\ l)(24\ hr/1\ d) = (1\ m^3/d)/(A_{membrane})$$

$$A_{membrane} = 2\ m^2$$

Since the UF provides 97% oil removal efficiency,

$$C_{out} = (0.03)(0.15)(1000\ mg/l)$$

$$= 4.5\ mg/l\ \text{(below the industrial effluent standard)}$$

Therefore, in order to acquire 1 m^3/d discharge under the environmental effluent standard, the following details is needed:

Coalescer diameter	14 cm
Decantation tank volume	62.5 L
Membrane area	2 m^2

CHAPTER 5

CONCLUSION AND RECOMMENDATION

5.1 CONCLUSIONS

This research work aims to investigate oil separation performance through various treatment processes, consisting of chemical destabilization, conventional coalescer, and membrane filtration. All processes were carried out under the optimal conditions obtained from this work as well as previous studies. The conclusions will be primarily described the practical manners of each separated technique. Then the performance of the integrated process will be evaluated.

5.1.1 Individual Treatment Process

This section describes the performance of several treatment processes in terms of oil removal efficiency. As seen from Table 5.1, the oil concentration appears to be an influential factor on oil separation. The functional conditions and limitations of each treatment process can be concluded as the following:

Table 5.1 *Oil removal efficiency of several treatment processes*

Oil conc. (% w/v)	**Treatment efficiency**				
	Decantation	**Coalescer**	**Destabilization**	**Destabilization & Coalescer**	**Cross-flow UF**
0.05	13.49%	25.24%	25.72%	42.02%	> 90%
0.1	14.25%	41.83%	53.19%	85.80%	
0.5	19.68%	6.76%	69.20%	91.65%	
1.0	15.99%	7.54%	74.46%	67.30%	-

Decantation

Since this process was operated under the gravitational force, it could not provide effective separation for highly stabilized oil droplets, which is extremely small and well dispersed in the continuous phase.

Coalescer

This technique could effectively act as a pretreatment for stabilized oily emulsions. Moreover, it was particularly suitable for the wastewater with moderate oil concentrations such as 0.05 and 0.1% w/v. However, the coalescer performance may vary depending on other parameters, for example, medium type, feed flow velocity, influent properties, and reactor configurations.

Chemical Destabilization

It should be noted that the coagulant dosage used in this study was optimized from a specific range, which was relatively low, in order to acquire least chemical effect on the system. Thus the results might be improved with a greater chemical amount.

For this process, the treatment efficiency was proportional to the oil concentration. Once the oily emulsion was destabilized, the system performance would be governed by the number of oil droplets presented in the water. Therefore, this might be one of the attractive methods for the treatment of stabilized oily wastewater.

Coupled Processes between Coalescer and Chemical Destabilization

It is clearly noticed that this system could greatly enhance oil separation efficiency. This process promoted twice oil droplet coalescence through the chemical and coalescing media, respectively. As a result, the oil droplets would form such a large diameter, which could be supported by the data in Table 4.4. On the other hands, when

dealing with too high oil concentrations (1% w/v), some coalesced oil droplets may rupture within the media bed and lead to adverse effects on the system.

Cross-flow UF

In general, under optimal conditions, oil removal efficiency of at least 90% could be achieved from the UF process. Nevertheless, the fouling problem during process frequently occurs, especially for high oil concentrations, leading to higher operating cost regarding cleaning agents and material replacement.

5.2.2 Combined Processes: destabilization, coalescer, and cross-flow UF

It is worth noting that the explanation in this phase was proposed based on 0.1% oily wastewater. The results obtained from this work obviously indicate the integrated process performance as follows:

- The treatment efficiency up to 97% could be achieved by the combined process. In other words, the residual COD of below 80 mg/l was detected in the effluent, which is acceptable for environmental discharge.
- The oil load upstream could be reduced before entrance the UF process, leading to better effluent quality and less intensity of flux decline. However, efficiency of the combined process in terms of the permeate flux was relatively low when compared to that of the sole membrane.
- The oily stream or retentate could be re-circulated to the coalescer, which may bring about enhanced oil recovery.
- Once the UF was located downstream, the decantation time of the coalescer could be lessened.

5.2 RECOMMENDATIONS

In order to make this combined process more useful, the following suggestions should be considered:

- A continuous mode of operation should be conducted to represent the system in real practice. Due to an extremely small membrane area, this action could not be completed in this study. An interesting alternative is to replace the membrane flat sheet by a hollow-fiber type, which provides a much more filtration area.
- The system should be carried out with produced oily wastewater for validating that this combined process is really applicable.
- The recovered oil content should be investigated in terms of characteristics and compositions to make sure of its stability to be reused.
- The oily structures or fouling mechanisms upon the membrane surface should be actually analyzed in order to verify the results from the mathematical models.

Additionally, it would be fascinating if the mechanisms taking place within the coalescer column could be noticeable. This would lead to better understanding of oil droplet activities during an operation. Moreover, the recirculation system should be observed in more aspects in order to attain novel perspectives, including enhanced overall process efficiency.

REFERENCES

American Public Health Association. (2005). Standard methods for the examination of water and wastewater. Washington, D.C.: APHA-AWWA-WEF.

Aurelle, Y. (1985). Treatment of Oil-Containing Wastewater. Bangkok: Chulalongkorn University, Department of Sanitary Engineering.

Bayramoglu, M., Kobya, M., Can, O. T., & Sozbir, M. (2004). Operating cost analysis of electrocoagulation of textile dye wastewater. Separation and Purification Technology, *37*(2), 117-125.

Bensadok, K., Belkacem, M., & Nezzal, G. (2007). Treatment of cutting oil/water emulsion by coupling coagulation and dissolved air flotation. Desalination, *206*(1–3), 440-448.

Chakrabarty, B., Ghoshal, A. K., & Purkait, M. K. (2008). Ultrafiltration of stable oil-in-water emulsion by polysulfone membrane. Journal of Membrane Science, *325*(1), 427-437.

Chakrabarty, B., Ghoshal, A. K., & Purkait, M. K. (2010). Cross-flow ultrafiltration of stable oil-in-water emulsion using polysulfone membranes. Chemical Engineering Journal, *165*(2), 447-456.

Chawaloesphonsiya, N. (2009). Enhancement of Cutting Oil Wastewater Treatment and Separation by Coalescer Process. Master degree, Chulalongkorn University.

Cheryan, M., & Rajagopalan, N. (1998). Membrane processing of oily streams. Wastewater treatment and waste reduction. Journal of Membrane Science, *151*(1), 13-28.

El Baradie, M. A. (1996). Cutting fluids: Part II. Recycling and clean machining. Journal of Materials Processing Technology, *56*(1–4), 798-806.

Elektorowicz, M., Habibi, S., & Chifrina, R. (2006). Effect of electrical potential on the electro-demulsification of oily sludge. Journal of Colloid and Interface Science, *295*(2), 535-541.

Eow, J. S., & Ghadiri, M. (2002). Electrostatic enhancement of coalescence of water droplets in oil: a review of the technology. Chemical Engineering Journal, *85*(2–3), 357-368.

Eow, J. S., & Ghadiri, M. (2003). Drop–drop coalescence in an electric field: the effects of applied electric field and electrode geometry. Colloids and Surfaces A: Physicochemical and Engineering Aspects, *219*(1–3), 253-279.

Grzesik, W. (2008). Chapter Ten - Cutting Fluids. In W. Grzesik (Ed.), *Advanced Machining Processes of Metallic Materials* (pp. 141-148). Amsterdam: Elsevier.

Hermia, J. (1982). CONSTANT PRESSURE BLOCKING FILTRATION LAWS - APPLICATION TOPOWER-LAW NON-NEWTONIAN FLUIDS. TRANS INST CHEM ENG, *V 60*(N 3), 183-187.

Hesampour, M., Krzyzaniak, A., & Nyström, M. (2008a). The influence of different factors on the stability and ultrafiltration of emulsified oil in water. Journal of Membrane Science, *325*(1), 199-208.

Hesampour, M., Krzyzaniak, A., & Nyström, M. (2008b). Treatment of waste water from metal working by ultrafiltration, considering the effects of operating conditions. Desalination, *222*(1–3), 212-221.

Hilal, N., Busca, G., Hankins, N., & Mohammad, A. W. (2004). The use of ultrafiltration and nanofiltration membranes in the treatment of metal-working fluids. Desalination, *167*(0), 227-238.

Hong, S., Faibish, R. S., & Elimelech, M. (1997). Kinetics of permeate flux decline in crossflow membrane filtration of colloidal suspensions. Journal of colloid and interface science, *196*(2), 267-277.

Ichikawa, T. (2007). Electrical demulsification of oil-in-water emulsion. Colloids and Surfaces A: Physicochemical and Engineering Aspects, *302*(1–3), 581-586.

Ichikawa, T., Dohda, T., & Nakajima, Y. (2006). Stability of oil-in-water emulsion with mobile surface charge. Colloids and Surfaces A: Physicochemical and Engineering Aspects, *279*(1–3), 128-141.

Ichikawa, T., Itoh, K., Yamamoto, S., & Sumita, M. (2004). Rapid demulsification of dense oil-in-water emulsion by low external electric field: I. Experimental evidence. Colloids and Surfaces A: Physicochemical and Engineering Aspects, *242*(1–3), 21-26.

Ii, M., Eda, H., Imai, T., Nishimura, M., Kawasaki, T., Shimizu, J., Yamamoto, T., & Zhou, L. (2000). Development of high water-content cutting fluids with a new

concept: Fire prevention and environmental protection. Precision Engineering, *24*(3), 231-236.

Khiewpuckdee, P. (2011). Treatment of Oily Wastewater by Ultrafiltration Process. Master degree, Chulalongkorn University.

Kongkangwarn, K. (2009). Improvement of Coalescer for Separation of Oil from Water with Surfactant. Master degree, Chulalongkorn University.

Li, J., & Gu, Y. (2005). Coalescence of oil-in-water emulsions in fibrous and granular beds. Separation and Purification Technology, *42*(1), 1-13.

Maiti, S., Mishra, I. M., Bhattacharya, S. D., & Joshi, J. K. (2011). Removal of oil from oil-in-water emulsion using a packed bed of commercial resin. Colloids and Surfaces A: Physicochemical and Engineering Aspects, *389*(1–3), 291-298.

Ministry of Science. (1996). *The Enhancement and Conservation of the National Environmental Quality Act, 1992*. the Royal Government Gazette.

Motta, A., Borges, C., Esquerre, K., & Kiperstok, A. (2014). Oil Produced Water treatment for oil removal by an integration of coalescer bed and microfiltration membrane processes. Journal of Membrane Science, *469*(0), 371-378.

Muniz, C. A. S., Castro Dantas, T. N., Dantas Neto, A. A., Moura, M. C. P. A., & Dantas, A. C. (2012). Cutting Fluid Oily Wastewater: Breakdown and Reuse of the Recovered Oil Phase. Brazilian Journal of Petroleum and Gas, *6*(1), 19-30.

Occupational Safety & Health Administration (OSHA). (1999). Metalworking Fluids: Safety and Health Best Practices Manual. Retrieved June 29, 2014, from https://www.osha.gov

Pacek, A. W., Man, C. C., & Nienow, A. W. (1998). On the Sauter mean diameter and size distributions in turbulent liquid/liquid dispersions in a stirred vessel. Chemical Engineering Science, *53*(11), 2005-2011.

Perez, M., Rodriguez-Cano, R., Romero, L. I., & Sales, D. (2007). Performance of anaerobic thermophilic fluidized bed in the treatment of cutting-oil wastewater. Bioresource Technology, *98*(18), 3456-3463.

Rachu, S. (2005). Computer Program Development for Oily Wastewater Treatment Process Selection, Design and Simulation. Doctoral dissertation, INSA-Toulouse.

Ríos, G., Pazos, C., & Coca, J. (1998a). Destabilization of cutting oil emulsions using inorganic salts as coagulants. Colloids and Surfaces A: Physicochemical and Engineering Aspects, *138*(2–3), 383-389.

Ríos, G., Pazos, C., & Coca, J. (1998b). Zeta potentials of cutting-oil water emulsions: Influence of inorganic salts. Journal of Dispersion Science and Technology, *19*(5), 661-678.

Salahi, A., Abbasi, M., & Mohammadi, T. (2010). Permeate flux decline during UF of oily wastewater: Experimental and modeling. Desalination, *251*(1–3), 153-160.

Salahi, A., Noshadi, I., Badrnezhad, R., Kanjilal, B., & Mohammadi, T. (2013). Nano-porous membrane process for oily wastewater treatment: Optimization using response surface methodology. Journal of Environmental Chemical Engineering, *1*(3), 218-225.

Sarfaraz, M. V., Ahmadpour, E., Salahi, A., Rekabdar, F., & Mirza, B. (2012). Experimental investigation and modeling hybrid nano-porous membrane process for industrial oily wastewater treatment. Chemical Engineering Research and Design, *90*(10), 1642-1651.

Sarkar, B., & De, S. (2011). Prediction of permeate flux for turbulent flow in cross flow electric field assisted ultrafiltration. Journal of Membrane Science, *369*(1–2), 77-87.

Shin, W.-T., Yiacoumi, S., & Tsouris, C. (2004). Electric-field effects on interfaces: electrospray and electrocoalescence. Current Opinion in Colloid & Interface Science, *9*(3–4), 249-255.

Shinnar, R. (1961). On the behaviour of liquid dispersions in mixing vessels. Journal of Fluid Mechanics, *10*(2), 259-275.

Sutherland, K. (2008). Machinery and processing: Managing cutting fluids used in metal working. Filtration & Separation, *45*(7), 20-23.

Titasupawat, S. (2009). Treatment and Separation of Oily Wastewater by Electrostatic Coalescer Process. Master degree, Chulalongkorn University.

Yoon, S.-H. (2015). Membrane Bioreactor Processes: Principles and Applications. United States: CRC Press.

APPENDICES

APPENDIX A
OIL DROPLET SIZE DISTRIBUTION

Table A-1 Volume distribution of the synthetic cutting oil emulsion of 0.05% w/v

Size (μm)	Volume (%)
0.100	0.00
0.112	0.00
0.126	0.03
0.142	0.76
0.159	2.95
0.178	5.67
0.200	6.79
0.224	7.57
0.252	7.60
0.283	7.16
0.317	6.52
0.356	5.82
0.399	5.16
0.448	4.49
0.502	3.76
0.564	3.01
0.632	2.27
0.710	1.58
0.796	0.99
0.893	0.59
1.002	0.41
1.125	0.46
1.262	0.64
1.416	0.85
1.589	1.01
1.783	1.09
2.000	1.10
2.244	1.04
2.518	0.94
2.825	0.81
3.170	0.70
3.557	0.62
3.991	0.58
4.477	0.58
5.024	0.64
5.637	0.73
6.325	0.86
7.096	1.00
7.962	1.14
8.934	1.27
10.024	1.38
11.247	1.44
12.619	1.46
14.159	1.42
15.887	1.33
17.825	1.18
20.000	0.98
22.440	0.75
25.179	0.54
28.251	0.32
31.698	0.02
35.566	0.00
39.905	0.00
44.774	0.00
50.238	0.00

Table A-2 Volume distribution of the synthetic cutting oil emulsion of 0.1% w/v

Size (μm)	Volume (%)
0.100	0.00
0.112	0.00
0.126	0.05
0.142	1.06
0.159	3.38
0.178	6.27
0.200	7.44
0.224	8.25
0.252	8.25
0.283	7.73
0.317	7.01
0.356	6.23
0.399	5.50
0.448	4.76
0.502	3.96
0.564	3.13
0.632	2.28
0.710	1.49
0.796	0.79
0.893	0.31
1.002	0.09
1.125	0.13
1.262	0.34
1.416	0.61
1.589	0.83
1.783	0.98
2.000	1.03
2.244	1.01
2.518	0.94
2.825	0.83
3.170	0.72
3.557	0.64
3.991	0.60
4.477	0.61
5.024	0.67
5.637	0.78
6.325	0.92
7.096	1.08
7.962	1.23
8.934	1.34
10.024	1.40
11.247	1.38
12.619	1.29
14.159	1.1
15.887	0.86
17.825	0.57
20.000	0.11
22.440	0.02
25.179	0.00
28.251	0.00
31.698	0.00
35.566	0.00
39.905	0.00
44.774	0.00
50.238	0.00

Table A-3 Volume distribution of the synthetic cutting oil emulsion of 0.5% w/v

Size (µm)	Volume (%)
0.100	0.00
0.112	0.00
0.126	0.00
0.142	0.00
0.159	0.00
0.178	0.00
0.200	0.03
0.224	0.66
0.252	1.34
0.283	2
0.317	2.63
0.356	3.18
0.399	3.62
0.448	3.94
0.502	4.11
0.564	4.13
0.632	3.98
0.710	3.69
0.796	3.27
0.893	2.76
1.002	2.22
1.125	1.7
1.262	1.27
1.416	0.96
1.589	0.79
1.783	0.77
2.000	0.83
2.244	0.94
2.518	1.05
2.825	1.13
3.170	1.2
3.557	1.22
3.991	1.21
4.477	1.18
5.024	1.13
5.637	1.07
6.325	1
7.096	0.94
7.962	0.88
8.934	0.82
10.024	0.76
11.247	0.7
12.619	0.63
14.159	0.57
15.887	0.51
17.825	0.47
20.000	0.45
22.440	0.49
25.179	0.59
28.251	0.74
31.698	0.96
35.566	1.22
39.905	1.51
44.774	1.81
50.238	2.07
56.368	2.29
63.246	2.45
70.963	2.54
79.621	2.56
89.337	2.52
100.237	2.41
112.468	2.24
126.191	1.99
141.589	1.68
158.866	1.33
178.250	1.00
200.000	0.70
224.404	0.48
251.785	0.33
282.508	0.21
316.979	0.12
355.656	0.02
399.052	0.00
447.744	0.00
502.377	0.00

Table A-4 Volume distribution of the synthetic cutting oil emulsion of 1% w/v

Size (µm)	Volume (%)
0.100	0.00
0.112	0.00
0.126	0.00
0.142	0.00
0.159	0.00
0.178	0.00
0.200	0.00
0.224	0.00
0.252	0.00
0.283	0.05
0.317	0.17
0.356	0.45
0.399	0.63
0.448	0.78
0.502	0.91
0.564	0.99
0.632	1.02
0.710	1.03
0.796	1
0.893	0.97
1.002	0.95
1.125	0.97
1.262	1.05
1.416	1.21
1.589	1.44
1.783	1.73
2.000	2.06
2.244	2.38
2.518	2.67
2.825	2.89
3.170	3.05
3.557	3.13
3.991	3.14
4.477	3.08
5.024	2.97
5.637	2.83
6.325	2.68
7.096	2.52
7.962	2.38
8.934	2.25
10.024	2.14
11.247	2.06
12.619	1.98
14.159	1.9
15.887	1.82
17.825	1.73
20.000	1.63
22.440	1.52
25.179	1.41
28.251	1.32
31.698	1.24
35.566	1.18
39.905	1.13
44.774	1.08
50.238	1.02
56.368	0.95
63.246	0.86
70.963	0.75
79.621	0.64
89.337	0.54
100.237	0.45
112.468	0.40
126.191	0.39
141.589	0.41
158.866	0.47
178.250	0.53
200.000	0.58
224.404	0.63
251.785	0.65
282.508	0.66
316.979	0.68
355.656	0.70
399.052	0.74
447.744	0.81
502.377	0.90
563.677	1.02
632.456	1.14
709.627	1.24
796.214	1.30
893.367	1.29
1002.374	1.21
1124.683	1.06
1261.915	0.87
1415.892	0.66
1588.656	0.47
1782.502	0.29
2000.000	0.16

Table A-5 Volume distribution of the 0.05% w/v emulsion via the decantation process

Size (µm)	Volume (%)
0.100	0.00
0.112	0.00
0.126	0.04
0.142	0.87
0.159	3.14
0.178	5.99
0.200	7.22
0.224	8.13
0.252	8.26
0.283	7.9
0.317	7.3
0.356	6.61
0.399	5.91
0.448	5.18
0.502	4.35
0.564	3.47
0.632	2.58
0.710	1.76
0.796	1.07
0.893	0.6
1.002	0.4
1.125	0.46
1.262	0.68
1.416	0.92
1.589	1.09
1.783	1.17
2.000	1.14
2.244	1.03
2.518	0.86
2.825	0.67
3.170	0.48
3.557	0.34
3.991	0.24
4.477	0.19
5.024	0.19
5.637	0.24
6.325	0.3
7.096	0.38
7.962	0.46

Size (µm)	Volume (%)
8.934	0.53
10.024	0.58
11.247	0.62
12.619	0.64
14.159	0.66
15.887	0.68
17.825	0.68
20.000	0.68
22.440	0.66
25.179	0.63
28.251	0.58
31.698	0.50
35.566	0.40
39.905	0.27
44.774	0.14
50.238	0.09
56.368	0.03
63.246	0.00
70.963	0.00
79.621	0.00
89.337	0.00
100.237	0.00

Table A-6 Volume distribution of the 0.1% w/v emulsion via the decantation process

Size (µm)	Volume (%)
0.100	0.00
0.112	0.00
0.126	0.00
0.142	0.00
0.159	1.66
0.178	4.09
0.200	5.12
0.224	6.01
0.252	6.3
0.283	6.21
0.317	5.92
0.356	5.55
0.399	5.15
0.448	4.69
0.502	4.13
0.564	3.52
0.632	2.89
0.710	2.32
0.796	1.84
0.893	1.54
1.002	1.44
1.125	1.52
1.262	1.7
1.416	1.88
1.589	1.97
1.783	1.96
2.000	1.84
2.244	1.63
2.518	1.38
2.825	1.1
3.170	0.84
3.557	0.64
3.991	0.50
4.477	0.42
5.024	0.4
5.637	0.44
6.325	0.5
7.096	0.58
7.962	0.65
8.934	0.71
10.024	0.74
11.247	0.75
12.619	0.74
14.159	0.71
15.887	0.68
17.825	0.66
20.000	0.64
22.440	0.63
25.179	0.63
28.251	0.64
31.698	0.65
35.566	0.66
39.905	0.64
44.774	0.60
50.238	0.53
56.368	0.43
63.246	0.33
70.963	0.21
79.621	0.08
89.337	0.02
100.237	0.00

Table A-7 Volume distribution of the 0.5% w/v emulsion via the decantation process

Size (µm)	Volume (%)
0.100	0.00
0.112	0.00
0.126	0.00
0.142	0.00
0.159	1.50
0.178	3.79
0.200	4.86
0.224	5.77
0.252	6.11
0.283	6.08
0.317	5.83
0.356	5.46
0.399	5.02
0.448	4.5
0.502	3.88
0.564	3.21
0.632	2.55
0.710	1.97
0.796	1.53
0.893	1.27
1.002	1.22
1.125	1.36
1.262	1.6
1.416	1.83
1.589	1.98
1.783	2.01
2.000	1.91
2.244	1.72
2.518	1.47
2.825	1.18
3.170	0.9
3.557	0.67
3.991	0.49
4.477	0.38
5.024	0.33
5.637	0.33
6.325	0.36
7.096	0.41
7.962	0.47
8.934	0.51
10.024	0.53
11.247	0.53
12.619	0.51
14.159	0.49
15.887	0.46
17.825	0.45
20.000	0.47
22.440	0.51
25.179	0.59
28.251	0.70
31.698	0.83
35.566	0.97
39.905	1.09
44.774	1.19
50.238	1.23
56.368	1.22
63.246	1.15
70.963	1.01
79.621	0.81
89.337	0.62
100.237	0.19
112.468	0.00
126.191	0.00
141.589	0.00
158.866	0.00
178.250	0.00
200.000	0.00

Table A-8 Volume distribution of the 1% w/v emulsion via the decantation process

Size (µm)	Volume (%)
0.100	0.00
0.112	0.00
0.126	0.00
0.142	0.00
0.159	0.00
0.178	0.00
0.200	0.00
0.224	0.00
0.252	0.00
0.283	0.05
0.317	0.17
0.356	0.45
0.399	0.63
0.448	0.78
0.502	0.91
0.564	0.99
0.632	1.02
0.710	1.03
0.796	1
0.893	0.97
1.002	0.95
1.125	0.97
1.262	1.05
1.416	1.21
1.589	1.44
1.783	1.73
2.000	2.06
2.244	2.38
2.518	2.67
2.825	2.89
3.170	3.05
3.557	3.13
3.991	3.14
4.477	3.08
5.024	2.97
5.637	2.83
6.325	2.68
7.096	2.52
7.962	2.38
8.934	2.25
10.024	2.14
11.247	2.06
12.619	1.98
14.159	1.9
15.887	1.82
17.825	1.73
20.000	1.63
22.440	1.52
25.179	1.41
28.251	1.32
31.698	1.24
35.566	1.18
39.905	1.13
44.774	1.08
50.238	1.02
56.368	0.95
63.246	0.86
70.963	0.75
79.621	0.64
89.337	0.54
100.237	0.45
112.468	0.40
126.191	0.39
141.589	0.41
158.866	0.47
178.250	0.53
200.000	0.58
224.404	0.63
251.785	0.65
282.508	0.66
316.979	0.68
355.656	0.70
399.052	0.74
447.744	0.81
502.377	0.90
563.677	1.02
632.456	1.14
709.627	1.24
796.214	1.30
893.367	1.29
1002.374	1.21
1124.683	1.06
1261.915	0.87
1415.892	0.66
1588.656	0.47
1782.502	0.29
2000.000	0.16

Table A-9 Volume distribution of the 0.05% w/v emulsion via the coalescer process

Size (µm)	Volume (%)
0.100	0.00
0.112	0.00
0.126	0.00
0.142	0.00
0.159	1.32
0.178	3.47
0.200	4.60
0.224	5.51
0.252	5.88
0.283	5.88
0.317	5.66
0.356	5.31
0.399	4.88
0.448	4.35
0.502	3.71
0.564	3.03
0.632	2.34
0.710	1.74
0.796	1.25
0.893	0.95
1.002	0.86
1.125	0.95
1.262	1.15
1.416	1.38
1.589	1.56
1.783	1.66
2.000	1.68
2.244	1.64
2.518	1.56
2.825	1.46
3.170	1.37
3.557	1.32
3.991	1.29
4.477	1.31
5.024	1.35
5.637	1.42
6.325	1.49
7.096	1.55
7.962	1.59
8.934	1.61
10.024	1.58
11.247	1.52
12.619	1.43
14.159	1.32
15.887	1.19
17.825	1.06
20.000	0.93
22.440	0.82
25.179	0.70
28.251	0.58
31.698	0.47
35.566	0.24
39.905	0.10
44.774	0.00
50.238	0.00
56.368	0.00
63.246	0.00
70.963	0.00
79.621	0.00
89.337	0.00
100.237	0.00

Table A-10 Volume distribution of the 0.1% w/v emulsion via the coalescer process

Size (µm)	Volume (%)
0.100	0.00
0.112	0.00
0.126	0.00
0.142	0.00
0.159	1.64
0.178	4.06
0.200	5.09
0.224	5.96
0.252	6.21
0.283	6.09
0.317	5.77
0.356	5.37
0.399	4.95
0.448	4.47
0.502	3.92
0.564	3.32
0.632	2.71
0.710	2.15
0.796	1.69
0.893	1.39
1.002	1.29
1.125	1.38
1.262	1.57
1.416	1.79
1.589	1.93
1.783	2.01
2.000	2.01
2.244	1.95
2.518	1.85
2.825	1.72
3.170	1.6
3.557	1.5
3.991	1.42
4.477	1.37
5.024	1.34
5.637	1.31
6.325	1.29
7.096	1.26
7.962	1.22

Size (µm)	Volume (%)
8.934	1.16
10.024	1.07
11.247	0.96
12.619	0.82
14.159	0.65
15.887	0.46
17.825	0.25
20.000	0.01
22.440	0.00
25.179	0.00
28.251	0.00
31.698	0.00
35.566	0.00
39.905	0.00
44.774	0.00
50.238	0.00
56.368	0.00
63.246	0.00
70.963	0.00
79.621	0.00
89.337	0.00
100.237	0.00

Table A-11 Volume distribution of the 0.5% w/v emulsion via the coalescer process

Size (µm)	Volume (%)
0.100	0.00
0.112	0.00
0.126	0.00
0.142	0.00
0.159	1
0.178	2.79
0.200	3.89
0.224	4.75
0.252	5.16
0.283	5.25
0.317	5.13
0.356	4.87
0.399	4.51
0.448	4.03
0.502	3.44
0.564	2.79
0.632	2.13
0.710	1.54
0.796	1.07
0.893	0.78
1.002	0.69
1.125	0.79
1.262	1.02
1.416	1.3
1.589	1.55
1.783	1.76
2.000	1.9
2.244	1.98
2.518	2.02
2.825	2.01
3.170	1.99
3.557	1.97
3.991	1.96
4.477	1.96
5.024	2
5.637	2.05
6.325	2.12
7.096	2.19
7.962	2.25
8.934	2.28
10.024	2.26
11.247	2.17
12.619	2
14.159	1.74
15.887	1.4
17.825	0.97
20.000	0.46
22.440	0.07
25.179	0.00
28.251	0.00
31.698	0.00
35.566	0.00
39.905	0.00
44.774	0.00
50.238	0.00
56.368	0.00
63.246	0.00
70.963	0.00
79.621	0.00
89.337	0.00
100.237	0.00

Table A-12 Volume distribution of the 1% w/v emulsion via the coalescer process

Size (µm)	Volume (%)
0.100	0.00
0.112	0.00
0.126	0.00
0.142	0.00
0.159	0.00
0.178	0.00
0.200	0.00
0.224	0.00
0.252	0.00
0.283	0.05
0.317	0.27
0.356	0.51
0.399	0.72
0.448	0.89
0.502	1.01
0.564	1.09
0.632	1.12
0.710	1.11
0.796	1.07
0.893	1.01
1.002	0.97
1.125	0.97
1.262	1.03
1.416	1.18
1.589	1.39
1.783	1.68
2.000	2.01
2.244	2.33
2.518	2.62
2.825	2.85
3.170	3.01
3.557	3.09
3.991	3.10
4.477	3.03
5.024	2.9
5.637	2.73
6.325	2.54
7.096	2.33
7.962	2.13

Size (µm)	Volume (%)
8.934	1.95
10.024	1.79
11.247	1.66
12.619	1.57
14.159	1.51
15.887	1.48
17.825	1.48
20.000	1.49
22.440	1.52
25.179	1.55
28.251	1.58
31.698	1.60
35.566	1.60
39.905	1.58
44.774	1.51
50.238	1.40
56.368	1.25
63.246	1.07
70.963	0.86
79.621	0.66
89.337	0.47
100.237	0.32
112.468	0.21
126.191	0.15
141.589	0.13
158.866	0.14
178.250	0.16
200.000	0.19
224.404	0.21
251.785	0.23
282.508	0.26
316.979	0.30
355.656	0.37
399.052	0.46
447.744	0.59
502.377	0.76
563.677	0.96
632.456	1.18
709.627	1.40

Size (µm)	Volume (%)
796.214	1.58
893.367	1.70
1002.374	1.73
1124.683	1.67
1261.915	1.52
1415.892	1.30
1588.656	1.04
1782.502	0.70
2000.000	0.41

Table A-13 Volume distribution of the 0.05% w/v emulsion via the coalescer coupled with destabilization process

Size (µm)	Volume (%)
0.100	0.00
0.112	0.00
0.126	0.00
0.142	0.00
0.159	0.00
0.178	0.00
0.200	0.00
0.224	0.06
0.252	0.68
0.283	1.48
0.317	2.05
0.356	2.68
0.399	3.19
0.448	3.6
0.502	3.89
0.564	4.03
0.632	4.01
0.710	3.85
0.796	3.54
0.893	3.12
1.002	2.64
1.125	2.13
1.262	1.67
1.416	1.29
1.589	1.05
1.783	0.93
2.000	0.92
2.244	1.01
2.518	1.17
2.825	1.4
3.170	1.67
3.557	1.97
3.991	2.27
4.477	2.55
5.024	2.79
5.637	2.95
6.325	3.03
7.096	3.01
7.962	2.89
8.934	2.69
10.024	2.41
11.247	2.08
12.619	1.73
14.159	1.40
15.887	1.09
17.825	0.85
20.000	0.68
22.440	0.57
25.179	0.53
28.251	0.54
31.698	0.57
35.566	0.61
39.905	0.64
44.774	0.67
50.238	0.68
56.368	0.70
63.246	0.72
70.963	0.76
79.621	0.82
89.337	0.90
100.237	0.96
112.468	1.00
126.191	0.98
141.589	0.85
158.866	0.70
178.250	0.35
200.000	0.00

Table A-14 Volume distribution of the 0.1% w/v emulsion via the coalescer coupled with destabilization process

Size (µm)	Volume (%)
0.100	0.00
0.112	0.00
0.126	0.00
0.142	0.00
0.159	0.00
0.178	0.00
0.200	0.00
0.224	0.04
0.252	0.52
0.283	1.19
0.317	1.72
0.356	2.31
0.399	2.87
0.448	3.39
0.502	3.87
0.564	4.29
0.632	4.68
0.710	5.02
0.796	5.31
0.893	5.53
1.002	5.68
1.125	5.73
1.262	5.64
1.416	5.39
1.589	4.99
1.783	4.43
2.000	3.79
2.244	3.1
2.518	2.42
2.825	1.81
3.170	1.3
3.557	0.91
3.991	0.64
4.477	0.49
5.024	0.44
5.637	0.46
6.325	0.53
7.096	0.61
7.962	0.69
8.934	0.73
10.024	0.75
11.247	0.72
12.619	0.67
14.159	0.61
15.887	0.54
17.825	0.48
20.000	0.46
22.440	0.47
25.179	0.52
28.251	0.59
31.698	0.67
35.566	0.71
39.905	0.71
44.774	0.64
50.238	0.50
56.368	0.33
63.246	0.10
70.963	0.00
79.621	0.00
89.337	0.00
100.237	0.00
112.468	0.00
126.191	0.00
141.589	0.00
158.866	0.00
178.250	0.00
200.000	0.00

Table A-15 Volume distribution of the 0.5% w/v emulsion via the coalescer coupled with destabilization process

Size (μm)	Volume (%)
0.100	0.00
0.112	0.00
0.126	0.00
0.142	0.00
0.159	0.00
0.178	0.00
0.200	0.00
0.224	0.00
0.252	0.00
0.283	0.00
0.317	0.00
0.356	0.00
0.399	0.09
0.448	0.31
0.502	0.78
0.564	1.13
0.632	1.56
0.710	1.99
0.796	2.43
0.893	2.87
1.002	3.29
1.125	3.67
1.262	4.00
1.416	4.23
1.589	4.35
1.783	4.34
2.000	4.19
2.244	3.91
2.518	3.52
2.825	3.07
3.170	2.59
3.557	2.13
3.991	1.72
4.477	1.4
5.024	1.17
5.637	1.04
6.325	1.01
7.096	1.05
7.962	1.15
8.934	1.27
10.024	1.40
11.247	1.51
12.619	1.61
14.159	1.67
15.887	1.72
17.825	1.75
20.000	1.78
22.440	1.8
25.179	1.82
28.251	1.85
31.698	1.86
35.566	1.87
39.905	1.85
44.774	1.80
50.238	1.71
56.368	1.60
63.246	1.45
70.963	1.29
79.621	1.13
89.337	0.98
100.237	0.84
112.468	0.72
126.191	0.61
141.589	0.49
158.866	0.39
178.250	0.20
200.000	0.00

Table A-16 Volume distribution of the 1% w/v emulsion via the coalescer coupled with destabilization process

Size (µm)	Volume (%)
0.100	0.00
0.112	0.00
0.126	0.00
0.142	0.00
0.159	0.00
0.178	0.00
0.200	0.00
0.224	0.00
0.252	0.00
0.283	0.00
0.317	0.00
0.356	0.00
0.399	0.00
0.448	0.00
0.502	0.00
0.564	0.00
0.632	0.02
0.710	0.05
0.796	0.07
0.893	0.07
1.002	0.08
1.125	0.09
1.262	0.11
1.416	0.13
1.589	0.15
1.783	0.18
2.000	0.2
2.244	0.23
2.518	0.25
2.825	0.27
3.170	0.29
3.557	0.3
3.991	0.3
4.477	0.3
5.024	0.3
5.637	0.29
6.325	0.28
7.096	0.27
7.962	0.26

Size (µm)	Volume (%)
8.934	0.24
10.024	0.22
11.247	0.20
12.619	0.18
14.159	0.17
15.887	0.16
17.825	0.17
20.000	0.19
22.440	0.22
25.179	0.28
28.251	0.35
31.698	0.44
35.566	0.54
39.905	0.63
44.774	0.72
50.238	0.79
56.368	0.83
63.246	0.84
70.963	0.84
79.621	0.83
89.337	0.85
100.237	0.94
112.468	1.13
126.191	1.47
141.589	1.99
158.866	2.71
178.250	3.58
200.000	4.59
224.404	5.64
251.785	6.61
282.508	7.41
316.979	7.90
355.656	8.02
399.052	7.74
447.744	7.07
502.377	6.08
563.677	4.89
632.456	3.62
709.627	2.40

Size (µm)	Volume (%)
796.214	1.33
893.367	0.62
1002.374	0.07
1124.683	0.00
1261.915	0.00
1415.892	0.00
1588.656	0.00
1782.502	0.00
2000.000	0.00

APPENDIX B
SEPARATION KINETICS AND JAR-TEST RESULTS

Table B-1 An area equivalent to the oil concentration from HPLC machine

Oil	0.025%	0.05%	0.1%	0.25%	0.5%
Area	93157	454562	1020514	2284405	5390141

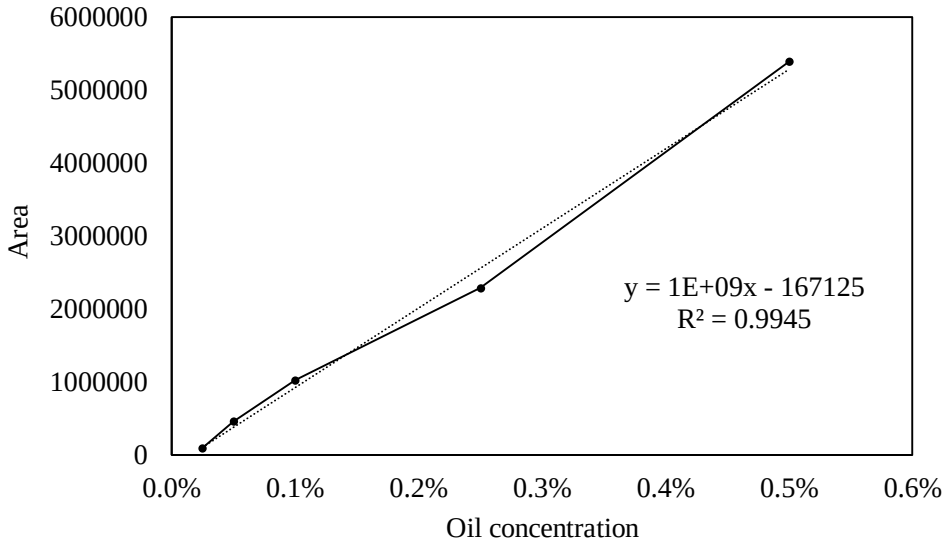

Figure B-1 Plots of the oil concentration standard curve

Table B-2 Turbidity as a function of time during the decantation process

Time (min)	**Turbidity (NTU)**			
	0.05%	**0.10%**	**0.50%**	**1%**
0	911	1822	10165	19655
20	905.4	2232	6436.5	19340
40	900.15	2003	9543	19250
60	899.75	1995	10470	20245
80	897.4	1974.5	9432	18750
100	893.05	1934	9030.5	18820
120	896.3	1754	10000	19285
140	893.7	1750	10030	18910
160	897.6	1766	10010	19475
180	896.4	1755	10000	19257

Table B-3 Separation kinetics of the coalescer apparatus

Time (min)	0.05% w/v emulsion		0.1% w/v emulsion	
	Oil conc. (% w/v)	Removal Eff. (%)	Oil conc. (% w/v)	Removal Eff. (%)
0	0.050	0	0.100	0
20	0.040	20	0.059	41.12
40	0.039	22.88	0.057	43.03
60	0.039	22.14	0.059	40.97
80	0.038	24.6	0.059	41.22
100	0.037	25.56	0.059	41.24
120	0.037	25.24	0.058	41.83
Time (min)	**0.5% w/v emulsion**		**1% w/v emulsion**	
	Oil conc. (% w/v)	**Removal Eff. (%)**	**Oil conc. (% w/v)**	**Removal Eff. (%)**
0	0.500	0	1.000	0
20	0.463	7.34	0.750	24.97
40	0.468	6.36	0.773	22.74
60	0.465	6.95	0.813	18.72
80	0.468	6.43	0.722	27.84
100	0.467	6.63	0.652	34.77
120	0.466	6.76	0.925	7.54

Table B-4 Effect of the coagulant dose on emulsion properties

$CaCl_2$ (g/l)	0.05% w/v emulsion		0.1% w/v emulsion	
	Oil conc. (% w/v)	Turbidity (NTU)	Oil conc. (% w/v)	Turbidity (NTU)
0	0.050	911	0.100	1822
0.5	0.025	789.5	0.068	1908
1.0	0.024	806	0.063	2172
1.5	0.028	865	0.069	2104.5
2.0	0.026	661	0.071	966
$CaCl_2$ (g/l)	**0.5% w/v emulsion**		**1% w/v emulsion**	
	Oil conc. (% w/v)	**Turbidity (NTU)**	**Oil conc. (% w/v)**	**Turbidity (NTU)**
0	0.500	10165	1.000	19655
0.5	0.382	8116.5	0.729	18190
1.0	0.403	9553	0.507	18810
1.5	0.359	9646.5	0.420	6746.5
2.0	0.242	2959.25	0.261	3025

APPENDIX C
CROSS-FLOW UF PERFORMANCE

Table C-1 Permeate flux as a function of time from different membrane types, operated with the 0.1% emulsion

Time (min)	PES Membrane Flux (l/m^2h)			PSU Membrane Flux (l/m^2h)		
	2 bar	**3 bar**	**4 bar**	**2 bar**	**3 bar**	**4 bar**
0	52	49	46	65	56	24
5	34	47	34	28	44	18
10	20	43	30	16	40	16
15	12	38	26	12	36	16
20	10	35	24	8	34	16
25	9	32	22	6	32	16
30	9	29	21	4.67	32	16
35	8	27	20	4	30	16
40	7.5	26	20	2.8	27.5	16
45	7	25	20	2.6	27	16
50	6	24	18	2.4	24	16
55	5	23	18	2.2	22	16
60	4.67	23	18	2	21	16

Table C-2 Normalized flux as a function of time from different membrane types, operated with the 0.1% emulsion

Time (min)	PES Membrane Normalized Flux			PSU Membrane Normalized Flux		
	2 bar	**3 bar**	**4 bar**	**2 bar**	**3 bar**	**4 bar**
0	1	1	1	1	1	1
5	0.65	0.96	0.74	0.43	0.79	0.75
10	0.38	0.88	0.65	0.25	0.71	0.67
15	0.23	0.78	0.57	0.18	0.64	0.67
20	0.19	0.71	0.52	0.12	0.61	0.67
25	0.17	0.65	0.48	0.09	0.57	0.67
30	0.17	0.59	0.46	0.07	0.57	0.67
35	0.15	0.55	0.43	0.06	0.54	0.67
40	0.14	0.53	0.43	0.04	0.49	0.67
45	0.13	0.51	0.43	0.04	0.48	0.67
50	0.11	0.49	0.39	0.04	0.43	0.67
55	0.10	0.47	0.39	0.03	0.39	0.67
60	0.09	0.47	0.39	0.03	0.38	0.67

Table C-3 Flux behaviors of each oil concentration under varied TMP, operated with PES membrane

Time (min)	0.05% w/v Flux (l/m^{2}h)			0.1% w/v Flux (l/m^{2}h)			0.5% w/v Flux (l/m^{2}h)		
	2 bar	3 bar	4 bar	2 bar	3 bar	4 bar	2 bar	3 bar	4 bar
0	67	75	82	48	53	54	28	38	42
15	62	73	73	34	52	30	23	30	14
30	54	68	61	27	50	20	14	22	11
45	46	63	54	21	47	13	5.5	21	8
60	36	59	48	16	41	10	4	19	7
75	28	56	45	14	37	8.5	3	18	6
90	26	54	41	13	32	6.67	2.33	17	5.5
105	22	51	38	9	26	6	2.33	14	4.67
120	20	48	36	8.5	24	4.67	1.67	12	4
135	18	46	35	7.5	22	4.67	1.67	10.5	4
150	18	44	32	7.5	17	4	1.67	9.5	4

Table C-4 Flux behaviors of each oil concentration under varied TMP in terms of normalized flux, operated with PES membrane

Time (min)	0.05% w/v Normalized Flux			0.1% w/v Normalized Flux			0.5% w/v Normalized Flux		
	2 bar	3 bar	4 bar	2 bar	3 bar	4 bar	2 bar	3 bar	4 bar
0	1.00	1.00	1.00	1.00	1.00	1.00	1.00	1.00	1.00
15	0.93	0.97	0.89	0.71	0.82	0.63	0.82	0.79	0.33
30	0.81	0.91	0.74	0.56	0.73	0.27	0.50	0.58	0.26
45	0.69	0.84	0.66	0.44	0.67	0.17	0.20	0.55	0.19
60	0.54	0.79	0.59	0.33	0.61	0.13	0.14	0.50	0.17
75	0.42	0.75	0.55	0.29	0.55	0.11	0.11	0.47	0.14
90	0.39	0.72	0.50	0.27	0.48	0.09	0.08	0.45	0.13
105	0.33	0.68	0.46	0.19	0.39	0.08	0.08	0.37	0.11
120	0.30	0.64	0.44	0.18	0.36	0.06	0.06	0.32	0.10
135	0.27	0.61	0.43	0.16	0.33	0.06	0.06	0.28	0.10
150	0.27	0.59	0.39	0.16	0.25	0.05	0.06	0.25	0.10

Table C-5 Flux behaviors of 0.1% emulsion under varied temperatures, operated with PES membrane

Time	Actual Flux (l/m^{2}h)			Normalized flux		
	16 °C	**28 °C**	**40 °C**	**16 °C**	**28 °C**	**40 °C**
0	47	49	76	1	1	1
10	24	43	48	0.51	0.88	0.63
20	20	35	36	0.43	0.71	0.47
30	17	29	30	0.36	0.59	0.39
40	14	26	26	0.3	0.53	0.34
50	14	24	24	0.3	0.49	0.32
60	13	23	20	0.28	0.47	0.26

Table C-6 Flux behaviors of 0.1% emulsion under varied pH, operated with PES membrane

Time	Actual Flux (l/m^{2}h)			Normalized flux		
	pH 5	**pH 7**	**pH 9**	**pH 5**	**pH 7**	**pH 9**
0	46	28	49	1	1	1
5	20	18	47	0.43	0.64	0.96
10	18	14	43	0.39	0.5	0.88
15	16	9	38	0.35	0.32	0.78
20	12.5	7.5	35	0.27	0.27	0.71
25	11	6	32	0.24	0.21	0.65
30	10	5	29	0.22	0.18	0.59
40	8.5	4	26	0.18	0.14	0.53
50	7	3.5	24	0.15	0.13	0.49
60	6.5	2.4	23	0.14	0.09	0.47

Table C-7 Flux behaviors of 0.1% emulsion under varied circulating lines

Time (min)	Actual Flux (l/m^{2}h)				Normalized flux			
	Hole 1	Hole 2	Hole 3	Hole 4	Hole 1	Hole 2	Hole 3	Hole 4
0	20	40	28	26	1	1	1	1
5	16	20	16	14	0.8	0.5	0.57	0.54
10	6	16	14	12	0.3	0.4	0.50	0.46
15	6	14	13	8	0.3	0.35	0.46	0.31
20	4.67	12	12	7	0.23	0.3	0.43	0.27
25	4	8.5	10	6	0.2	0.21	0.38	0.23
30	3.33	7	9	5.5	0.16	0.18	0.32	0.21
35	3	6	8	5	0.15	0.15	0.28	0.19
40	2.5	5	8	4.67	0.13	0.13	0.28	0.18
45	2	4.33	7.5	4	0.1	0.11	0.27	0.15
50	1.67	4	7	3.33	0.08	0.10	0.25	0.13
55	1.57	3	7	2.75	0.08	0.08	0.25	0.11
60	1.57	3	7	2.5	0.08	0.08	0.25	0.10

Table C-8 Flux behaviors of 0.1% emulsion under different residence times

Time (min)	Actual Flux (l/m^{2}h)					Normalized flux				
	Sole MB	30 min	45 min	1 hr	2 hr	Sole MB	30 min	45 min	1 hr	2 hr
0	58	28	26	20	20	1	1	1	1	1
5	32	15	14	18	16	0.55	0.54	0.54	0.90	0.80
10	26	12	14	14	14	0.45	0.43	0.54	0.70	0.70
15	22	10	12	14	12	0.38	0.36	0.46	0.70	0.60
20	19	9	10	12	12	0.33	0.32	0.39	0.60	0.60
25	18	8	8	12	10	0.31	0.29	0.31	0.60	0.50
30	16	7.50	6	10	8	0.28	0.27	0.23	0.50	0.40
35	15	7	6	8	7	0.26	0.25	0.23	0.40	0.35
40	14	6.5	6	8	7	0.24	0.23	0.23	0.40	0.35
45	14	6	4.67	7.5	7	0.24	0.21	0.18	0.38	0.35
50	13	5.33	3.33	7	6.50	0.22	0.19	0.13	0.35	0.33
55	12	5	3	7	6	0.21	0.18	0.12	0.35	0.30
60	12	5	2.75	7	6	0.21	0.18	0.11	0.35	0.30

Table C-9 Flux behaviors of 0.1% emulsion under an external electric field

Time (min)	Flux (l/m^2h)					Normalized flux				
	Sole MB	**30 min**	**30 min w/ E-field**	**1 hr**	**1 hr w/ E-field**	**Sole MB**	**30 min**	**30 min w/ E-field**	**1 hr**	**1 hr w/ E-field**
0	58	28	20	20	15	1	1	1	1	1
5	32	15	14	18	14	0.55	0.54	0.70	0.90	0.93
10	26	12	12	14	12	0.45	0.43	0.60	0.70	0.80
15	22	10	12	14	12	0.38	0.36	0.60	0.70	0.80
20	19	9	10	12	11	0.33	0.32	0.50	0.60	0.73
25	18	8	8	12	10	0.31	0.29	0.40	0.60	0.67
30	16	7.50	6	10	10	0.28	0.29	0.30	0.50	0.67
35	15	7	5.5	8	7	0.26	0.25	0.28	0.40	0.47
40	14	6.5	5	8	7	0.24	0.23	0.25	0.40	0.47
45	14	6	5	7.5	6	0.24	0.21	0.25	0.38	0.40
50	13	5.33	3.33	7	5	0.22	0.19	0.17	0.35	0.33
55	12	5.00	3.33	7	5	0.21	0.18	0.17	0.35	0.33
60	12	5.00	3	7	5	0.21	0.18	0.15	0.35	0.33

Table C-10 R^2 values from different TMP at 28 ºC and pH of 9

TMP (bar)	R^2 value from pore blocking model			
	Complete	**Standard**	**Intermediate**	**Cake formation**
2	0.848	0.936	**0.967**	0.895
3	0.959	0.972	0.981	**0.988**
4	0.833	0.875	0.910	**0.955**

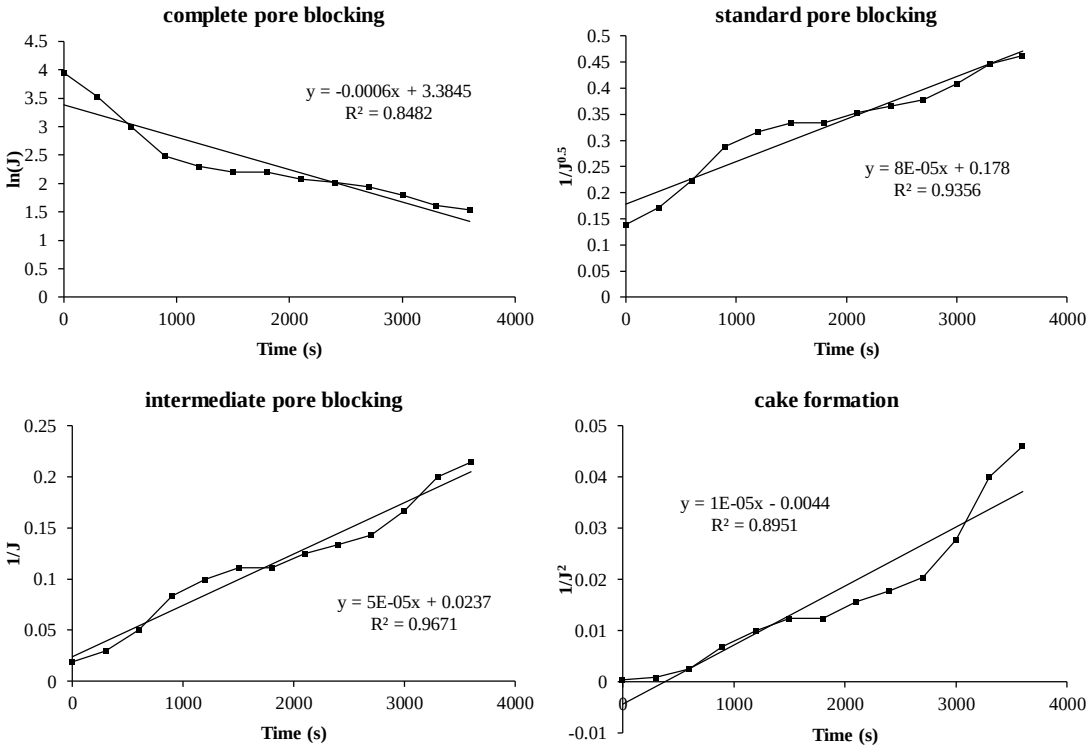

Figure C-1 Different R^2 values under 2 bar

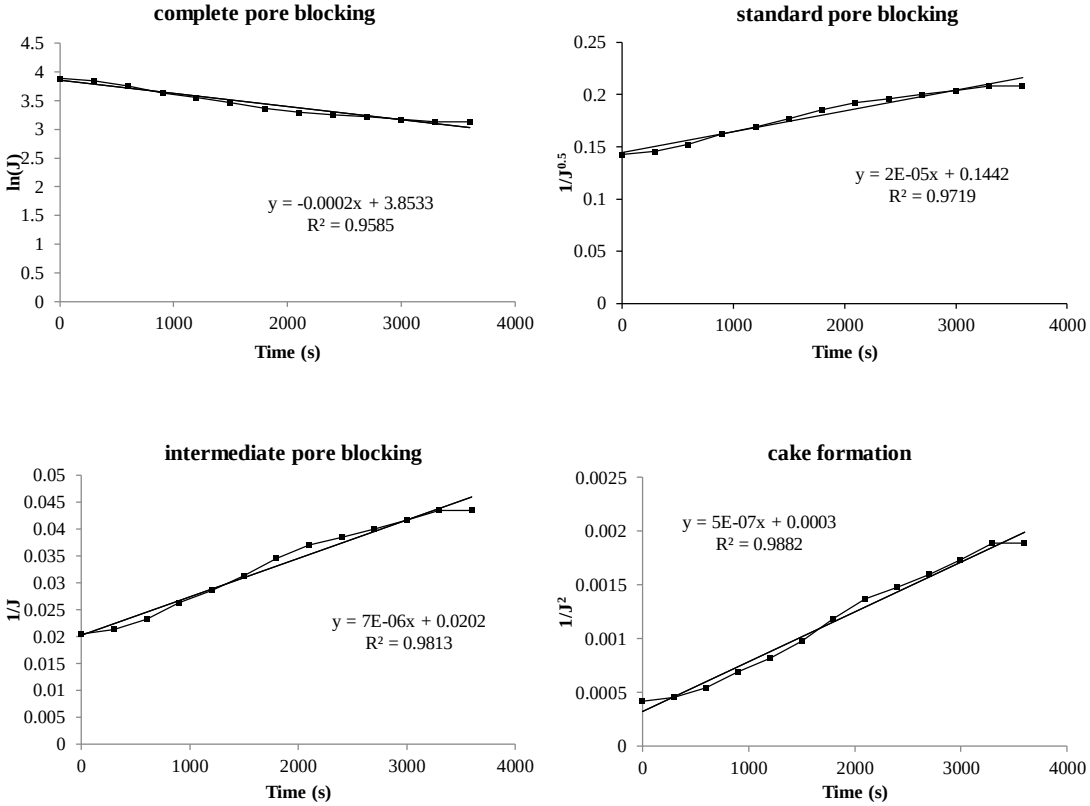

Figure C-2 Different R^2 values under 3 bar

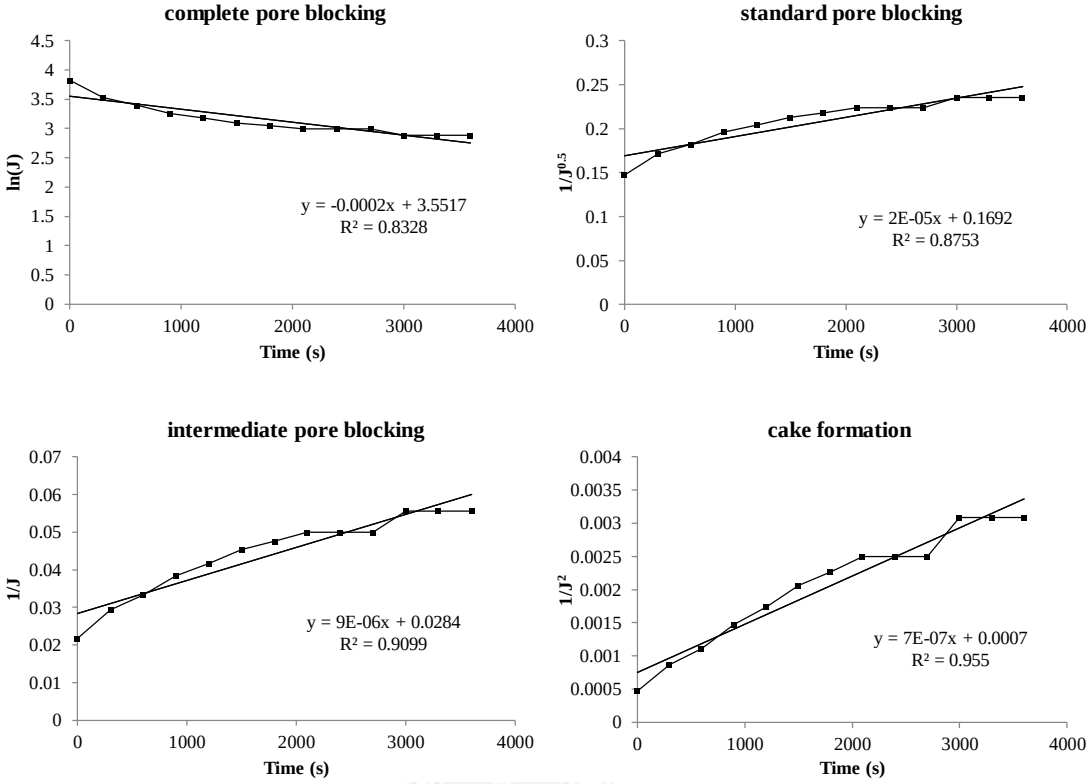

Figure C-3 Different R^2 values under 4 bar

Table C-11 R^2 values from different temperatures at 3 bar and pH of 9

Temp (°C)	R^2 value from pore blocking model			
	Complete	**Standard**	**Intermediate**	**Cake formation**
16	0.820	0.881	0.926	**0.970**
28	0.957	0.970	0.980	**0.987**
40	0.927	0.968	**0.989**	0.974

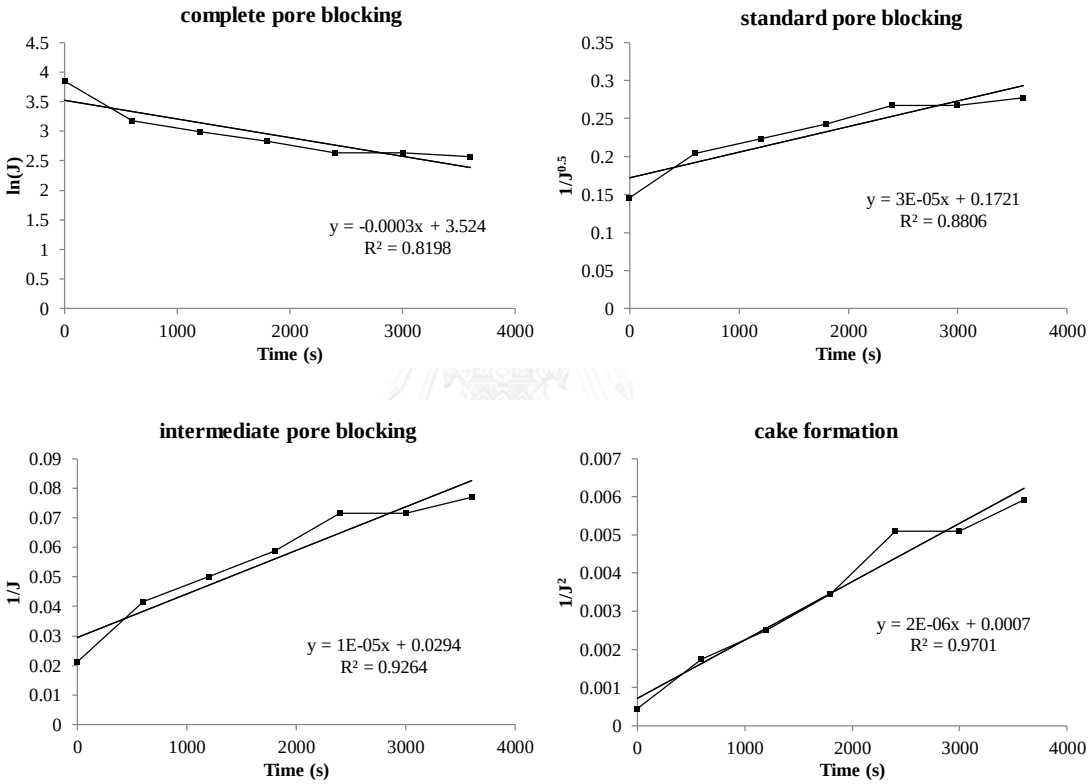

Figure C-4 Different R^2 values under 16 °C

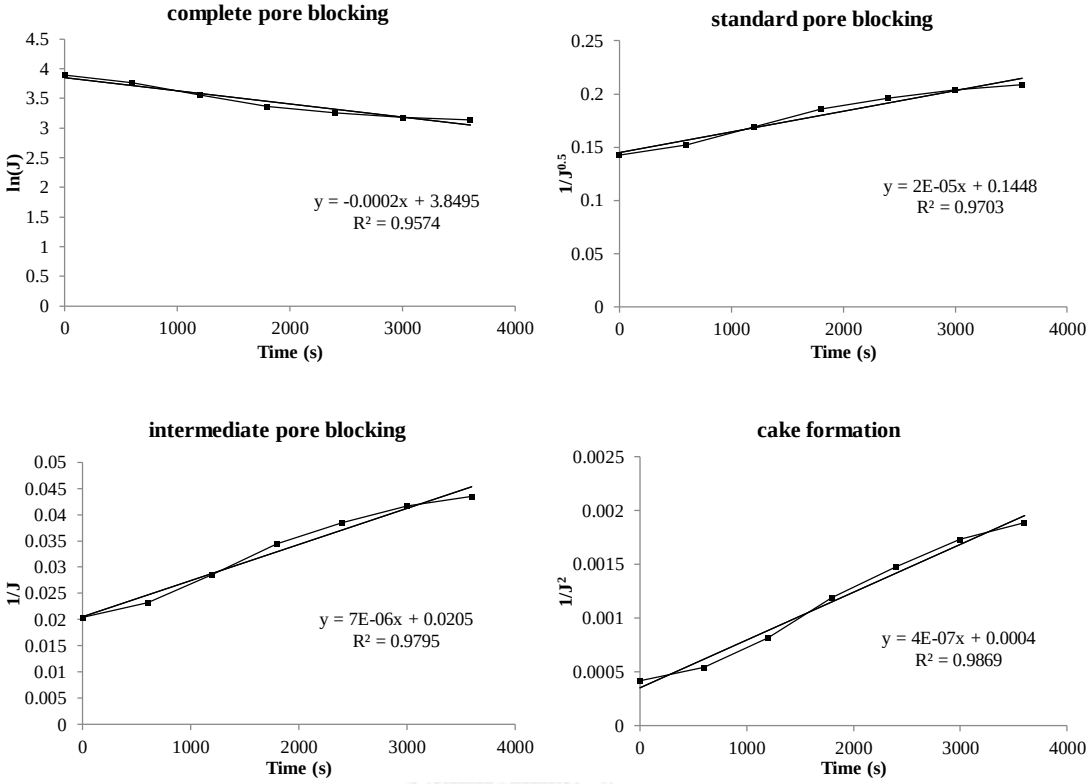

Figure C-5 Different R^2 values under 28 °C

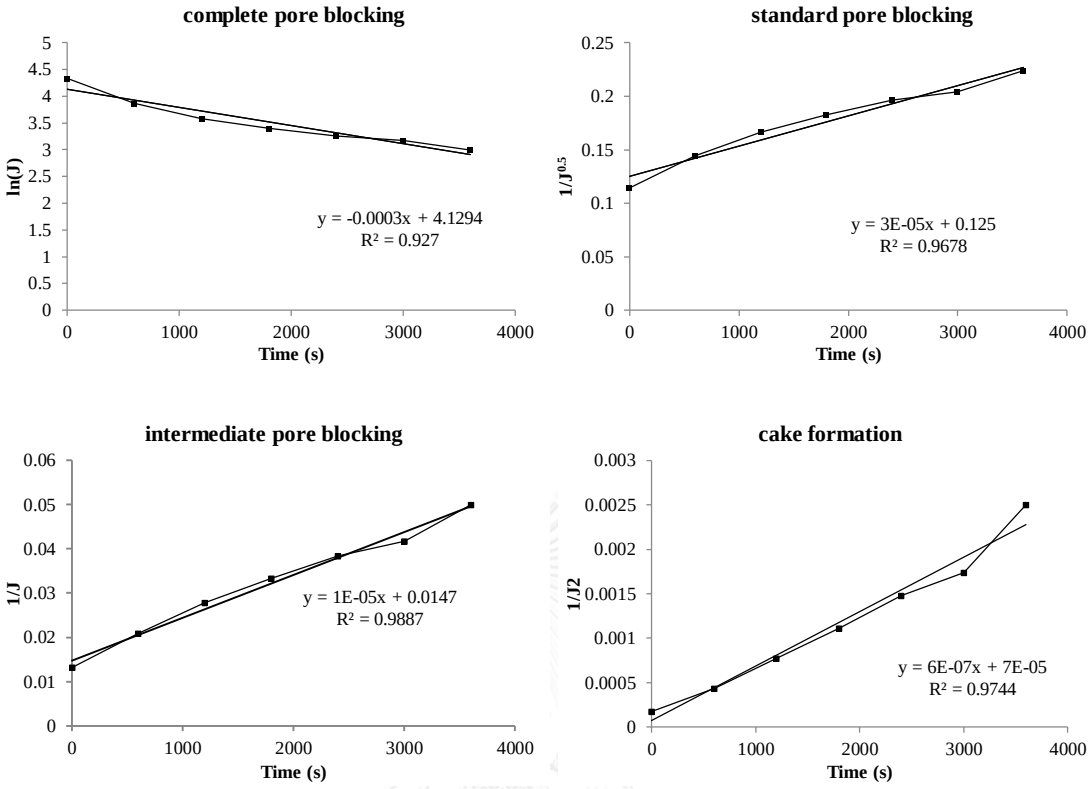

Figure C-6 Different R^2 values under 40 °C

Table C-12 R^2 value from different pH at 3 bar and 28 ºC

pH	R^2 value of pore blocking model			
	Complete	**Standard**	**Intermediate**	**Cake formation**
5	0.835	0.933	**0.982**	0.980
7	0.927	**0.983**	0.976	0.846
9	0.957	0.972	0.982	**0.988**

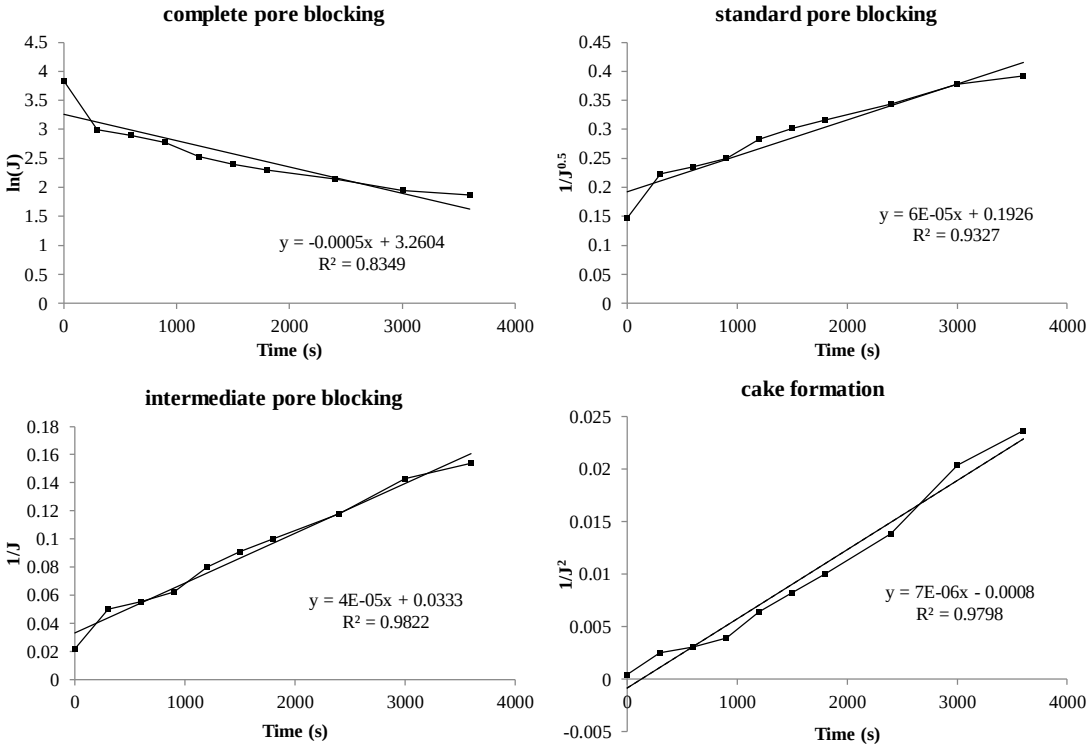

Figure C-7 Different R^2 values under pH 5

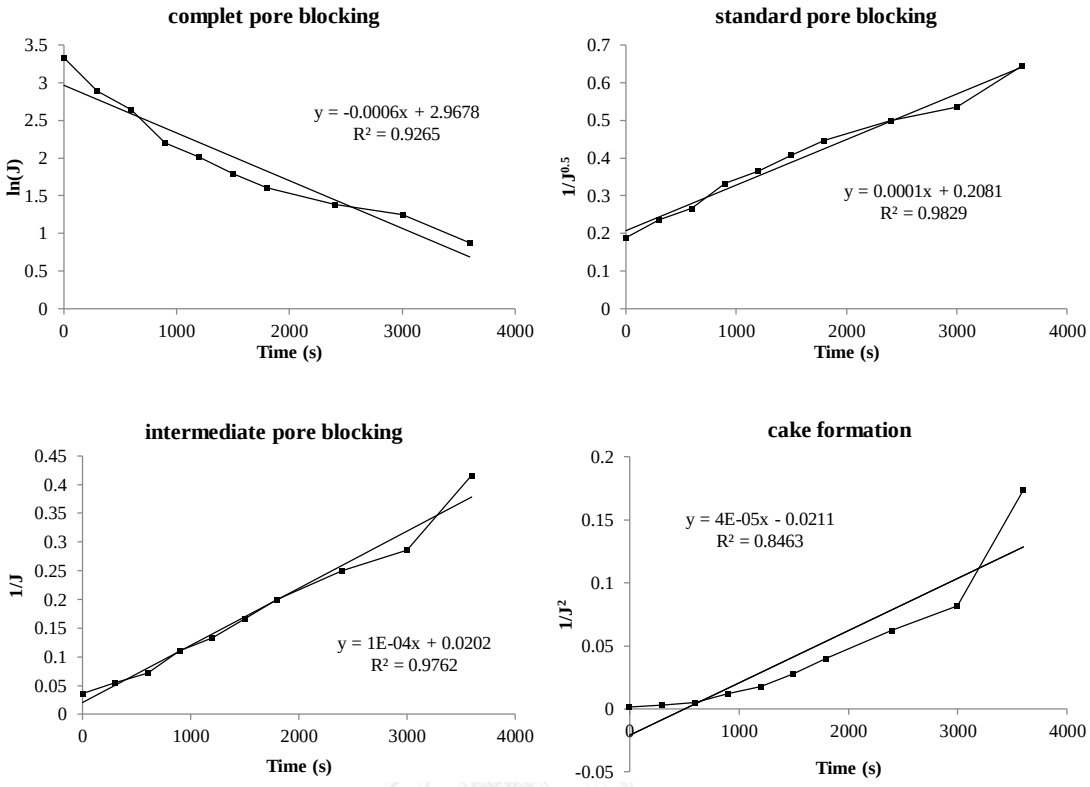

Figure C-8 Different R^2 values under pH 7

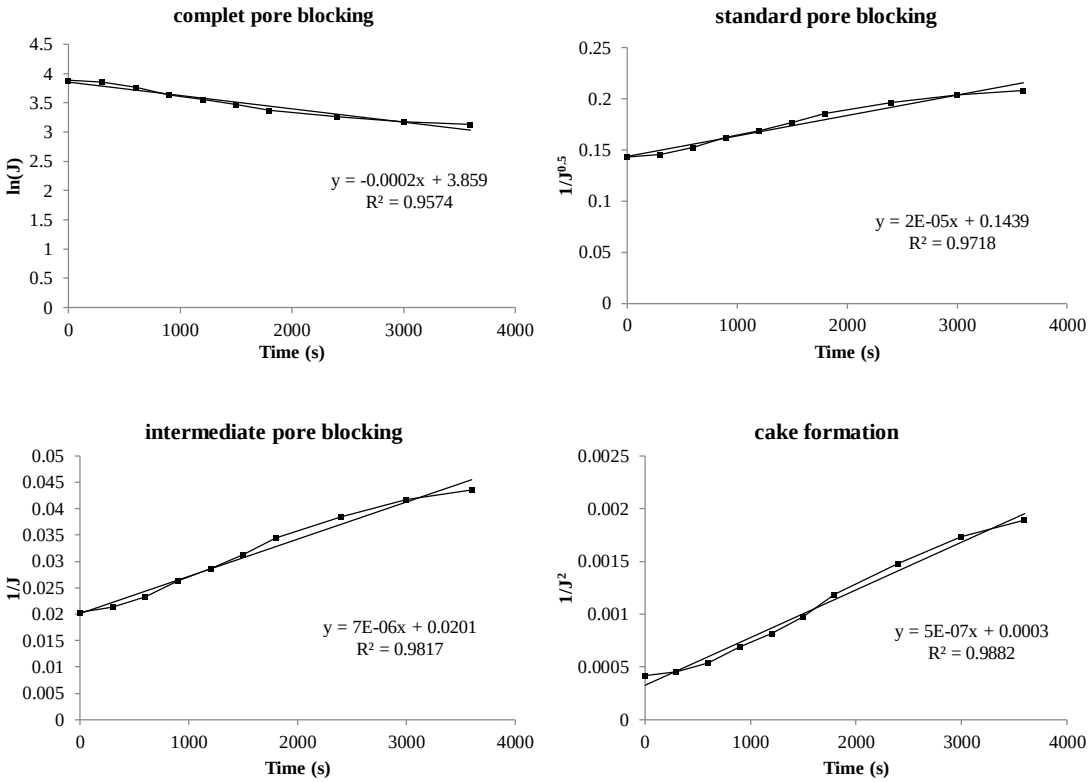

Figure C-9 Different R^2 values under pH 9

VITA

Miss Thaksina Poyai was born on March 16, 1991 in Lopburi, Thailand. She graduated a Bachelor's Degree in 2013 from Department of Environmental Engineering, Faculty of Engineering, Chulalongkorn University. Then she started a Master's Degree of Science at International Program in Hazardous Substance and Environmental Management, Graduate School, Chulalongkorn University in May 2013.